Warren A. Shaw

L 5-1

UNCLASSIFIED

Project NY 340 030-11
Technical Memorandum M-130

ELASTO-PLASTIC RESPONSE OF BEAMS TO DYNAMIC LOADS

3 March 1958

U. S. NAVAL CIVIL ENGINEERING
RESEARCH AND EVALUATION
LABORATORY
PORT HUENEME, CALIFORNIA

AD 160282

ELASTO-PLASTIC RESPONSE OF BEAMS TO DYNAMIC LOADS

Final Report

3 March 1958

by

J. R. Allgood
W. A. Shaw

U.S. NAVAL CIVIL ENGINEERING
Research and Evaluation
LABORATORY
Port Hueneme, California

SUMMARY

OBJECT OF PROJECT

To carry out a comprehensive research and development program which will provide adequate designs and techniques to afford protection to structures and resolve existing data on loading and response of structural elements and structures.

OBJECT OF SUBPROJECT

To perform basic dynamic tests and studies on structural components in order to contribute to available knowledge in this field.

OBJECT OF THIS REPORT

To present the results of experiments and studies made to define the elasto-plastic response of beams to transient loads.

RESULTS

Design criteria are established and curves are provided for the rapid determination of the maximum initial deflection of beams subjected to step-function loading. Present knowledge of dynamic elasto-plastic response is summarized. Experimental results are compared with the theory.

ABSTRACT

The study was designed to provide and substantiate a simple method for determining the elasto-plastic response of beams subjected to pulse loads. Design charts are presented, and the theory is compared with the results of over sixty beam tests.

It was found that deflection can be predicted by the spring-mass approximation with accuracy sufficient for design purposes. Further, it was found that the dynamic reactions were in the range from 1.5 to 2 times the corresponding static values.

Experimental resistance curves have been developed from a simple force-equilibrium relation. The influence of the rise-time of the load is demonstrated. Definite ranges of behavior have been established for step loading.

CONTENTS

TABLES

ILLUSTRATIONS

INTRODUCTION

This is a final report on the small-scale beam tests and related studies which have been conducted at the Laboratory (U. S. Naval Civil Engineering Research and Evaluation Laboratory), Port Hueneme, California, under Project NY 340 030, authorized by the BUDOCKS (Bureau of Yards and Docks). The work was undertaken to provide data which would extend existing knowledge of the dynamic behavior of beams.

The study was planned to determine the characteristics of resistance, establish the relative importance of the higher modes of vibration, determine the accuracy to be expected from fundamental mode analysis, establish shear requirements, measure the strain rate and the increase in yield point, and evaluate the gain in capacity from permitting plastic action.

These determinations will help in setting forth an intelligent approach for designing structures to resist loads of the type imposed by nuclear explosions.

Early dynamic beam tests[1] were made starting about 1948. Small reinforced concrete beams were tested in which different spans, sizes, steel percentages, and support conditions were used. The results showed that the energy absorbed by beams under dynamic loading is greater than the energy absorbed under static loading.

More recent tests[2] were conducted on nine steel beams in which the variables were the shape of the cross section, the orientation of the cross section with respect to lateral load, and the lower yield stress. It was noted that in the early stages of response, the resistance exhibited a time-dependent character.

In the Laboratory experiments it was decided to test a relatively large number of beams of one type to establish positively the dynamic load-deflection relation and the resistance throughout the range of plastic behavior. Thus, scope of the tests was limited so that a sufficient number of closely controlled tests could be run to insure confidence in the results.

In the following paragraphs the experimental work is described briefly, then the results are interpreted and compared with the behavior of the spring-mass system. Distinction is drawn between the response to step-loads and rapidly decaying loads. The influence of rise-time of the load is also considered.

Theoretical developments are confined to appendices wherever expediency permits. An appendix is given which shows how the material in the text and other appendices is used in the design of a one-way panel.

EXPERIMENTATION

Test Beams

Reinforced concrete beams having the section shown in figure 1 were tested. They measured 3 1/2 in. (inch) by 4 1/2 in. by 78 in., and comprised two groups, series B and series C (pilot tests, series A,

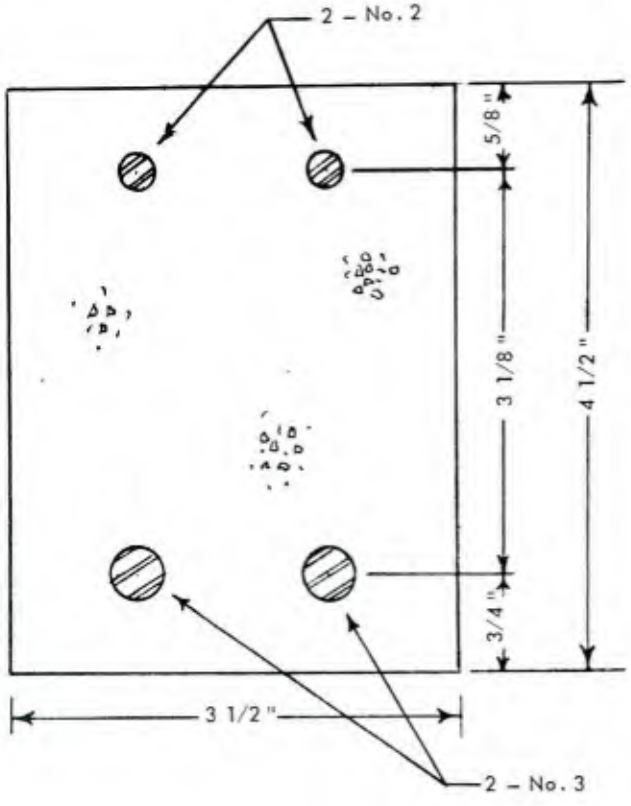

Figure 1. Typical section of the test beams.

are not included) which differed in steel properties. The steel of the series B beams had a tensile yield stress of 44,400 psi (pounds per square inch) while that used in the series C beams had a tensile yield of 50,400 psi. The distances from the top of the beam to the center of the compression and tension steel were 5/8 in. and 3-3/4 in., respectively. Stirrups, of 1/4-in. diameter, were spaced every 9 in. along the length of the beam. A photograph of the reinforcing steel with gages attached is shown in figure 2. The members were designed to fail by yielding of the tensile steel.

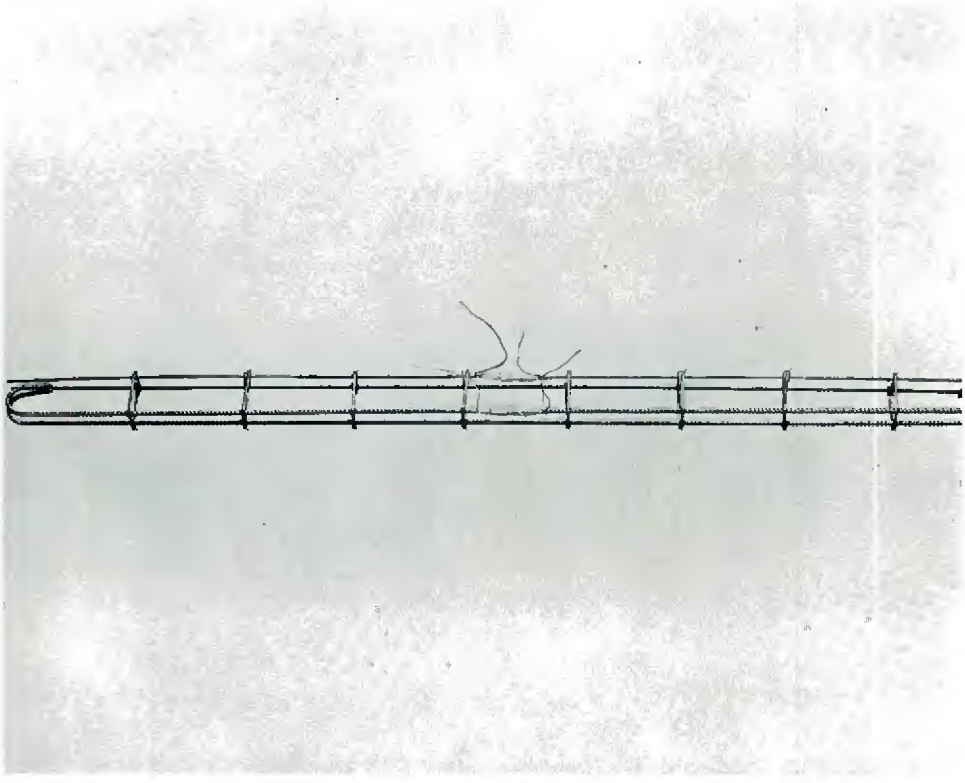

Figure 2. Reinforcing steel with strain gages attached.

The reasons for choosing reinforced concrete members were as follows:

1. A reinforced concrete beam has discrete tensile elements, thereby avoiding complex tensile stress fields on formation of the plastic-hinge.

2. The damping of a reinforced concrete beam reduces high frequency oscillations, making it easier to interpret the data.

The Rapid Load Machine

The rapid load machine (shown in figure 3) is essentially a pneumatic cylinder-piston arrangement by means of which concentrated static or dynamic loads may be applied to a member. Loads up to

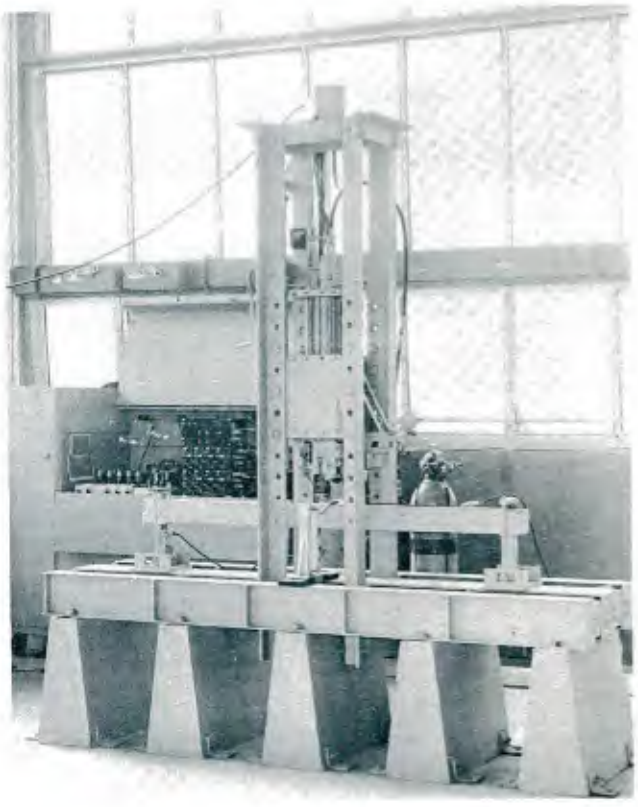

Figure 3. View of rapid load machine.

10,000 lb (pounds) may be obtained in as little as 1 msec (millisecond). Rise-time and decay of the load may be varied, or the load may be maintained at essentially a constant value for any desired time.

The cylinder of the machine is 17 in. in length. This length is sufficient to keep the volume change caused by deflection of the beam within acceptable limits. It is possible to vent the cylinder and thus reduce the load to zero in about 20 msec. The piston and piston rod are made of aluminum to minimize inertia effects of the moving parts.

The load is initiated by releasing a trip-lever system controlled by a solenoid. The load release is controlled by a second solenoid and is accomplished by puncturing a thin brass diaphragm.

Instrumentation

One of the main problems in impulsive load testing is accurate, reproducible time control. In order to provide this control, electronic equipment referred to as the "interval controller" was designed and built at NAVCERELAB.[3]

Functions of the interval controller are:

1. Starting the high-speed camera, and the rotating-drum deflection gage, or both.

2. Starting the recording oscillograph.

3. Activating the solenoid which initiates application of the load.

4. Actuating a second solenoid which initiates the load-release mechanism.

5. Turning off all instrumentation and equipment.

Time intervals associated with these various operations may be varied and controlled to within a few milliseconds.

Load, reaction, deflection, acceleration, and strain measurements were made at the stations shown in figure 4. The transient signals were obtained by an oscillographic recording and measuring system.

Load was measured by means of a strain gage bridge mounted on the piston rod, sometimes called the load strut. The gages were placed to enable cancellation of any effects of bending. The load strut was calibrated statically and dynamically, against a load cell. During the dynamic tests, an approximate check on applied loads was afforded by knowledge of the cylinder pressure and the friction between the piston and cylinder. The cylinder temperature was maintained within ± 5 F of a preselected nominal value chosen to minimize loss of the nitrogen gas used and to maintain a relatively constant value of friction. Since

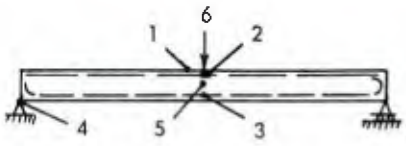

1 accelerometer
2 SR-4's top and bottom
3 SR-4 gage
4 load cell
5 translatory potentiometer
6 load

Figure 4. Instrumentation stations.

the load for many of the tests was essentially a step function, it was necessary to check the response of the galvanometer in the load-strut circuit. The galvanometer used was found to follow the signal adequately.

Considerable emphasis was placed on the measurement of the load transmitted to the supports. The simple setup used consisted of a load cell placed under the test beam, anchored to the support, and preloaded with tie-down rods. A stiff spring was placed between the top of the beam and the crossbar of the tie-down rods shown in figure 5. These supports allowed the ends of the beam to rotate as well as move in a longitudinal direction.

The measurement of deflection was complicated by the high velocities encountered. After some searching and trial, a linear potentiometer was found which would accommodate the 100 ips (inches per second) velocities encountered in the tests.

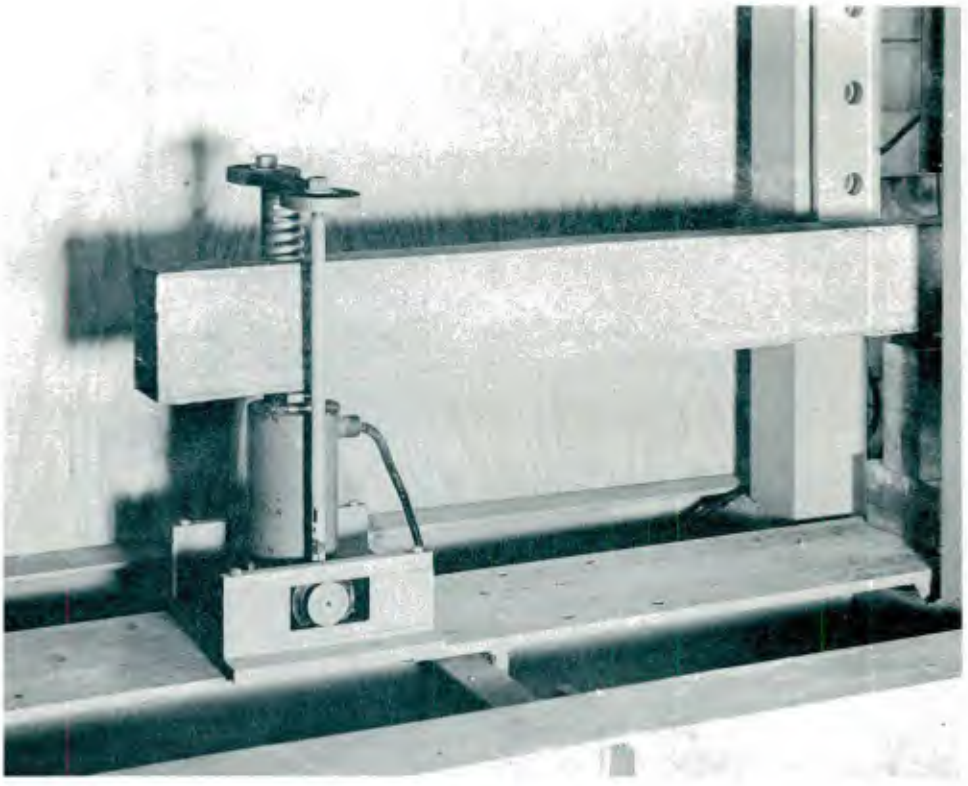

Figure 5. End support.

A rotating-drum deflection gage (shown in figure 6) was devised in order to provide a reliable check on maximum deflection. The gage, which rotates at a constant speed, is made of a drum (with paper attached) placed at the center of the test beam. A spring-loaded pencil, fastened to the beam, rests against the paper on the drum. As the beam deflected the pencil traced the position of the beam versus time. These time values, of course, were not as accurate as those obtained from the oscillograph.

Steel strain measurements were made on about one-third of the series C beams with type A-12 and post yield PA-3 gages. All gages were located at mid-span except for beams C-2 and C-41. For these members gages also were placed 6 in., 15 in., and 24 in. off center. A-9 gages were used to determine concrete strains on beam B-2. These measurements were found to be of little value and hence were not taken on other beams.

Figure 6. Rotating drum-deflection gage.

All but a few of the first acceleration measurements were made using a ± 50 g strain gage-type pickup. Calibration showed that the accelerometer was linear within 3 percent up to 1.5 times rated capacity at 107 cps (cycles per second). At ± 5 g, output varied 8 percent over the frequency range 25 to 107 cps.

Other supplemental measurements were made. For example, high speed motion pictures were made for several beams. These films afforded an excellent check on deflections and provided information on crack formation. This method of obtaining information was extremely laborious and was used in only a few instances.

TEST PROCEDURE

The rapid load machine was used for static loading as well as for dynamic loading.

Static Tests

In the static tests, the load was applied by slowly admitting nitrogen into the cylinder with the trip-lever system released. The magnitude of the load was obtained from output signals of the strain gage bridge on the load strut. Deflection was determined by a translatory potentiometer and a 0.001 in. dial indicator. For some of the beams, strains in the reinforcing steel and the concrete were recorded.

Dynamic Tests

For the dynamic tests, the beams were placed and clamped on the supports in the rapid load machine. A view of a beam in place in the test machine is shown in figure 3.

In preparing for a test, the sequence adhered to was as follows:

1. Clearance was provided between the load strut and the bearing plate on the beam. This clearance was 0.012 in. for members loaded at 1 msec rise-time.

2. Instrumentation cables were attached, and the amplifying, recording, and measuring system was checked out.

3. Nitrogen was admitted to the cylinder with the trip-lever system restraining the piston.

4. The interval controller was energized, automatically completing the test.

RESULTS

The primary characteristics of beam behavior, and deductions therefrom, are given in this section. The consequences of dynamic characteristics observed will be discussed later in respect to the theoretical behavior of the equivalent spring-mass system.

Concrete Properties

The average ultimate compressive strength of the concrete in the B beams was 2980 psi while the corresponding strength for the C beams was 5100 psi.

Steel Properties

Standard tension tests were performed on samples taken from the reinforcing steel as delivered. Also, steel samples were taken from the beams after they had been subjected to dynamic tests. These samples were taken from near the ends of the beams where the stress had not exceeded the yield point. The results of the tension tests are presented in table I. For the B beams, the average yield point from 16 specimens was 44,300 psi with a maximum variation of 4 1/2 percent. This variation is well within the normal limits of variation expected from such tests.

Static Beam Tests

Reasonably consistent results were obtained from the static tests as may be seen from the summary of static test data given in table II. However, beams B-17 and B-31 displayed a higher yield load than the other B beams. An investigation was made to determine the reasons for this variation. Representative beams were sawed in half to establish the exact location of the reinforcement. It was noted that the steel was not always in the design location, despite precautions taken in fabrication, but varied a maximum of 1/8 in. in the vertical direction. This variation would only account for a difference in the yield load of $\pm$ 1 1/2 percent. The expected total maximum variation in yield load of the test beams was $\pm$ 6 percent. The actual variation was found to be $\pm$ 7 1/2 percent. A plot of the average static load-deflection curve is shown in figure 7.

Curves showing the experimental variation of strain in the concrete, top steel, and bottom steel and deflection of the beam are shown in figure 8. As expected, a linear relationship exists among the various strains and the deflection up to the yield load of the beam and good agreement exists between theoretical and experimental results.

Table 1. Summary of Static Test Data (Series B Beams)

Beam	Yield load lb	Yield deflection in.	Experimental EI lb-ft^2	Elastic slope, k_1 lb/ft	Plastic slope, k_2 lb/ft
B-1	1725	0.329	284,000	72,940	2724
B-17	1875	0.295	308,000	76,270	1266
B-22	1750	0.275	288,000	76,360	408
B-31	1933	0.318	318,000	72,950	612
Average	1821	0.304	299,500	74,630	1253
Theoretical	1750	0.32	288,000	67,460	2070

Steel properties (average of 9 or more specimens)

Size bar	Yield stress psi	Ultimate stress psi	Elongation in 8 in. percent	Modulus of Elasticity psi
3/8	44,400	67,700	22.9	29,000,000
1/4	53,200	82,000	18.5	29,900,000

Concrete properties (average of 14 specimens)

Cylinder size	Ultimate strength (at time of testing beams) psi
6 in. by 12 in.	2980

Table II. Summary of Static Test Data (Series C Beams)

Beams	Yield load lb	Yield deflection in.	Experimental EI $lb\text{-}ft^2$	Elastic slope, k_1 lb/ft	Plastic slope, k_2 lb/ft
C-1	2140	0.378	305,700	67,940	1270
C-2	1907	0.354	290,900	64,640	1428
C-3	1907	0.364	282,900	62,870	1428
C-37	2230	0.371	324,600	72,130	1010
Average	2046	0.367	301,000	66,900	1284
Theoretical	1960	0.30	353,000	78,400	1870

Steel properties (average of 6 or more specimens)

Size bar	Yield stress psi	Ultimate stress psi	Elongation in 8 in. percent	Modulus of Elasticity psi
3/8	50,400	73,280	22.0	29,710,000
1/4	50,030	66,540	15.3	31,030,000

Concrete properties (average of 10 specimens)

Cylinder size	Ultimate strength (at time of testing beams) psi
6 in. by 12 in.	5100

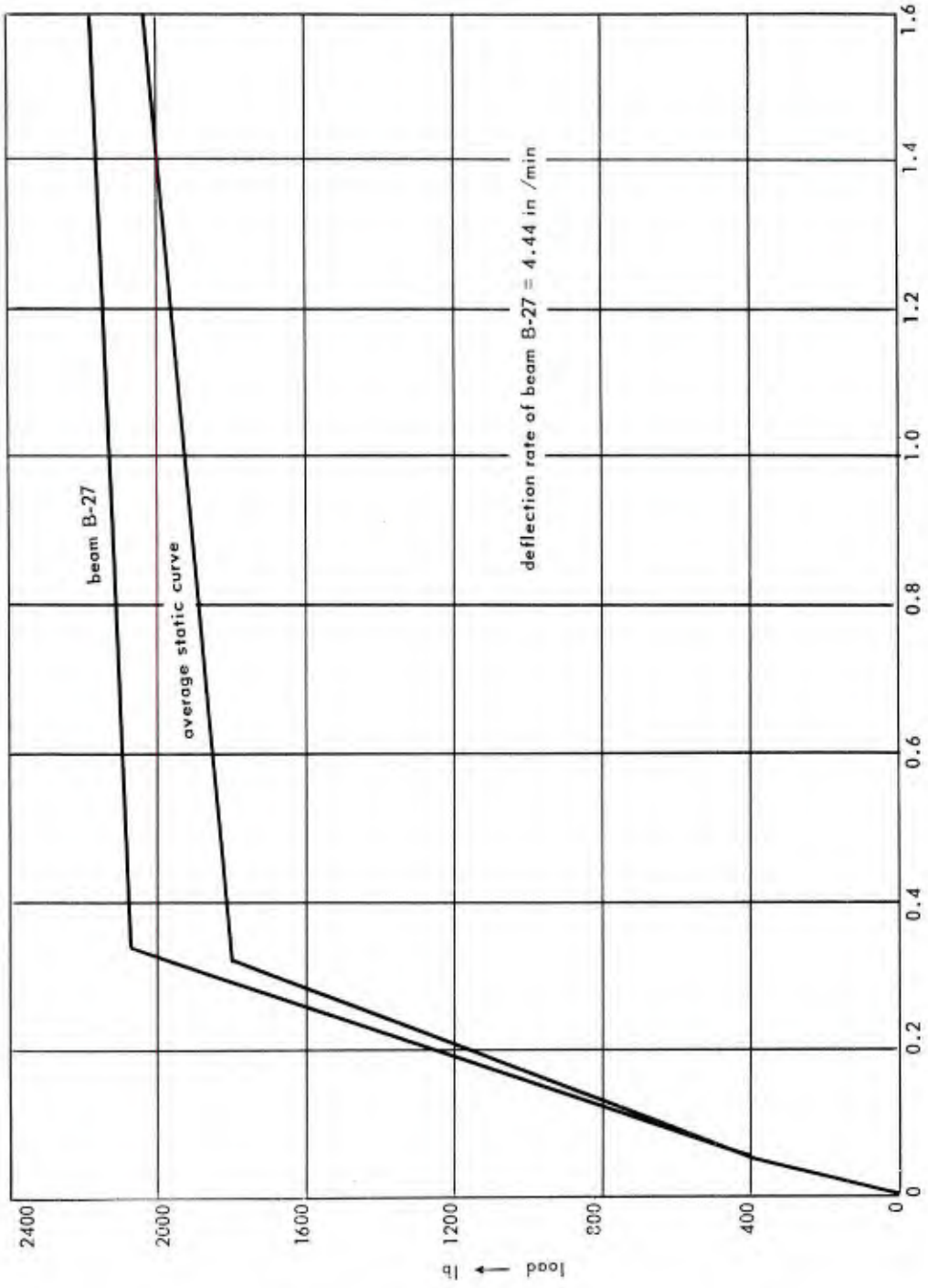

Figure 7. Static load deflection curves for series B beams.

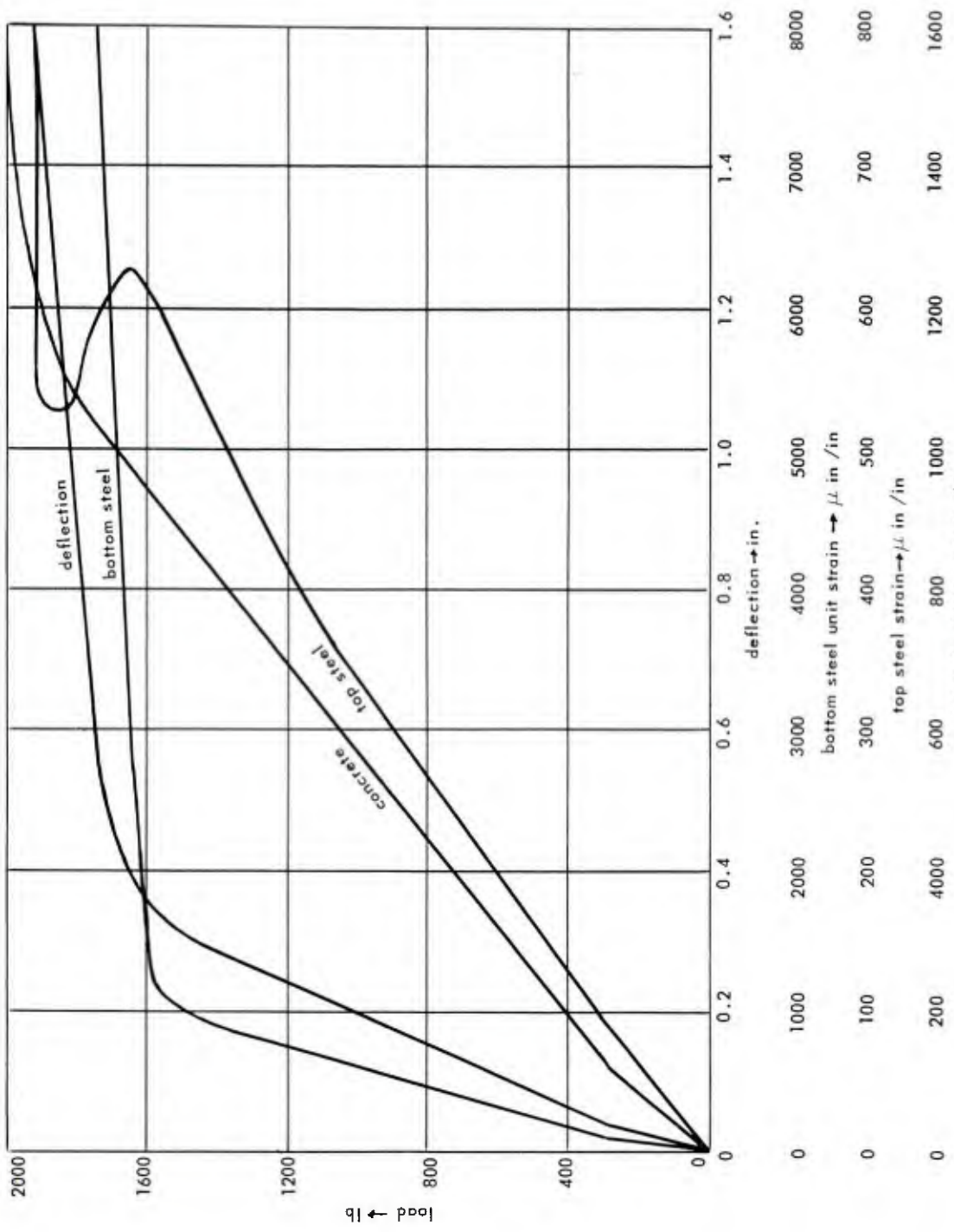

Figure 8. Static test curves for beam B-2.

As yielding began, the strain in the top steel was initially relieved because of continued upward shifting of the neutral axis. With continued yielding, the compression strain in the top steel increased as the ultimate load of the beam was approached. The static ultimate load of the beam was governed by the ultimate strength of the concrete. The compression failure and the crack pattern near mid-span are shown in figure 9.

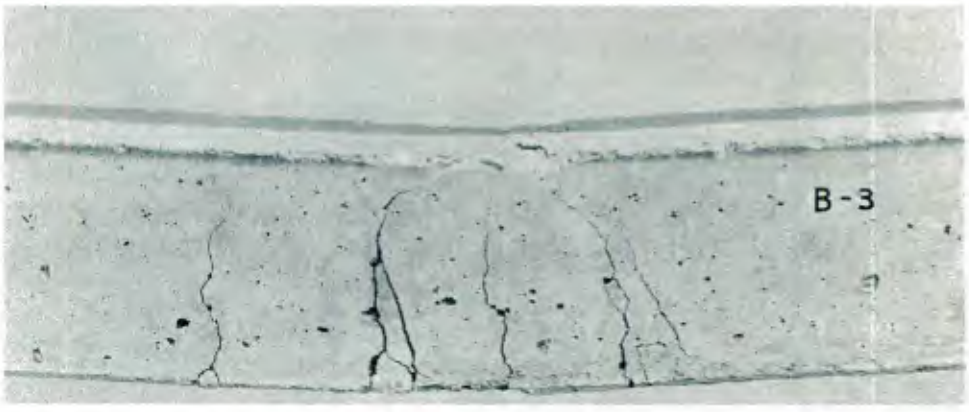

Figure 9. Crack pattern near mid-span from static loading.

In an elasto-plastic theoretical analysis, the slope of the static load-deflection curve in the plastic range is often assumed to be horizontal. This implies that the yield load would cause failure if maintained for a long period of time. The plastic-range slopes of the load-deflection curves for the test beams are not horizontal but have a rather definite slope.

Some idea of the influence of time on the load-deflection curve is given by two tests run under conditions where the time could be determined. These tests were run at a deflection rate of 4.44 ipm (inches per minute). The results from beam B-27 are plotted in figure 7 and show that the yield load of the beam was increased by 12 percent over static loading. It is interesting to note, however, that the plastic-range slope changed only slightly.

Response to Step Load

In general, the response of a beam to a step load (figure 10, diagram (a)) of between 0.8 and 1.1 times the static yield load is as follows:

1. The beam deflects to an initial maximum deflection. (The term initial maximum deflection is used to distinguish the peak deflection reached during the oscillatory phase of the behavior from the deflection reached prior to release of the load, which may or may not be greater than the initial maximum value.)

2. It remains at or near this value for a short time, then deflects at a relatively slow rate until the load is released.

3. It then recovers elastically.

The beam is left with a permanent deflection equal to the maximum deflection prior to release of the load minus the elastic recovery. The time from load application to initial maximum deflection lasts less than 70 msec for most of the beams tested.

From the typical oscillograms (figures 11 through 17) it may be seen that the load reached a peak value in 1 msec and stabilized in 4 to 5 msec. Most of the load traces were equally as good; however, in one or two of the tests the load was more erratic.

The mid-point of the beam did not experience detectable deflection until 1 1/2 to 2 msec after the load was applied. This delay resulted from large inertial forces which caused the ends of the beam to rise and negative reactions to develop.

In nine tests at loads from 1880 lb to 2184 lb the maximum negative (downward) reaction ranged from 44 to 50 percent of the static reaction. After the first 2 or 3 msec the reaction became positive, reaching a maximum value of 151 to 166 percent of the static reaction. The reaction stabilized in approximately 70 msec to the static value of one-half of the applied load. It is reasonable to expect the increase in shear stress to be at least as great as the increase in reaction; hence, shear design[4] should be based on dynamic analysis rather than on static requirements. (See development, page 53.)

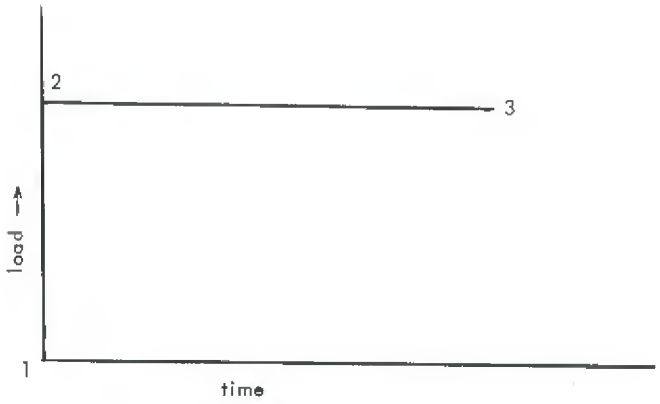

(a) Step load (zero rise time).

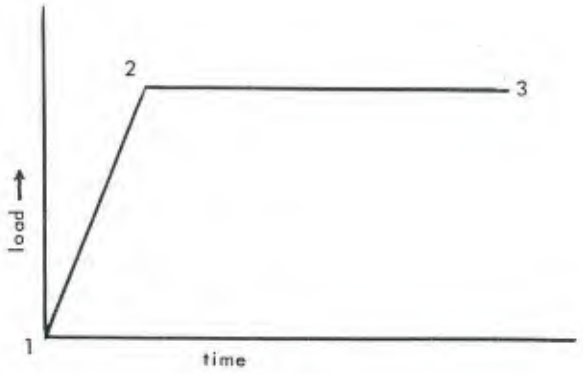

(b) Step load with finite rise time.

Figure 10. Theoretical load curves.

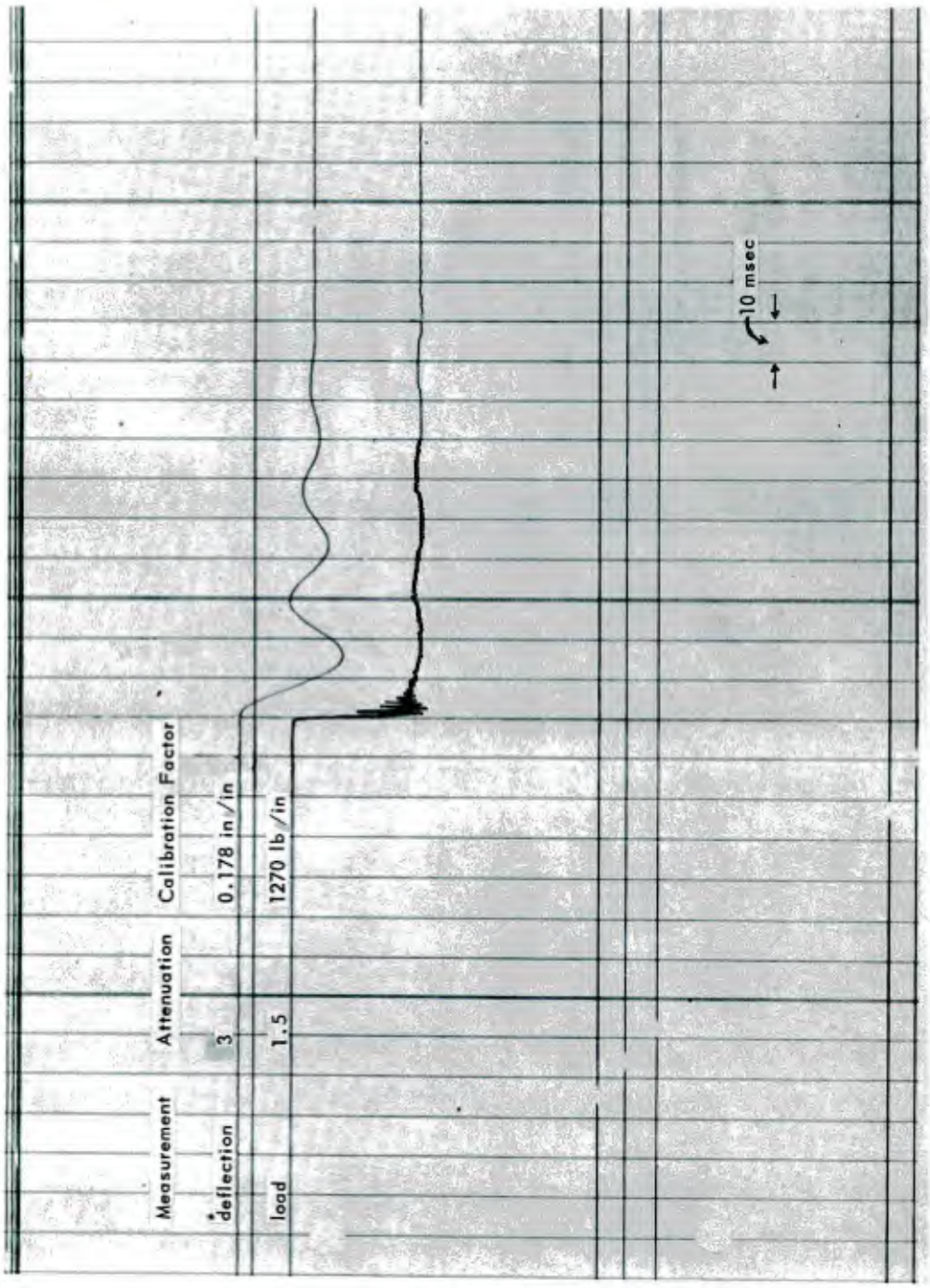

Figure 11. Oscillogram for beam B-15.

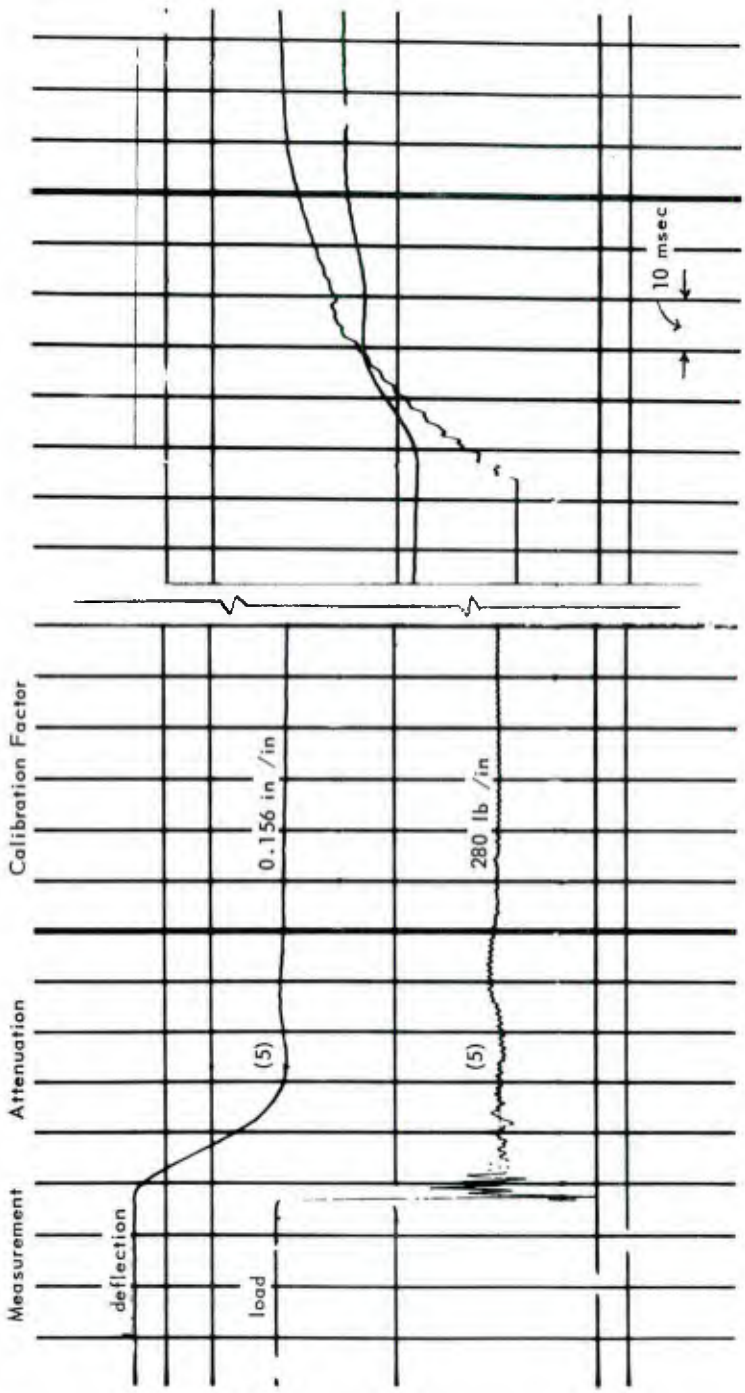

Figure 12. Oscillogram for beam B-26.

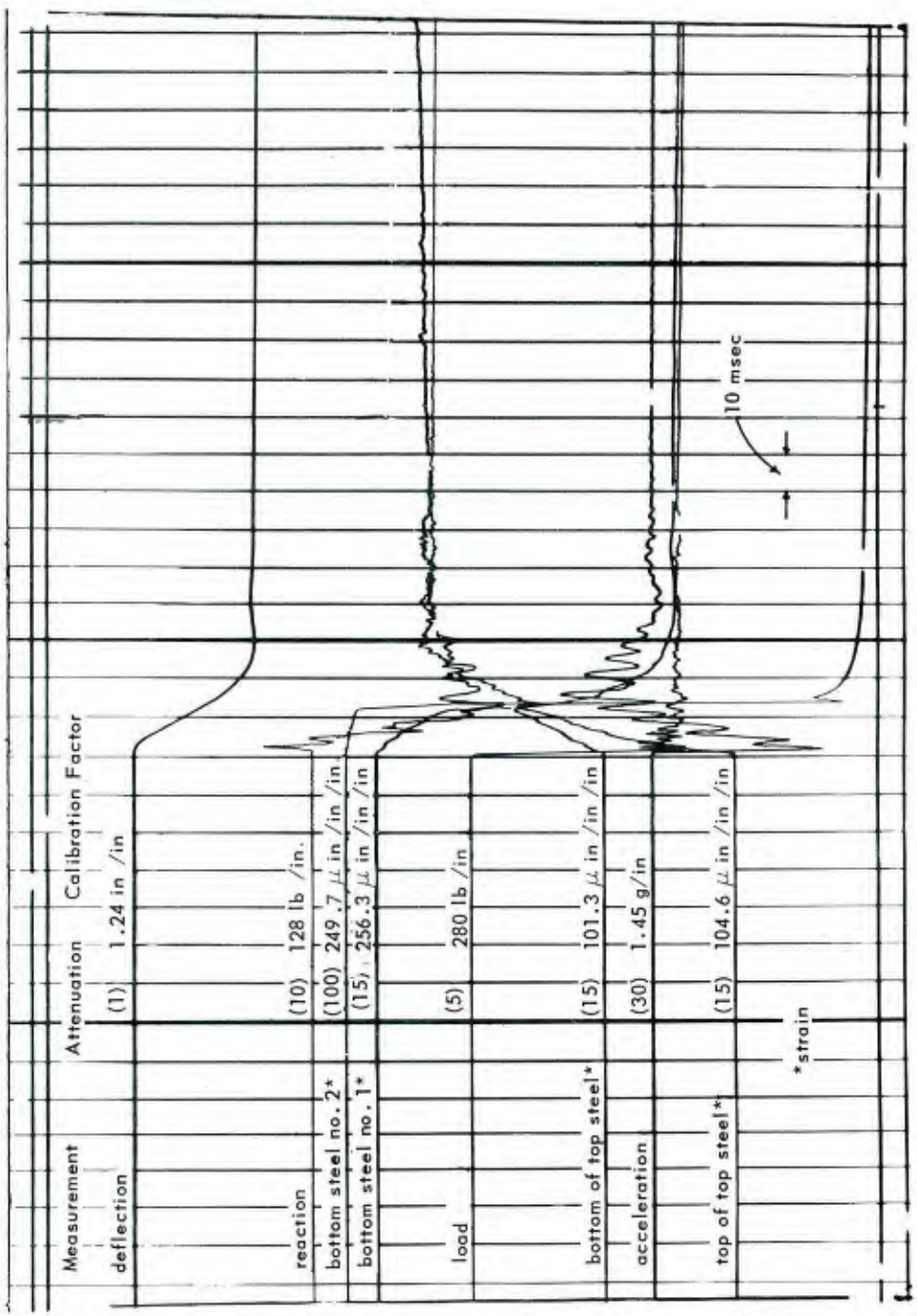

Figure 13. Oscillogram for beam C-4.

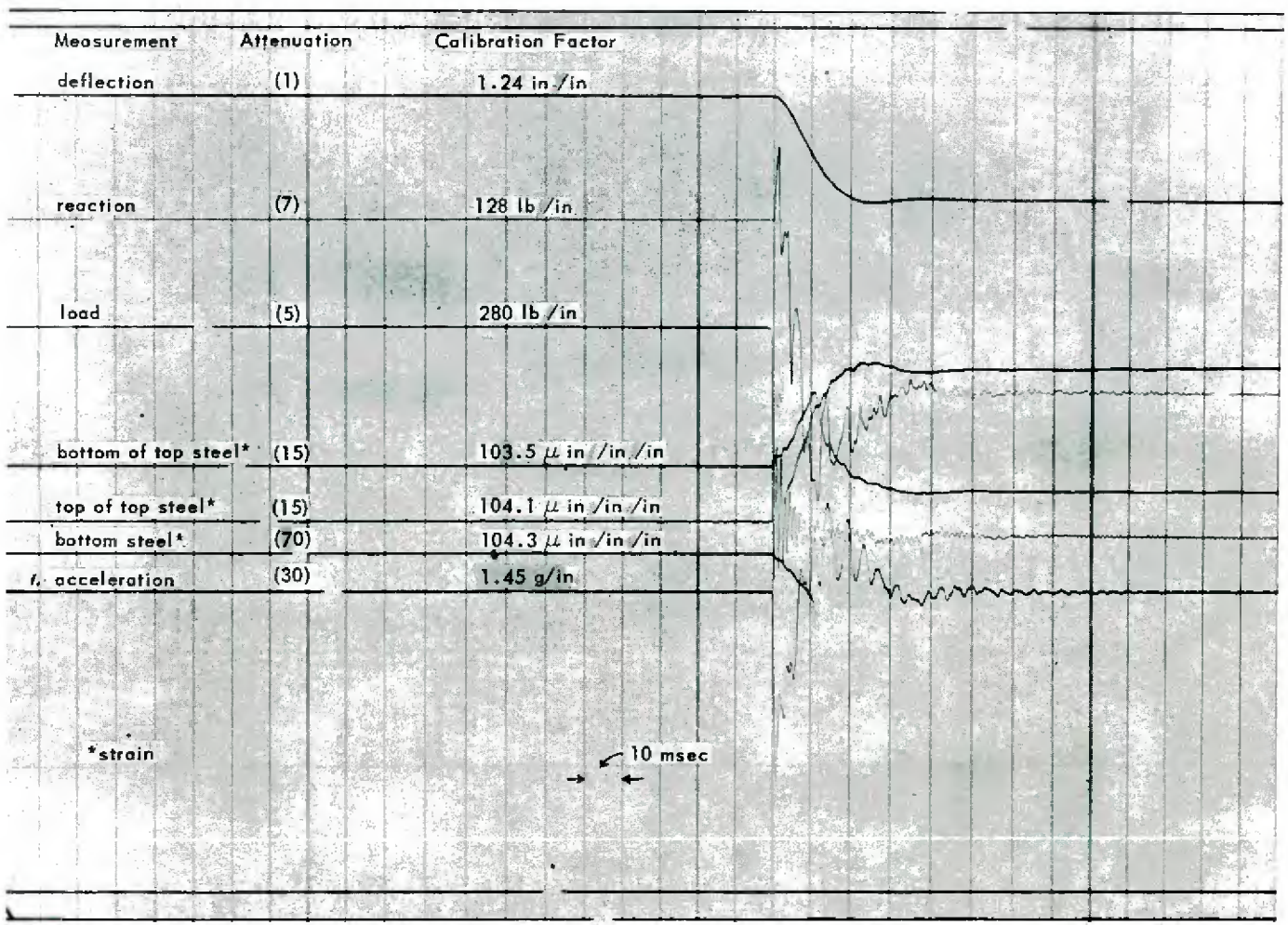

Figure 14. Oscillogram for beam C-5.

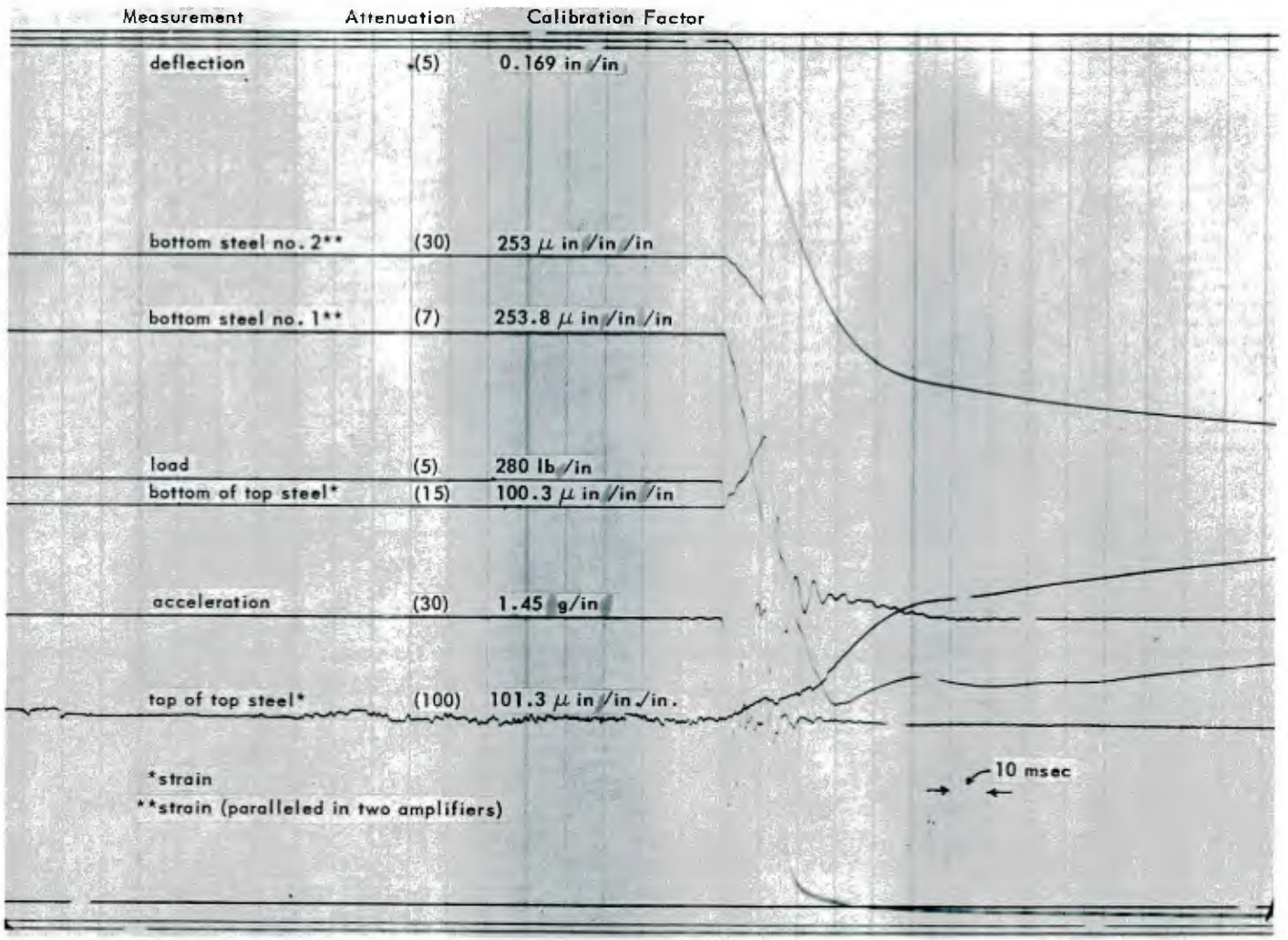

Figure 15. Oscillogram for beam C-9.

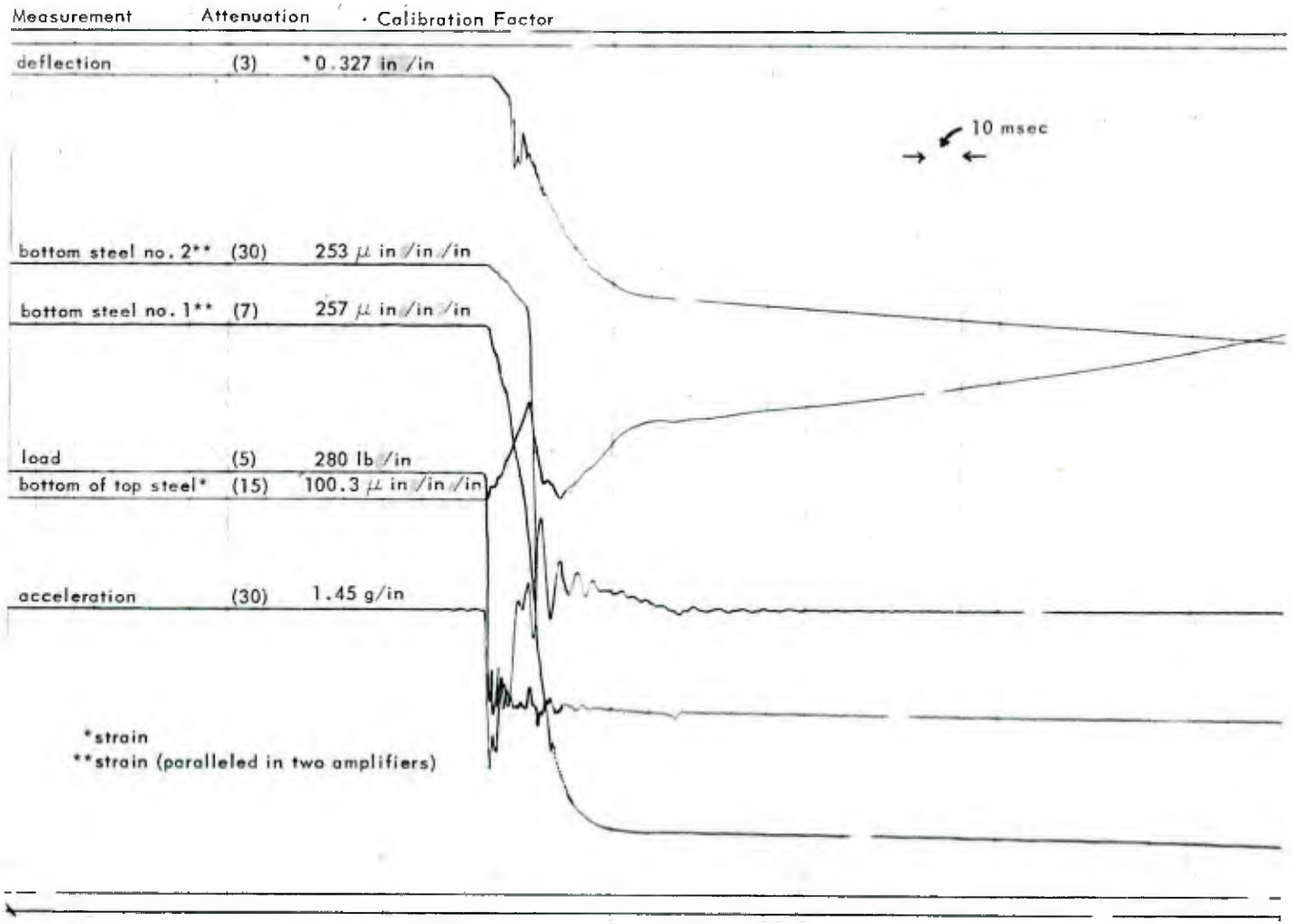

Figure 16. Oscillogram for beam C-12.

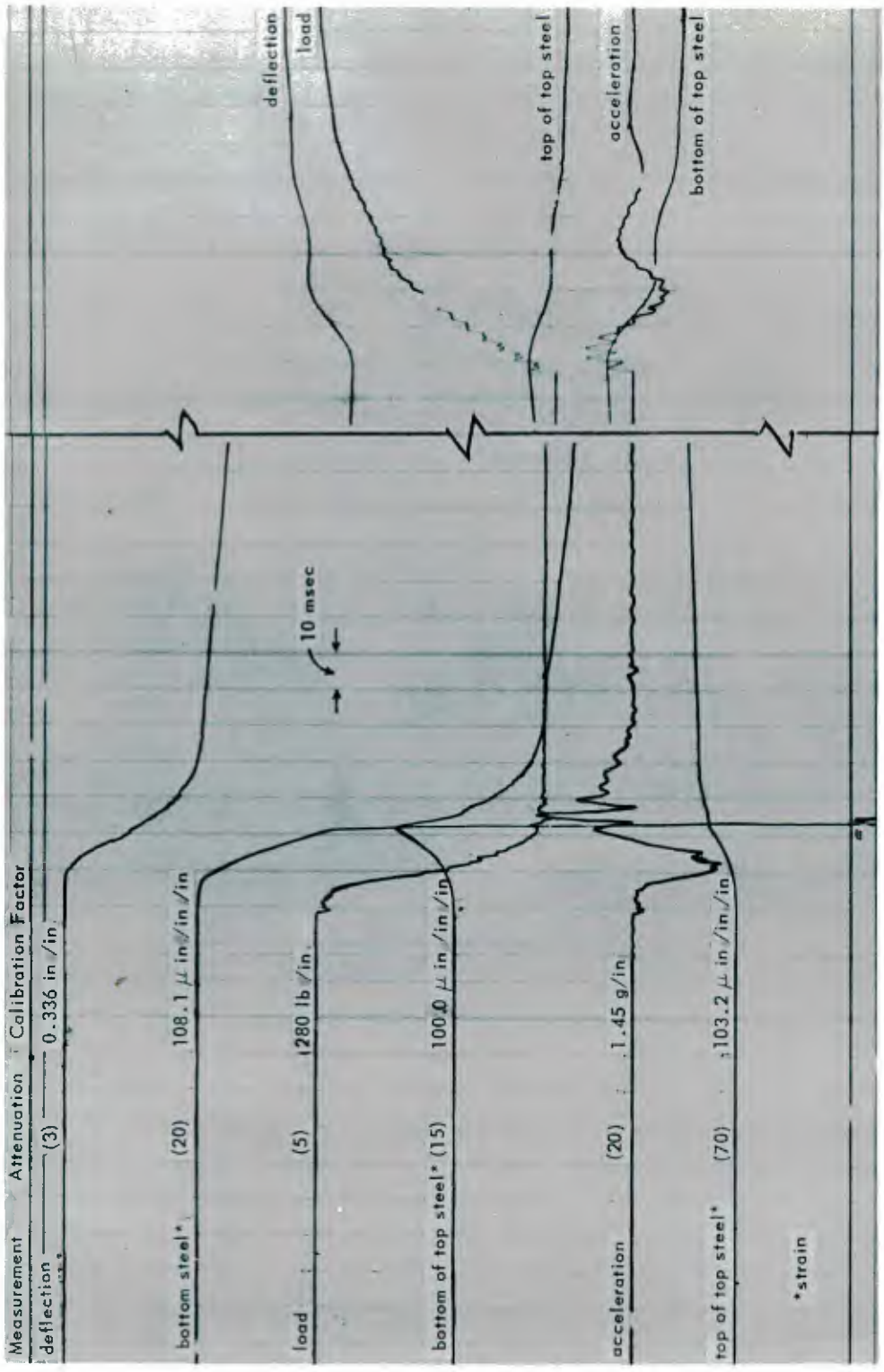

Figure 17. Oscillogram for beam C-14.

Strain records of the tension steel given in figure 13 show that strain increased almost linearly with time until yield. After yield was reached, plastic straining proceeded at a high rate until strain hardening began. The average increase in upper yield point, based on the static lower yield point, was 40 percent. For a discussion of the dynamic properties of steel, see appendix A and reference 5 and 6. Strain records also showed that for dynamic loads of the order of the static yield load, the plastic region was within the middle one-sixth of the beam.

Observation of the compression steel strains revealed that the neutral axis moved upward into the top steel and, generally, remained there. The strain on the bottom of the top bar changed from compression to tension. The top bar underwent bending. This indicates the importance of compression steel in "consolidating and containing" the compression zone. Study is needed to determine how much compression steel should be used with a given amount of tensile steel.

Investigators[1] have found that, in beams having compression steel, the dynamic response of the beams is not appreciably influenced by the strength of the concrete. This was also borne out in this series of tests.

Acceleration was perhaps the most useful measurement for providing new information on beam behavior. As can be seen in figure 13, the acceleration traces contained oscillations of higher frequency (comparable to the third mode) than the fundamental oscillation. If the fundamental oscillation is singled out, it can be used in a simple force-equilibrium study from which the resistance curve, corresponding to that assumed in the spring-mass analogy, may be determined. The details of this procedure are included under "Results versus Theory".

The records show that acceleration (and net inertial force) was in a direction which opposed motion of the beam during the initial 7 msec, then reversed direction to help the load produce deflection.

Deflection traces for various loads are shown in figure 18. Initial peak is referred to as initial maximum deflection. Deflection data necessarily comprised the primary basis for comparison of experiment and theory. The final deflected shape of several typical beams is shown in figures 19 and 20. Data from the oscillograms are presented in tables III and IV.

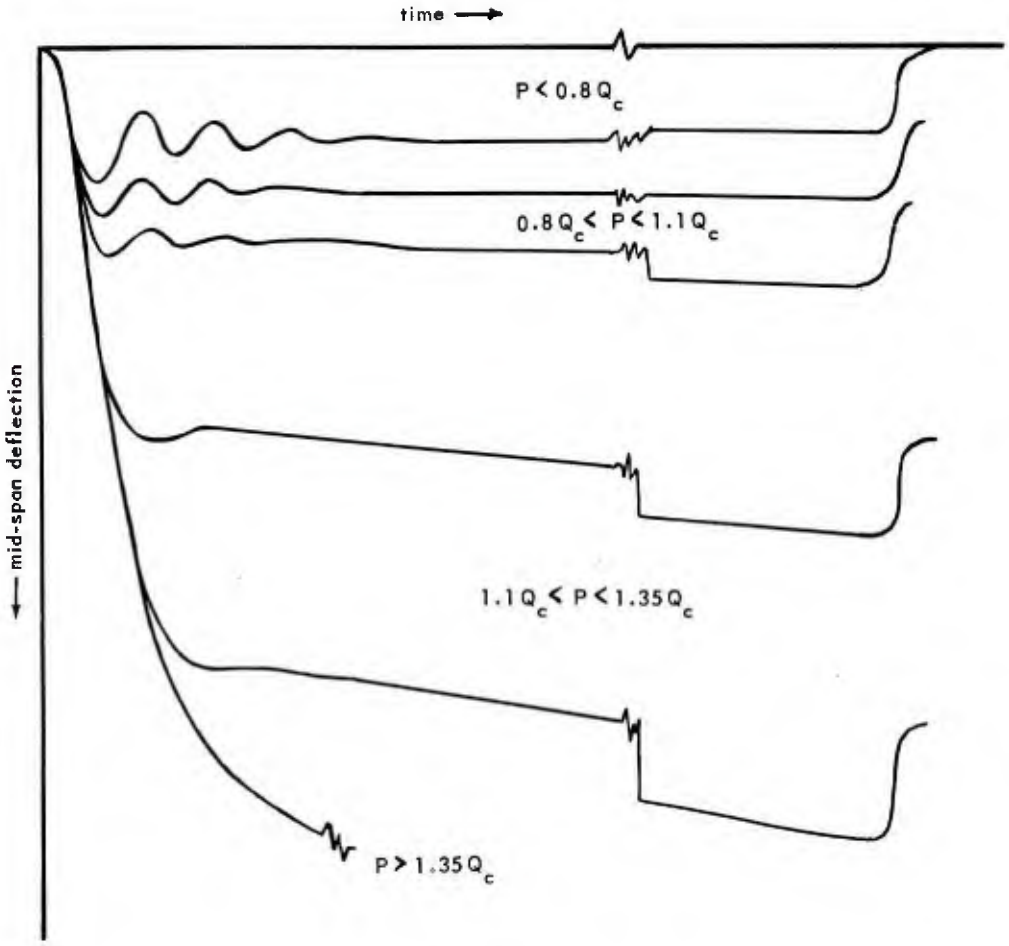

Figure 18. Deflection traces for different loads.

Table III. Summary of Dynamic Test Data (Series B Beams)

	Load			Deflection				
Beam No.	Initial lb	Final lb	Load Duration msec	Initial Maximum Deflection in.	Time to Initial Maximum msec	Final Maximum Deflection msec	Permanent Deflection In.	Rate of Deflection in /sec
B-7	Variable	--	--	1.32	40	2.59	2.14	1.27
B-10	2110	2160	997	--	--	--	--	1.90
B-11	Variable	--	--	1.45	--	--	--	1.42
B-12	2275	2300	1007	1.43	38	2.59	2.09	1.30
B-13	Variable	--	--	1.35	39	2.51	2.09	1.13
B-14-2	2120	2260	977	1.56	35	2.81	2.31	1.33
B-15-2	2195	Short	No Record	1.06	29	2.22	1.81	1.25
B-16-2	2185	2290	969	1.37	31	2.25	1.80	0.87
B-18-2	2160	2260	973	1.38	38	2.39	1.97	1.14
B-19-2	2145	2310	973	1.22	33	2.41	1.97	1.37
B-23	2240	2310	986	1.34	36	2.38	1.95	1.04
B-24	2230	2370	954	1.26	36	2.48	2.03	1.28
B-25	2190	2310	956	1.22	35	2.61	2.19	1.40
B-29	2100	2220	964	0.95	30	2.00	1.60	1.05
Average Values	2175			1.30	35	2.44	2.00	1.27
B-4	1940			0.72	28	1.38	0.99	0.71
B-5	Variable	--	--	0.78	26	1.34	0.96	0.75
B-6	Variable	--	--	0.75	24	1.12	0.75	0.48
B-8	2055	2210	1007	0.76	26	1.36	1.00	0.62
B-9	2085	2210	998	0.69	22	1.01	0.63	0.35
B-20-2	1950	2050	955	0.68	20	1.26	0.89	0.67
B-21	2020			0.78	23	--	--	--
B-26	1975			0.84	26	1.54	1.15	0.73
B-28	1950	2085	954	0.89	28	1.51	1.11	0.63
B-30	2045	2220	952	1.19	34	1.78	1.41	0.84
Average Values	2000			0.81	26	1.37	0.99	0.64
B-14	1685	1790	992	0.47	17	0.30	0	0.47
B-15	1665	1735	982	0.42	16	0.30	0.06	0.42
B-16	1715	1770	970	0.47	16	0.40	0.14	0.47
B-32	1690	1775	970	0.58	19	0.65	0.33	0.58
Average Values	1690			0.49	17	0.41	0.13	0.49
B-18	1205			0.28	15	0.23	0.04	0.28
B-19	1205	1270	984	0.31	16	0.23	0.04	0.31
B-20	1350	1400	942	0.29	15	0.21	0.02	0.29
Average Values	1225			0.29	16	0.22	0.03	0.29

Note: Time-of-rise of load = 1 msec
Load duration = 1 sec

Table IV. Summary of Dynamic Test Da

Beam No.	Load lb	Deflection					Bottom Steel						
		Initial max. defl. in.	Time to initial max. msec	Final max. defl. in.	Perm. defl. in.	Rate of defl. in /sec	Strain at yield μ-in /in	Increase in yield point § percent	Rate of strain in /in /sec	Time to yield msec	Initial max. strain μ-in /in	Final max. strain μ-in /in	Perm. strain μ-in /in
C-40	1650	0.53	18	0.43	0.10	42.7	-	-	-	not instrumented		-	-
C-42	1665	0.53	24	0.31	‡	15.2	2250	31.4	0.126	19	2810	3290	‡
C-44	1650	0.41	18	0.33	0.07	34.9	did not yield		0.125	-	1600	1340	300
Average Values	1655	0.49	20	0.36	0.09	30.9							
C-38	1820	0.54	18	0.56	0.22	49.5	-	-	-	not instrumented		-	-
C-4	2185	1.12	30	1.64	1.18	70.9	2060	20.3	0.188	11	gage failed (excessive strain)		
C-5	2115	0.96	26	1.18	0.79	69.1	2445	42.8	0.244	11	*	*	31,100
Average Values	2150	1.04	28	1.41	0.98	70.0							
C-10	2295	1.24	32	1.85	1.56	64.4	-	-	-	not instrumented		-	-
C-11	2260	1.42	40	2.73	2.28	64.1	-	-	-	not instrumented		-	-
C-13	2295	1.44	40	2.54	1.95	64.8	-	-	-	not instrumented		-	-
Average Values	2285	1.37	37	2.37	1.93	64.4							
C-7	2380	2.23	60	2.54	2.10	72.1	-	-	-	not instrumented		-	-
C-8	2340	2.15	57	3.70	3.52	78.3	2360	37.8	0.289	10	gage failed (excessive strain)		
C-9	2420	2.00	55	3.97	3.41	76.3	2550	49.1	0.233	11	gage failed (excessive strain)		
C-12	2395	1.78	46	2.82	electrical short circuit	68.0	2470	44.3	0.231	10	31,600	38,300	38,000
Average Values	2385	2.04	55	3.26	3.01	73.7							

* Transient measurements exceeded the range of the recording equipment
† + indicates tension strain; - indicates compression strain
‡ Load did not release properly; unable to record valid permanent deflection and strain data
§ Based on static yield strain of 1710 μ-in /in

Note: Time-of-rise of load = 1 msec
Load duration = 0.7 - 0.8 sec

	Top Side of Top Steel				Bottom Side of Top Steel						Acceleration	
Perm. strain μ-in /in	Rate of strain in /in /sec	Initial max. strain μ-in /in	Final max. strain μ-in /in	Perm. strain μ-in /in	Max. Comp. strain μ-in /in	Time to max. comp. strain msec	Initial max. tens. strain μ-in /in	Time to max. tens. strain msec	Final max. strain † μ-in /in	Perm. strain† μ-in /in	Peak pos. value g's	Peak neg. value g's
-	-	not instrumented		-	-	-	not instrumented		-	-	19	23
‡	0.08	1100	950	‡	-	-	not instrumented		-	-	28	22
300	0.06	940	820	100	-	-	not instrumented		-	-	20	16
											22	20
-	-	not instrumented		-	-	-	not instrumented		-	-	33	21
lve strain)	0.172	3750	5560	4930	1010	11	820	38	+1540	+2330	43	30
31,100	0.131	1810	2060	850	860	11	310	36	+ 530	+1380	58	28
											50	29
-	-	not instrumented		-	-	-	not instrumented		-	-	57	27
-	-	not instrumented		-	-	-	not instrumented		-	-	59	28
-	-	not instrumented		-	-	-	not instrumented		-	-	49	26
											55	27
-	-	not instrumented		-	-	-	not instrumented		-	-	71	30
ive strain)	0.175	not instrumented		51,700	-	-	not instrumented		-	-	accelerometer fallure	
ive strain)	0.153	8970	35,300	32,200	770	11	2140	20	†	-9600	57	30
38,000	-	bad gage		-	1090	11	-25	20	†	-4080	59	28
											58	29

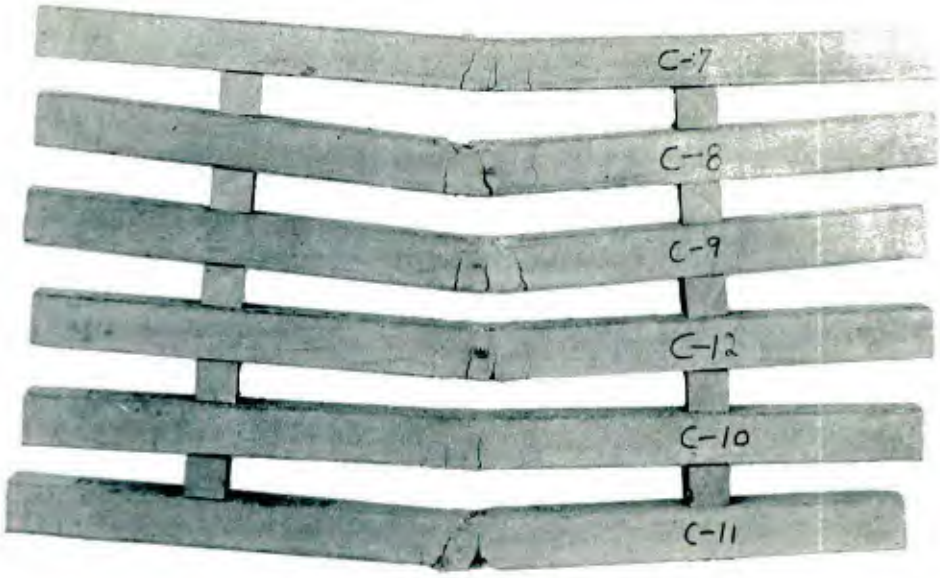

Figure 19. Crack pattern of beams C-7 through C-12.

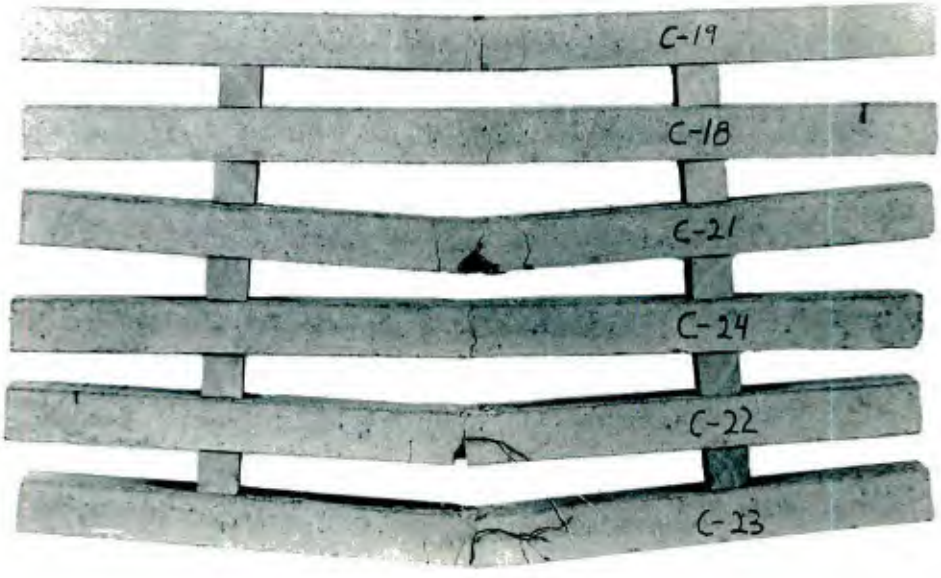

Figure 20. Crack pattern of beams C-18 through C-24.

Response to Load with Rise-Time

If the load has a rise-time which is a significant fraction of the natural period of the beam, the response is markedly changed. An oscillogram for a beam with rise-time of load of 16 msec is given in figure 17. Data taken from this and other similar oscillograms are given in table V. The traces are essentially of the same form as corresponding traces for 1 msec rise-time. However, there is a marked decrease in the magnitude of the high frequency oscillations on the acceleration traces.

THEORY

Load Characteristics

The loading from a nuclear explosion is dependent upon the orientation of the structure. It also depends upon whether the structure is a "diffraction" or a "drag" target.[7]

For many members the actual loading may be approximated by a simple step load. This is generally true if the ratio of the duration of the blast to the natural period of the member is 8 or higher.[8] Such is often the case, especially for high yield weapons.

Since a large number of problems are amenable to analysis by step loading and since a considerable simplification results therefrom, step load and step load with a rise-time (see figure 10) will be the only loadings treated. The methods presented are, incidentally, applicable to other types of loading.

The Spring-mass Analogy

Numerous theories have been developed for predicting the maximum deflection a beam will experience under an imposed dynamic load; in general they may be classified as follows:

1. Rigid-plastic analyses.[9]
2. Equivalent static load approach.[10]
3. Spring-mass analogy.[11]
4. Exact multiple-mode analysis.[12, 13]

Table V. Summary of Dynamic Test Data (Series C Beams)

Beam No.		Load		Deflection					Bottom Steel							Top Side of Top Steel				
		Magnitude lb	Time-of-rise msec	Initial max. defl. in.	Time to initial max. msec	Final max. defl. in.	Perm. defl. in.	Rate of defl. in /sec	Strain at yield μ-in /in	Increase in yield point§ percent	Rate of strain in /in /sec	Time to yield msec	Initial max. strain μ-in/in	Final max. strain μ-in/in	Perm. strain μ-in/in	Rate of strain in /in /sec	Initial max. strain μ-in /in	Final max. strain μ-in /in	Perm. strain μ-in /in	Max. comp. strain μ-in /in
C-21	1	1980	17	0.64	26	0.55	0.18	39.6	-	-	not instrumented		-	-	-	-	not instrumented		-	-
C-22	1	1940	22	0.55	28	0.48	0.14	42.5	2160	26.2	0.111	28	4640	7300	5950	0.08	1290	1100	120	690
C-24	1	2030	18	0.56	26	0.50	0.15	43.9	-	-	not instrumented		-	-	-	-	not instrumented		-	-
Average Values		1980	19	0.58	27	0.51	0.16	42.0												
C-17	1	2320	20	0.70	28	1.03	0.68	43.6	2360	37.9	0.170	23	gage failed (excessive strain)			0.08	1650	2550	1150	670
C-18	1	2340	18	0.69	32	0.79	0.42	43.6	-	-	not instrumented		-	-	-	-	not instrumented		-	-
C-20	1	2260	20	0.80	36	1.14	0.74	37.7	2290	33.8	0.164	24	gage failed (excessive strain)			0.11	1590	2320	870	720
C-24	2	2320	20	0.69	33	1.00	0.55	43.5	-	-	not instrumented		-	-	-	-	not instrumented		-	-
C-30	1	2300	21	0.58	26	0.89	0.49	36.5	-	-	not instrumented		-	-	-	-	not instrumented		-	-
C-35	1	2300	23	0.55	27	0.97	0.57	35.3	2250	31.5	0.111	30	*	*	22,800	0.06	1050	1140	40	710
C-35	2	2300	23	0.51	26	0.84	0.41	33.4	2340	36.8	0.173	21	4080	3970	1630	0.12	1340	1510	250	620
Average Values		2310	21	0.65	30	0.95	0.55	39.1												
C-22	2	2380	15	1.13#	46	2.73	2.21	51.5	2380	39.0	0.307	15	gage failed (excessive strain)			0.12	3230	27,900	22,800	740
C-29	1	2420	18	0.59	24	1.28	0.86	42.2	-	-	not instrumented		-	-	-	-	not instrumented		-	-
C-32	1	2340	21	0.56	26	0.94	0.51	44.7	2185	27.8	0.122	27	gage failed (excessive strain)			0.14	2640	1850	310	1260
Average Values		2380	18	0.76	32	1.65	1.19	46.1												
C-14	1	2470	16	1.07	47	2.24	1.73	47.9	2400	40.2	0.192	19	gage failed (excessive strain)			0.11	2060	11,700	9390	680
C-15	1	2430	15	1.23	45	2.45	1.96	58.2	-	-	not instrumented		-	-	-	-	not instrumented		-	-
C-16	1	2430	17	0.92	54	2.35	1.83	40.0	2440	42.5	0.197	20	gage failed (excessive strain)			0.10	2700	8670	6580	590
C-19	1	2460	19	1.14	44	1.33	0.95	47.6	-	-	not instrumented		-	-	-	-	not instrumented		-	-
C-26	1	2440	14	1.16	58	2.99	2.47	47.2	2460	43.7	0.187	19	gage failed (excessive strain)			0.20	2600	12,100	11,600	750
Average Values		2450	16	1.10	50	2.27	1.79	48.2												
C-34	1	2080	31	0.44	31	0.41	0.09	27.1	-	-	not instrumented		-	-	-	-	not instrumented		-	-
C-34	2	2110	26	0.38	26	0.35	0.01	27.4	-	-	not instrumented		-	-	-	-	not instrumented		-	-
C-36	2	2070	26	0.39	24	0.35	0.01	30.0	-	-	not instrumented		-	-	-	-	not instrumented		-	-
C-39	1	2140	30	0.42	24	0.40	0.10	16.0	-	-	not instrumented		-	-	-	-	not instrumented		-	-
C-39	2	2090	31	0.36	30	0.33	0.01	24.0	-	-	not instrumented		-	-	-	-	not instrumented		-	-
Average Values		2100	29	0.40	27	0.37	0.04	24.9												
C-33	1	2280	30	0.52	31	0.80	0.43	31.5	did not exhibit dynamic yield		0.131	-	2320	17,600	16,200	0.06	970	1160	140	560
C-39	3	2390	29	0.43	28	0.85	0.46	30.9	-	-	not instrumented		-	-	-	-	not instrumented		-	-
Average Values		2340	30	0.48	30	0.83	0.45	31.2												
C-27	1	2510	25	0.81#	45	2.04	1.60	42.6	-	-	not instrumented		-	-	-	-	not instrumented		-	-
C-33	2	2510	22	0.66#	32	2.24	‡	37.5	2320	35.7	0.209	18	11,500#	20,100	‡	0.09	1190	6490	‡	670
C-34	3	2600	23	0.52	27	2.15	1.66	37.0	-	-	not instrumented		-	-	-	-	not instrumented		-	-
C-36	3	2510	25	0.57#	32	2.53	2.02	37.9	-	-	not instrumented		-	-	-	-	not instrumented		-	-
Average Values		2530	24	0.64	34	2.24	1.76	38.8												

* Transient measurements exceeded the range of the recording equipment
+ - indicates tension strain; - indicates compression strain
‡ Load did not release properly; unable to record valid permanent deflection and strain data
§ Based on static yield strain of 1710 μ-in. in
# Beam continued deflecting

Note: Load duration = 0.7 - 0.9 sec

Summary of Dynamic Test Data (Series C Beams)

Bottom Steel				Top Side of Top Steel				Bottom Side of Top Steel						Acceleration	
Time to yield msec	Initial max. strain μ-in/in	Final max. strain μ-in/in	Perm. strain μ-in/in	Rate of strain in /in /sec	Initial max. strain μ-in /in	Final max. strain μ-in /in	Perm. strain μ-in /in	Max. comp. strain μ-in /in	Time to max. comp. strain msec	Initial max. tens. strain μ-in /in	Time to max. tens. strain msec	Final max. strain † μ-in /in	Perm. strain † μ-in /in	Peak pos. value g's	Peak neg. value g's
instrumented	-	-	-	-	not instrumented		-	-	-	not instrumented		-	-	15	16
28	4640	7300	5950	0.08	1290	1100	120	690	28	compression only		-460	+180	13	19
instrumented	-	-	-	-	not instrumented		-	-	-	not instrumented		-	-	13	19
														14	18
23	gage failed (excessive strain)			0.08	1650	2550	1150	670	22	60	47	+370	+1240	17	17
instrumented	-	-	-	-	not instrumented		-	-	-	not instrumented		-	-	accelerometer failure	
24	gage failed (excessive strain)			0.11	1590	2320	870	720	24	70	50	+580	+1780	19	18
instrumented	-	-	-	-	not instrumented		-	-	-	not instrumented		-	-	17	13
instrumented	-	-	-	-	not instrumented		-	-	-	not instrumented		-	-	13	14
30	*	*	22,800	0.06	1050	1140	40	710	27	compression only		+500	+1250	10	13
21	4080	3970	1630	0.12	1340	1510	250	620	22	compression only		-380	+440	12	12
														15	15
15	gage failed (excessive strain)			0.12	3230	27,900	22,800	740	15	600	50	-3150	-1210	20	13
instrumented	-	-	-	-	not instrumented		-	-	-	not instrumented		-	-	13	15
27	gage failed (excessive strain)			0.14	2640	1850	310	1260	24	compression only		-360	+580	12	14
														15	14
19	gage failed (excessive strain)			0.11	2060	11,700	9390	680	21	1950	358	+1950	+2780	20	21
instrumented	-	-	-	-	not instrumented		-	-	-	not instrumented		-	-	19	27
20	gage failed (excessive strain)			0.10	2700	8670	6580	590	20	2480	199	+2160	+2960	18	24
instrumented	-	-	-	-	not instrumented		-	-	-	not instrumented		-	-	18	25
19	gage failed (excessive strain)			0.20	2600	12,100	11,600	750	19	450	99	‡	-4600	18	18
														19	23
instrumented	-	-	-	-	not instrumented		-	-	-	not instrumented		-	-	8	11
instrumented	-	-	-	-	not instrumented		-	-	-	not instrumented		-	-	9	12
instrumented	-	-	-	-	not instrumented		-	-	-	not instrumented		-	-	10	12
instrumented	-	-	-	-	not instrumented		-	-	-	not instrumented		-	-	8	10
instrumented	-	-	-	-	not instrumented		-	-	-	not instrumented		-	-	8	11
														9	11
-	2320	17,600	16,200	0.06	970	1160	140	560	28	compression only		+460	+1020	10	12
instrumented	-	-	-	-	not instrumented		-	-	-	not instrumented		-	-	10	13
														10	13
instrumented	-	-	-	-	not instrumented		-	-	-	not instrumented		-	-	11	12
18	11,500#	20,100	‡	0.09	1190	6490	‡	670	19	1280	332	+950	‡	13	12
instrumented	-	-	-	-	not instrumented		-	-	-	not instrumented		-	-	13	14
instrumented	-	-	-	-	not instrumented		-	-	-	not instrumented		-	-	14	14
														13	13

An exact analytical treatment becomes lengthy and involved. Hence, one of the other methods is better to use in interpreting the experimental behavior of beams. The spring-mass analogy seems to offer the most promise for physical interpretation throughout the range of beam behavior. Consequently, that theory is used in this paper.

As a further simplification, the discussion assumes symmetry of load, beam, and support conditions with respect to the transverse center line of the beam. Violation of these conditions might alter the response significantly.

The spring-mass analogy is based on the observation that under load the mid-span deflection of a beam describes a path similar to

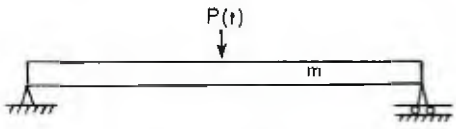

(a) The beam.

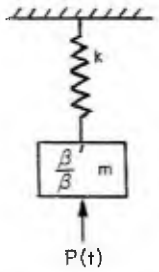

(b) The model.

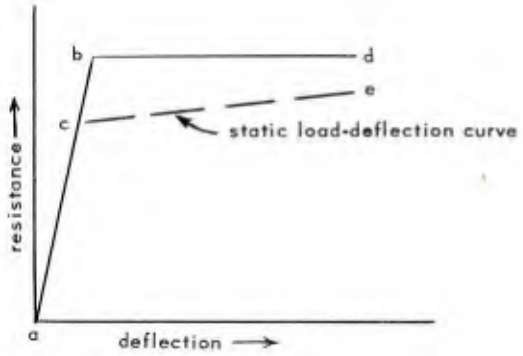

(c) The resistance curve.

Figure 21. The beam and its equivalent system.

that of the spring-mass system. As shown in figure 21, (a), (b), and (c), the model has an equivalent mass and is subjected to the same load as

the beam. The equivalency ratio $\frac{\beta'}{\beta}$ is developed in appendix B. It is shown that a value of 0.769 can be adopted for all beams if the stiffness is taken as the mid-span stiffness due to a uniformly distributed load. In fact, for step loads, mass (and hence the equivalency ratio) has no influence on maximum deflection (see appendix C).

Past practice has been to establish the resistance of the model from the static load-deflection characteristics of the beam. This is done by increasing the static yield point an amount dependent upon the strain rate which can be estimated by the method given in appendix D. The percent increase in yield point subsequently is determined from appendix A (figure 36). The plastic range stiffness is considered small enough that any increase in resistance therefrom may be neglected. Thus, the familiar "flat-topped" resistance curve of figure 21 is obtained with which a dynamic analysis can be readily made.

The resistance of a beam of partial fixity is determined by the method of appendix E.

For a step load the equation of motion of the equivalent system may be expressed as

$$m_e \frac{d^2y}{dt^2} = P - Q = I \qquad (1)$$

Equivalent mass times acceleration is given as inertial force (I). The simple relation of equation 1 is used here as a basis for determining the experimental resistance. It should be noted that the discontinuous resistance results in a non-linear problem.

The problem represented by equation 1 has been solved[14] using the non-linear resistance of figure 21, and is plotted in non-dimensional form in figure 40. The theory presented in appendix C is used to develop the curves of figure 40. Solutions are available for various ratios of plastic to elastic stiffness;[14] however, only the curve for a stiffness ratio equal to zero (zero plastic slope) is given. From this curve it is easy to determine initial maximum deflection (y_m). Only the dynamic yield load (Q_b) and deflection (y_b), and the applied load need be known (see the example of appendix F). The curve of figure 40 shows that the initial maximum deflection varies with static yield load and deflection. As previously noted, for a step load, mass has no influence on the initial maximum deflection which will be reached, although it does govern the frequency and hence the time to initial maximum deflection.

A numerical example demonstrating the use of the theory is given in appendix F. A one-way panel is selected for the roof of a warehouse based on the criteria established in the following section and a megaton bomb loading of 4.5 psi. The panel is assumed to be 80 percent fixed, which requires that a modified elastic slope be used as given in appendix E.

Equations for determining the response to a load with a rise-time are developed in appendix G and the solutions are plotted in figures 45 and 46. The relations do not include damping, yet the development is quite involved. A much simpler solution is obtained by graphical methods as is demonstrated in appendix H.

RESULTS VERSUS THEORY

In considering the theory several questions arise. How good an approximation to actual behavior is the motion of the model? What are the load-deflection characteristics? What is the form of an actual resistance curve? What is the influence of damping? Can shear be estimated accurately? What is the relative influence of rise-time? Answers to these queries are sought in the study which follows.

Response to Step Loading

The experimental and theoretical load versus the initial maximum deflection is shown in figures 22 and 23. From these results it appears that deflections may be predicted with an error of less than 25 percent even for the relatively crude assumptions of constant increase in yield point, zero damping, and a plastic to elastic stiffness ratio of zero.

Better agreement between theory and experiment can be obtained by using the correct increase in yield point corresponding to the applied load, by including elastic damping, and using a rounded resistance. Including damping shifts the theoretical curve to the left on the load-deflection curve (figure 22). Rounding of the resistance curve, approximating the actual plot, increases the curvature and lowers the theoretical curve at high loads ($P=1.1Q_c$).

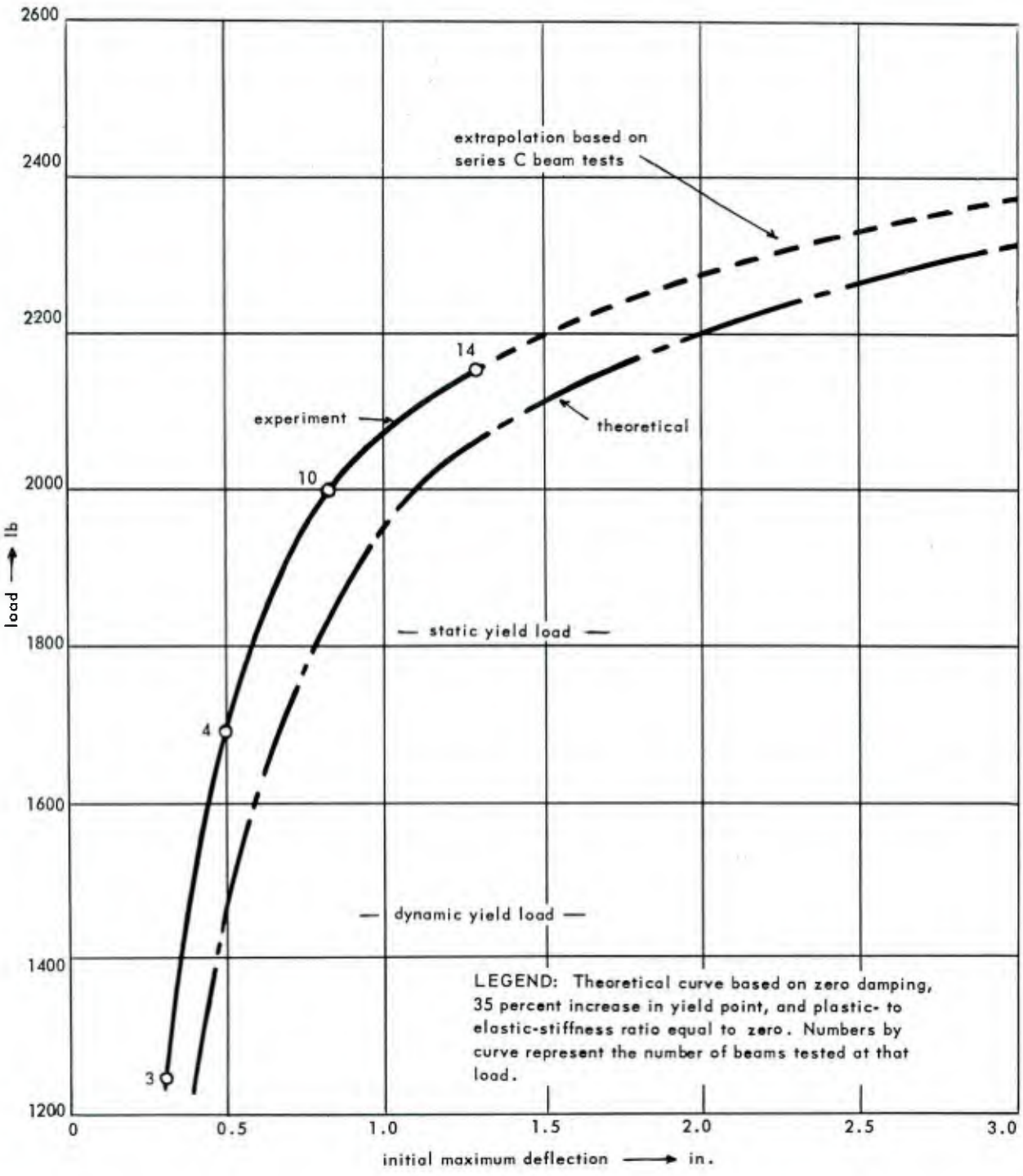

Figure 22. Load-deflection curves for series B beams.

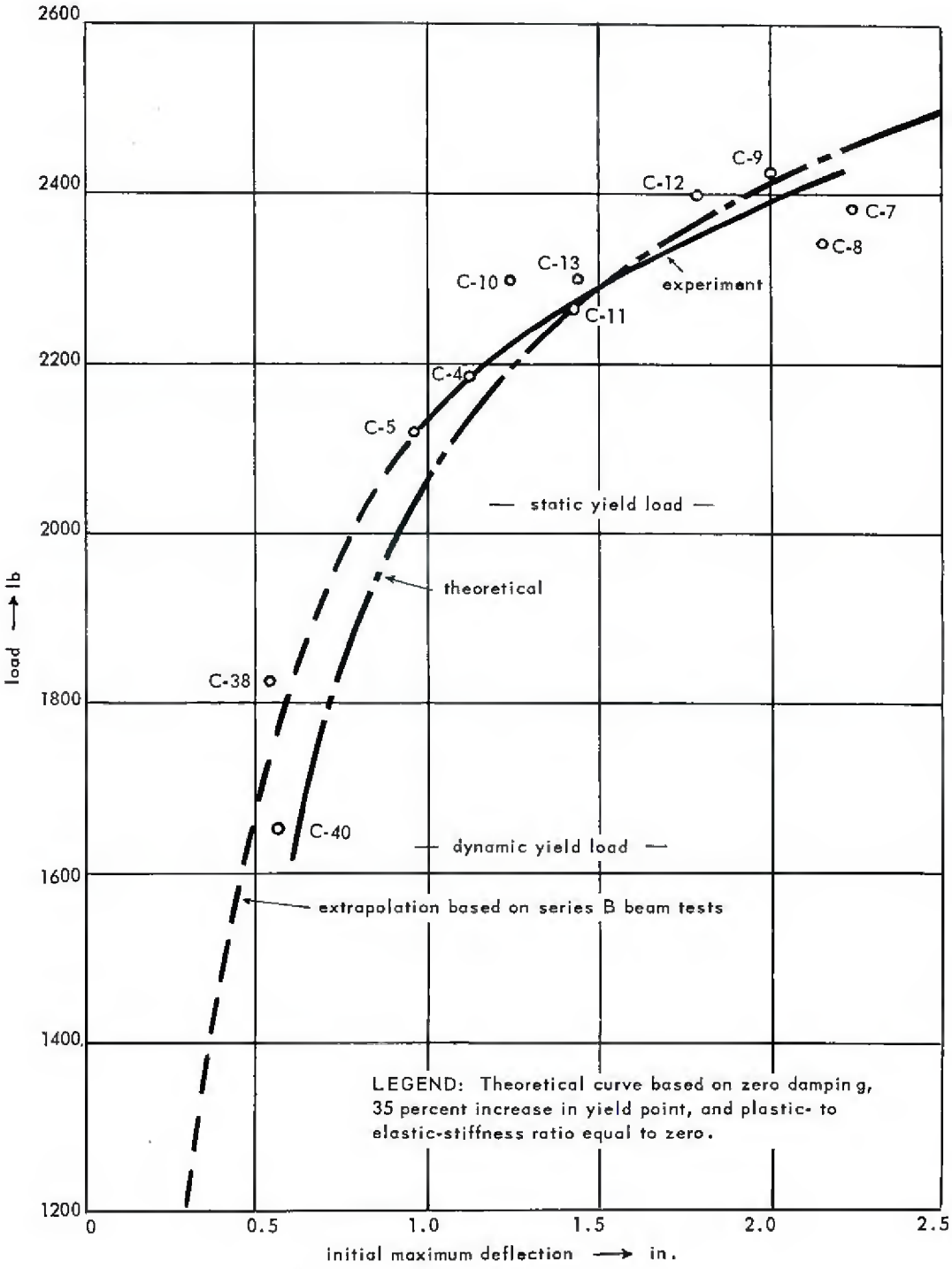

Figure 23. Load-deflection curves for series C beams.

Denoting the static yield point by Q_c, for a step-load the dependence of behavior on load may be stated as follows:

1. $0 < P < 0.8Q_c$ The beam remains elastic.

2. $0.8Q_c \leq P < 1.1Q_c$ The beam goes plastic, eventually reaching a state of equilibrium; the final maximum deflection may or may not be larger than the initial maximum deflection depending on the duration of the load and whether P is greater or less than Q_c.

3. $1.1Q_c \leq P < 1.35Q_c$ The beam reaches an initial maximum deflection, recovers slightly, then continues deflecting to values greater than the initial maximum. Deflection continues at a rate dependent upon the load until the load is released.

4. $1.35Q_c < P$ The beam does not experience an initial maximum deflection, but continues deflecting until the load is released or until the ultimate deflection is reached.

From the above classification it would appear that a load of $1.1Q_c$ is a reasonable criteria for design against loads from megaton weapons. As may be determined from appendix C, figure 40, assuming a 35 percent increase in yield stress, the load criteria of $1.1Q_c$ requires that the ultimate deflection of the beam be at least 2.75 (1.35) = 3.71 times the static yield deflection. Obviously it would be preferable to have the ratio of the ultimate deflection to static yield deflection several times the 3.71 value.

Arbitrarily using the load condition $P = 1.35Q_c$ and the experimental dynamic yield load as criteria, the gain in capacity from plastic action may be determined as

$$\frac{1.35 - 0.8}{0.8} \quad (100) = 70 \text{ percent} \qquad (2)$$

The value of 0.8 is determined from the ratio of the increase in yield strain to the strain magnification in the tensile steel (strain magnification is the amount by which strain is increased under dynamic loading above the corresponding strain which would be produced by a static load of the same magnitude).

A much greater increase in load capacity from plastic action is possible for rapidly decaying loads. An inclusive percent increase cannot be given, however, because it depends upon such parameters as the ratio of the decay time to the natural frequency of the particular member under consideration. Each case must be considered separately.

Determination of Experimental Resistance

Actual resistance may be determined by using the experimental acceleration and load in equation 1. For this purpose the high frequency oscillations are ignored. Using an equivalent mass equal to one-half the actual mass, resistance was plotted versus time for several beams which were subjected to different applied loads (see figure 24). These curves show that for a step load, the time to peak resistance and the magnitude of that resistance is independent of the magnitude of the load. It is significant to observe that the stress corresponding to peak resistance is well above the level for which a significant time-delay-to-yield would be possible.

To investigate further the increased resistance from plastic action, resistance was plotted versus deflection for several beams (shown in figures 25 through 31). These curves are compared with the corresponding theoretical curve. An increased rounding of the resistance curves occurs with successively larger loads which also increases the rate of deflection in the final stages of behavior (shown in figure 32). If better accuracy is required than that provided by the simplified resistance curve, figure 21 (c), a time and velocity dependent resistance relation should be used.

Damping

For the beams tested the elastic damping was 6 percent. Its primary influence was reduction of velocity at yield. A maximum reduction of 10 percent was experienced from 6 percent damping. Multiplying the damping constant by the maximum velocity gave the maximum force from damping. For beam C-4 this force was 12 percent of static yield load.

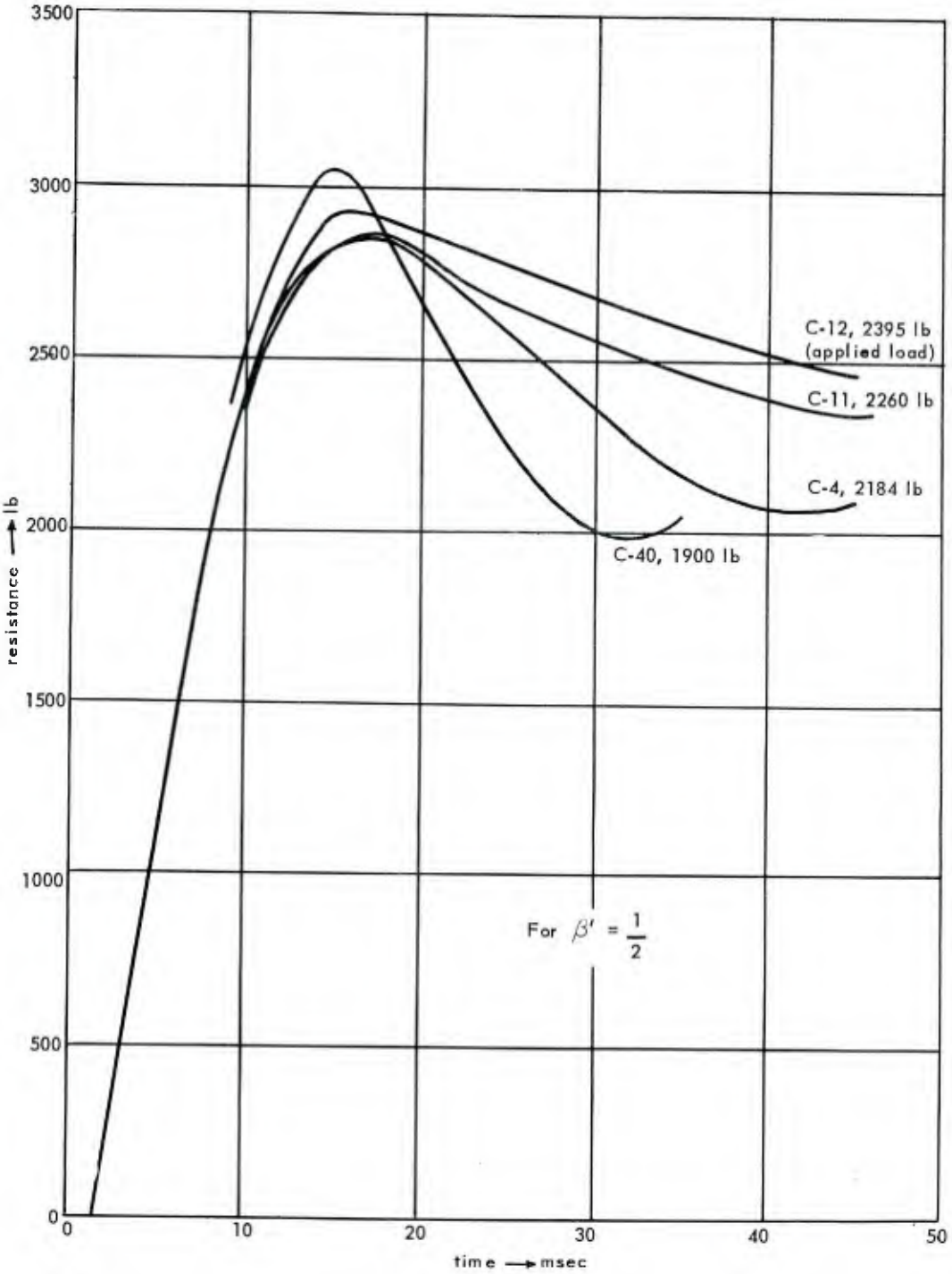

Figure 24. Composite plot of resistance time curves.

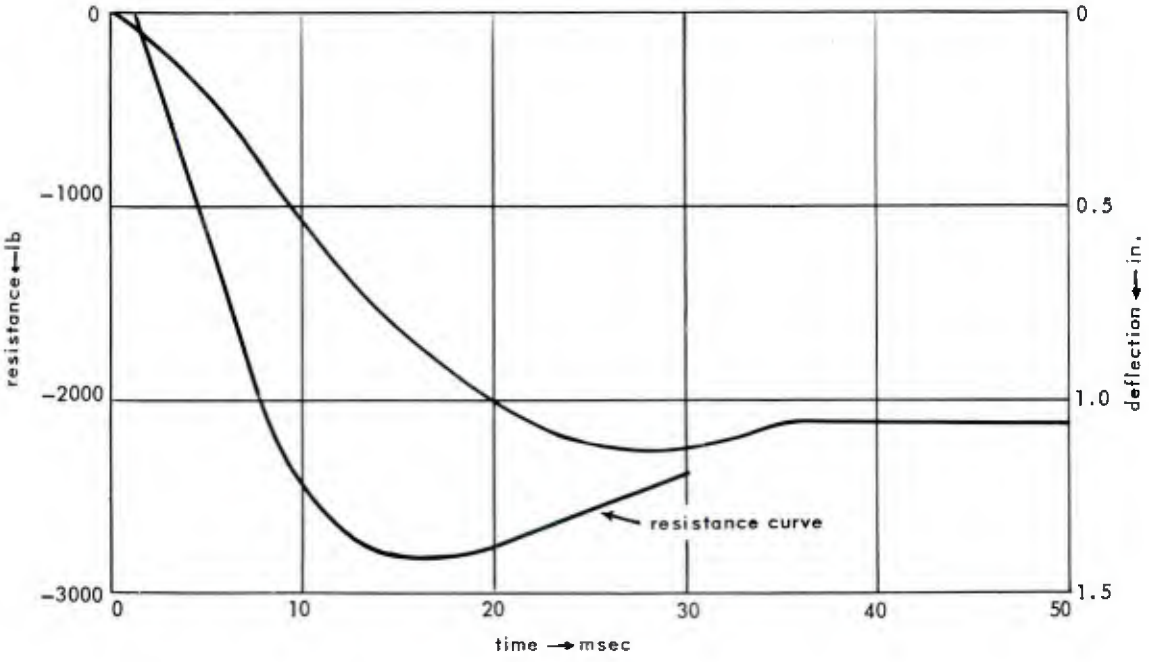

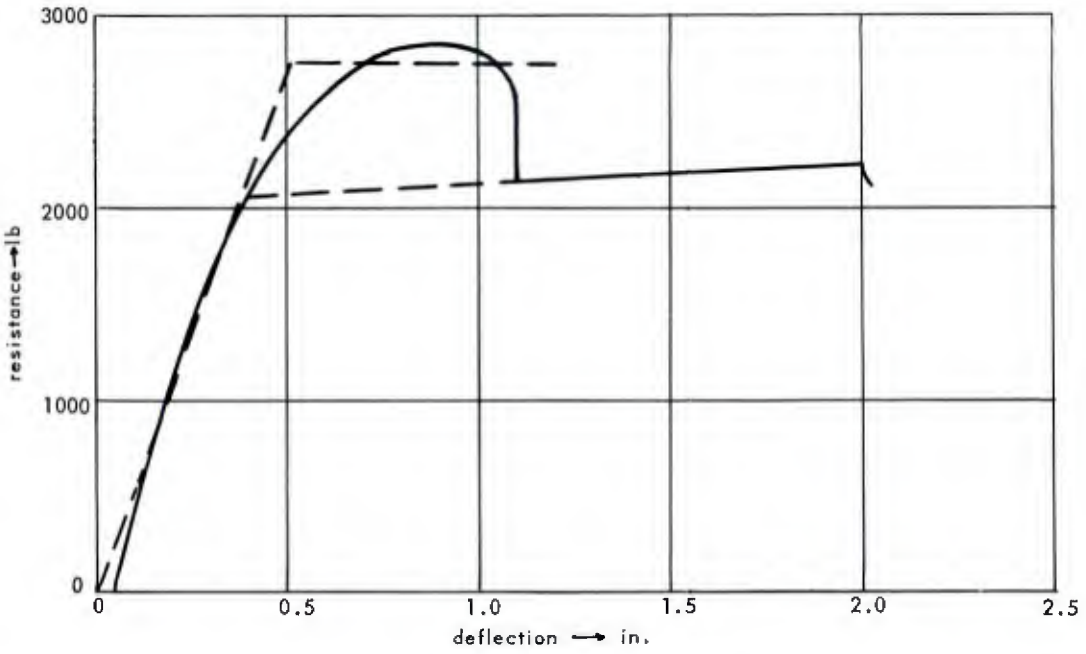

Figure 25. Resistance curve, beam C-4.

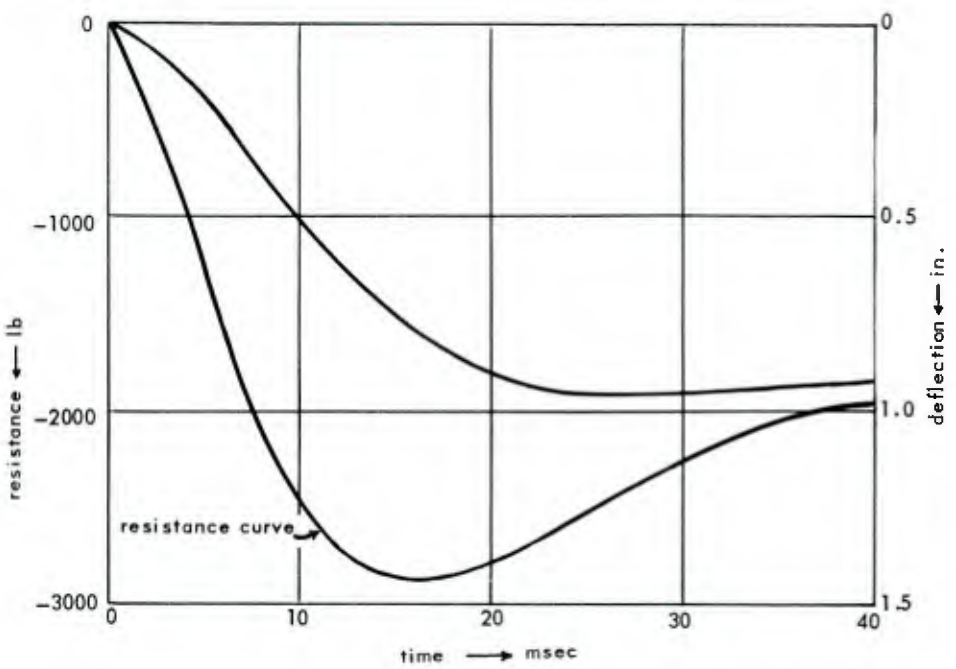

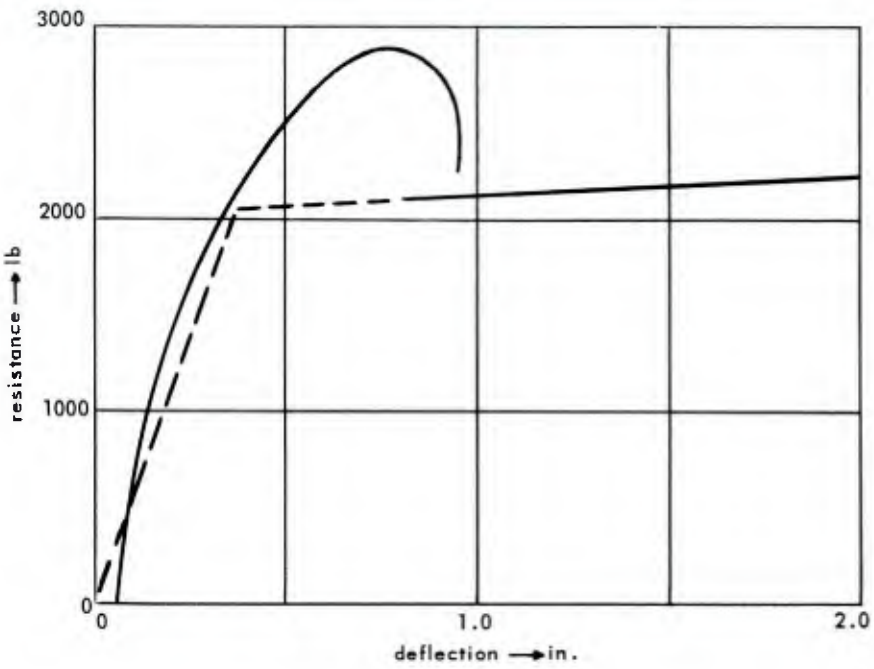

Figure 26. Resistance curve, beam C-5.

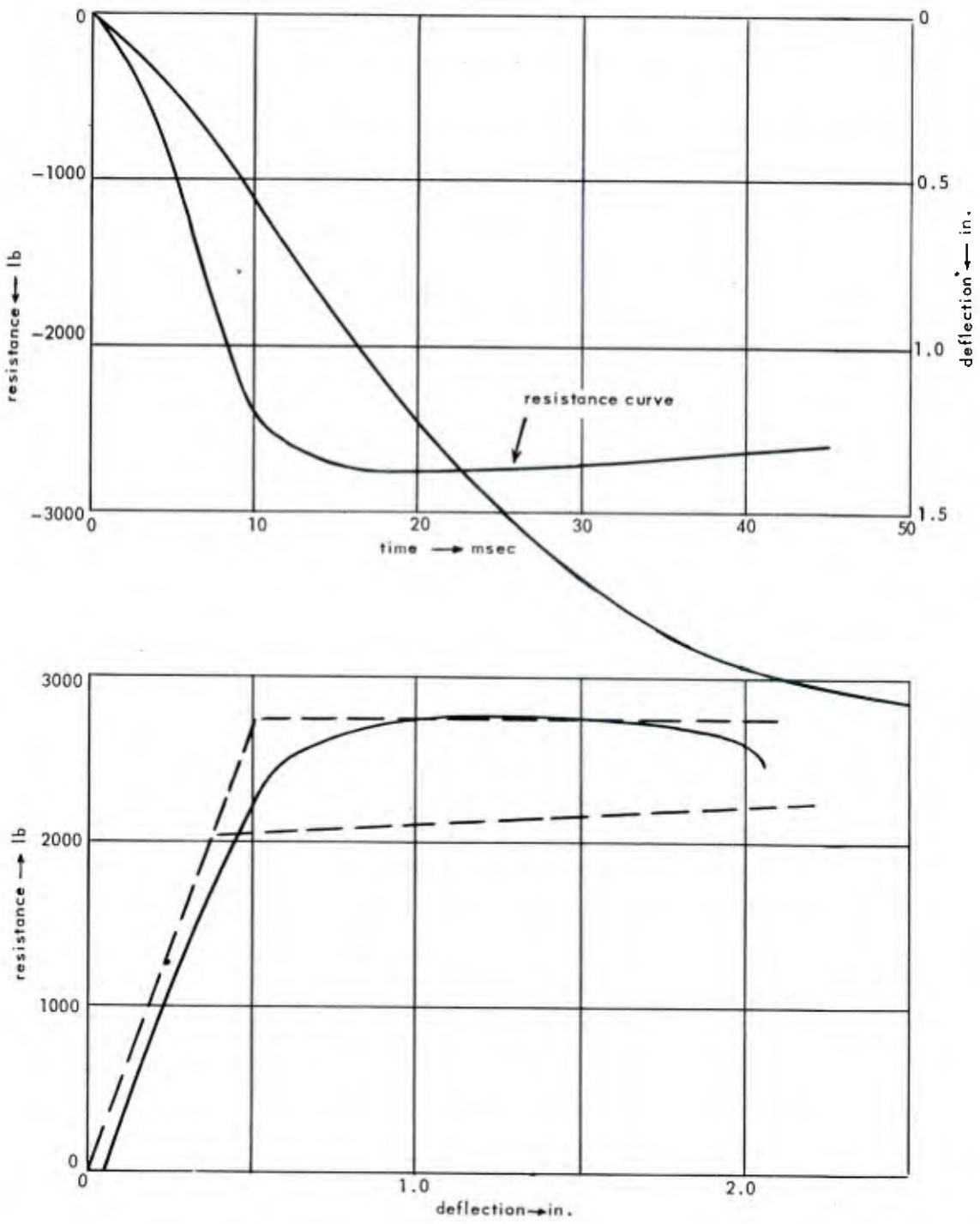

Figure 27. Resistance curve, beam C-9.

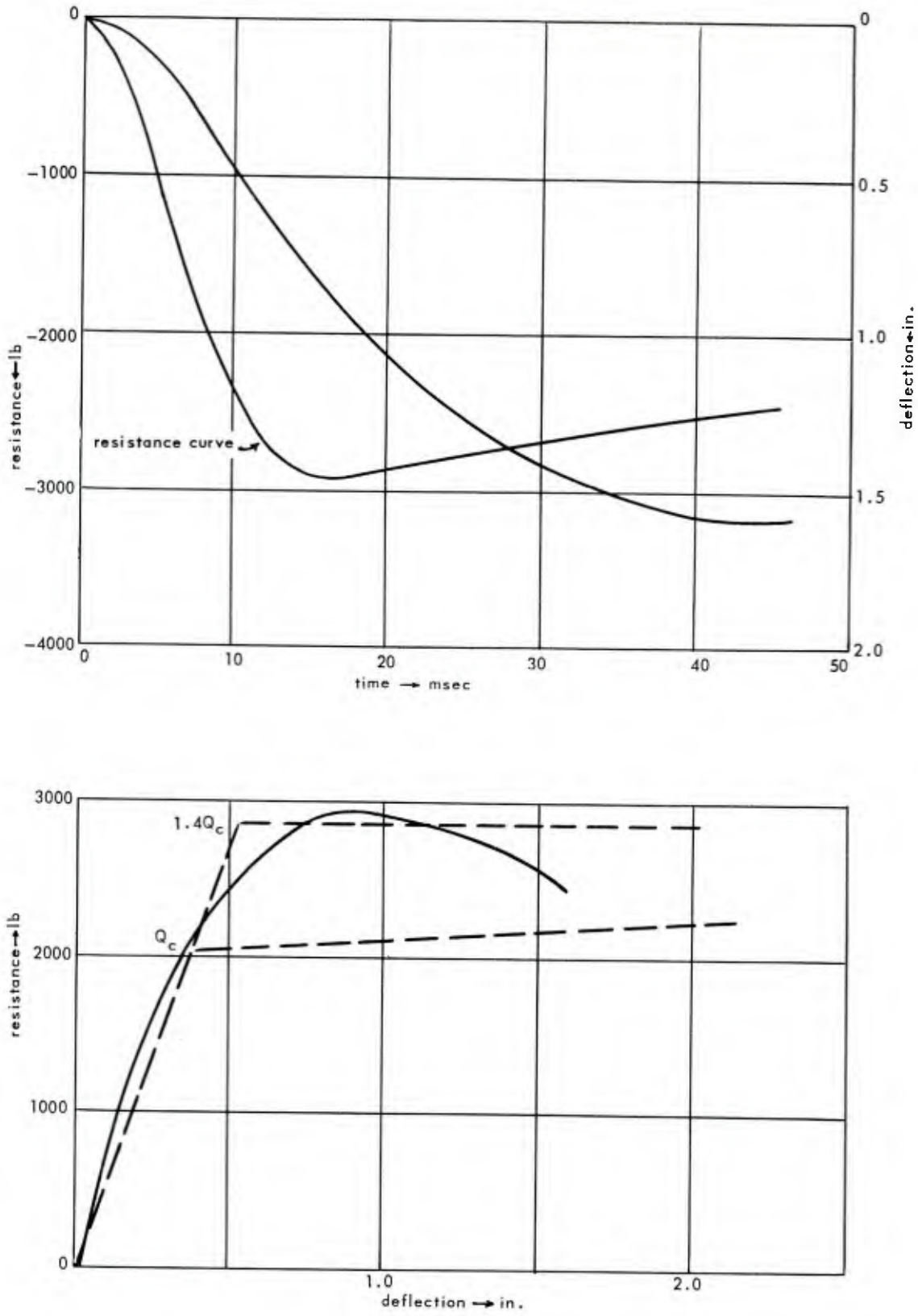

Figure 28. Resistance curve, beam C-12.

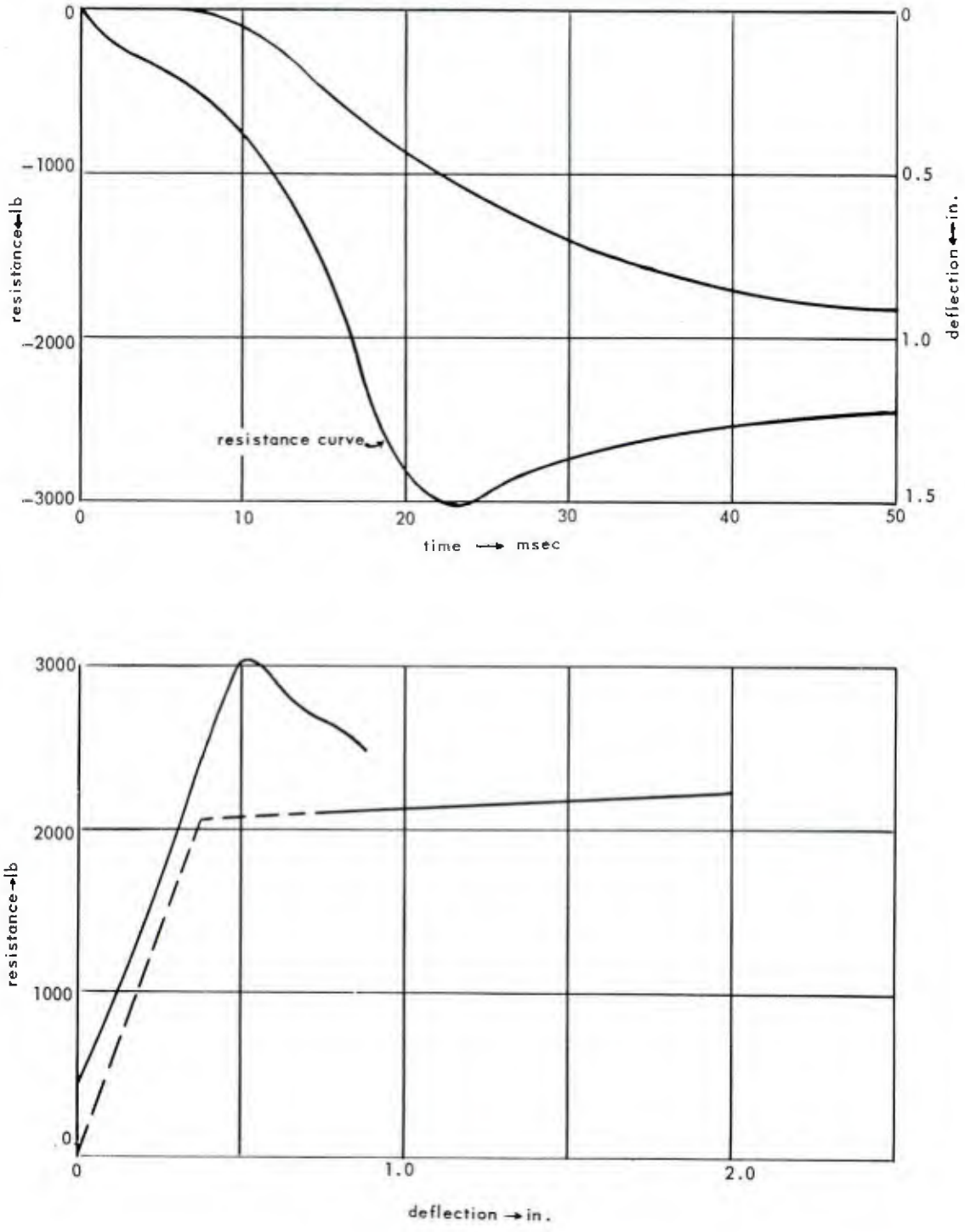

Figure 29. Resistance curve, beam C-16.

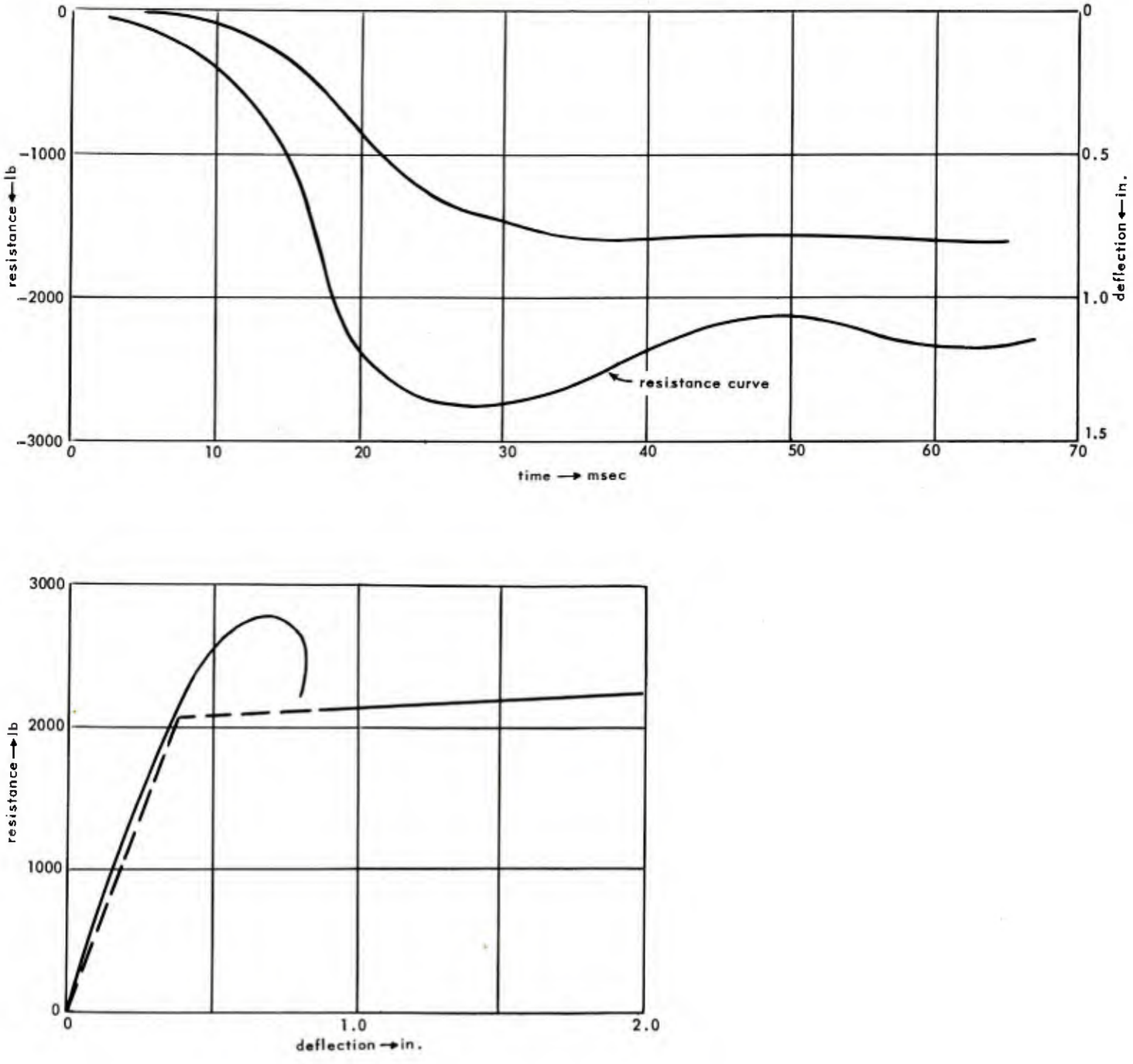

Figure 30. Resistance curve, beam C-20.

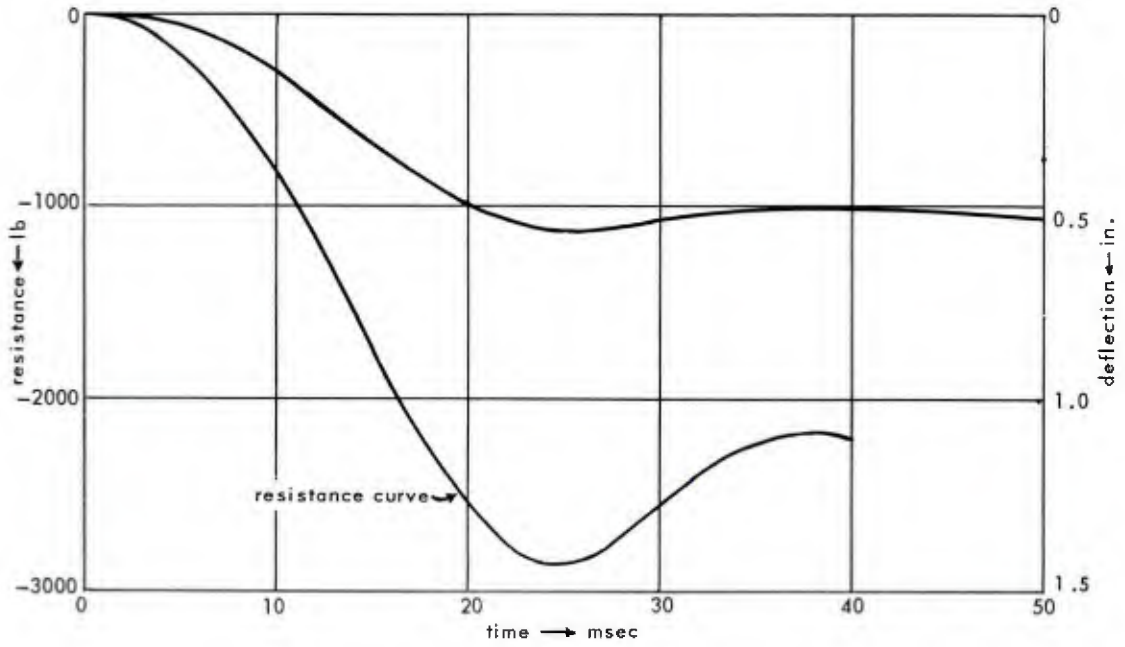

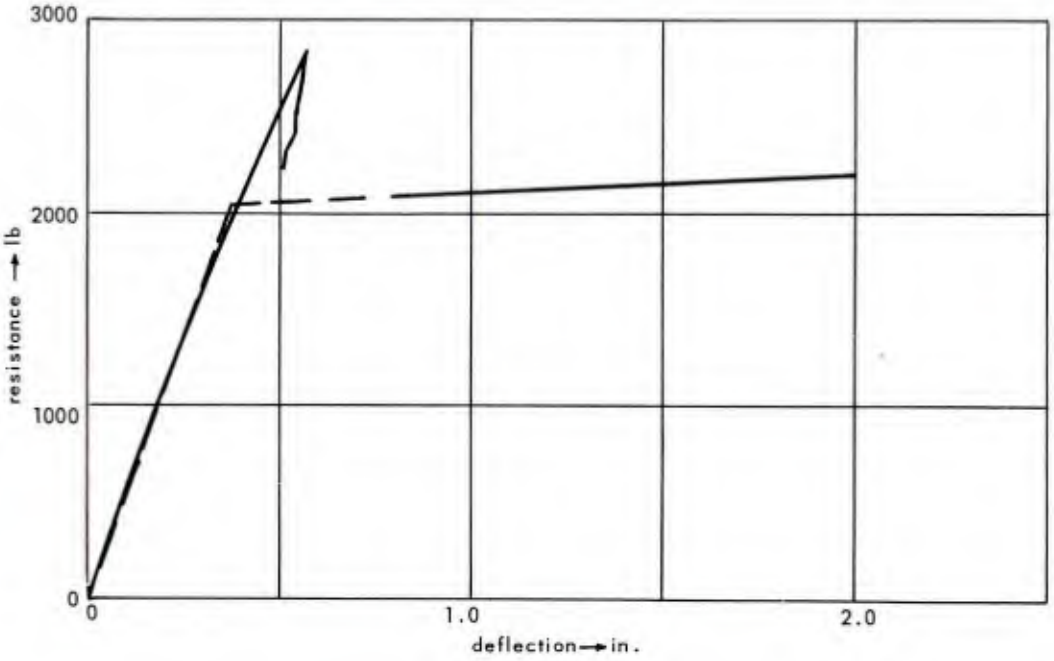

Figure 31. Resistance curve, beam C-32.

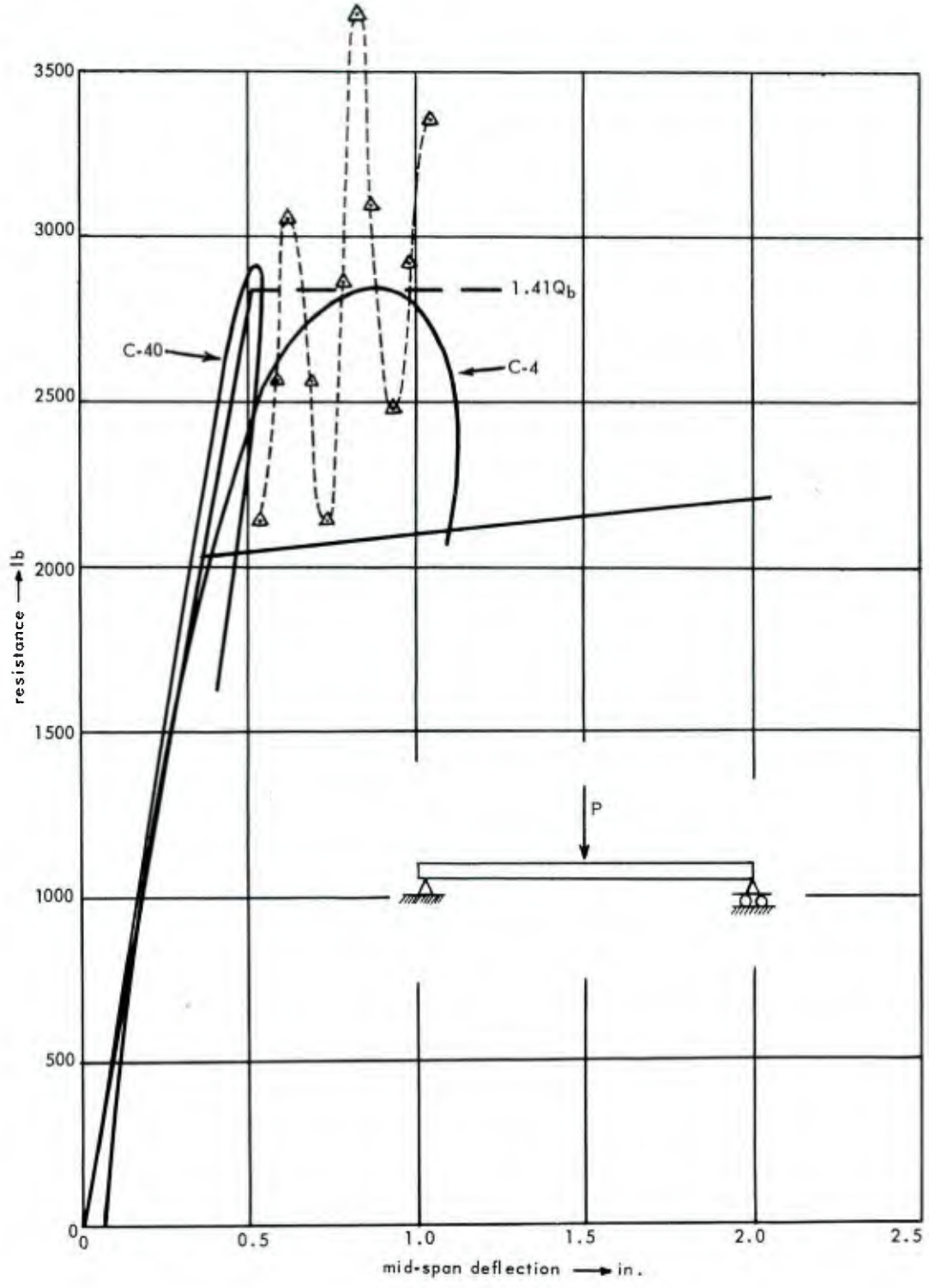

Figure 32. Resistance curve ($m_e = \frac{1}{2} m$).

Damping is generally attributed to internal friction plus small windage and support friction. Plastic straining also results in a loss of energy from internal molecular friction. Hence, attempting to separate damping from plastic action seems scarcely worth the effort. The concept of a plastic range damping is useful for research purposes but is of doubtful value in practical design. In making calculations of response for beams, tests indicate that the use of $\frac{k_2}{k_1} = 0$ curve of appendix C, figure 40 with zero damping gives satisfactory results.

Such calculations are based on fundamental mode response. Symmetry of load, reaction, and member with respect to the center line is assumed. For other conditions it would be quite possible for the maximum moment and shear to occur at sections other than those critical under static loading.

Determination of Shear

The maximum shear force to which a beam is subjected may be quickly estimated by using a free body of one-half the beam (see figure 33).

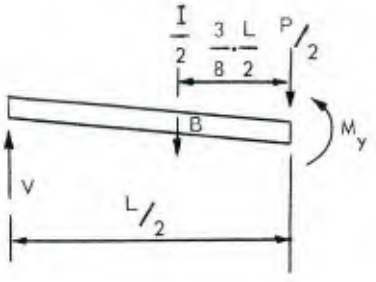

Figure 33. Free body of one-half of beam.

Assuming that the inertial force is lumped at the centroid of the half-parabolic area included by the reference axis, the elastic line, and the center line, the equation of moment equilibrium is

$$M_c = \frac{P}{2}\left(\frac{3}{8}\right)\left(\frac{L}{2}\right) + V\left[\frac{L}{2} - \frac{3}{8}\left(\frac{L}{2}\right)\right] \qquad (3)$$

or

$$V = \frac{M_c - \frac{3}{32} PL}{\frac{5}{16} L} \qquad (4)$$

For the series C beams, with a 2000-lb load, the calculated shear was 1600 lb, which gives a dynamic reaction 1.6 times the static reaction. Experimentally determined values for loads between 1880 lb and 2184 lb were in the range 1.51 to 1.66. The shear ratio for the load with a rise-time was appreciably reduced.

The Influence of Rise-Time

For elasto-plastic response in purely elastic behavior,[8] if the rise-time is 8 or greater times the natural period, maximum deflection is markedly reduced. The theoretical load-deflection relation for a 20 msec rise-time is given in figure 34. Test results corrected to 20 msec rise-time are given for comparison. Also the theoretical curve for zero rise-time is included showing the large difference in maximum deflection resulting from an increased rise-time. Agreement between theory and experiment is excellent.

The Deflected Shape

The shape that the beam assumes during the deflection can be deduced by considering the equilibrium of the beam at successive times during each of the positive and negative acceleration periods. During the first 5 to 10 msec, acceleration would be in the direction of motion (positive). The D'Alembert force, if lumped in two components and considered as a time-varying load, would be as shown in figure 35, diagram (a). Later, the acceleration would reverse direction, and the inertial forces would be as shown in figure 35, diagram (b). Thus, after the first few milliseconds but prior to hinge formation, the deflected shape would not be much different from the shape of the elastic curve under uniform static loading. This deduction is supported by measurements.

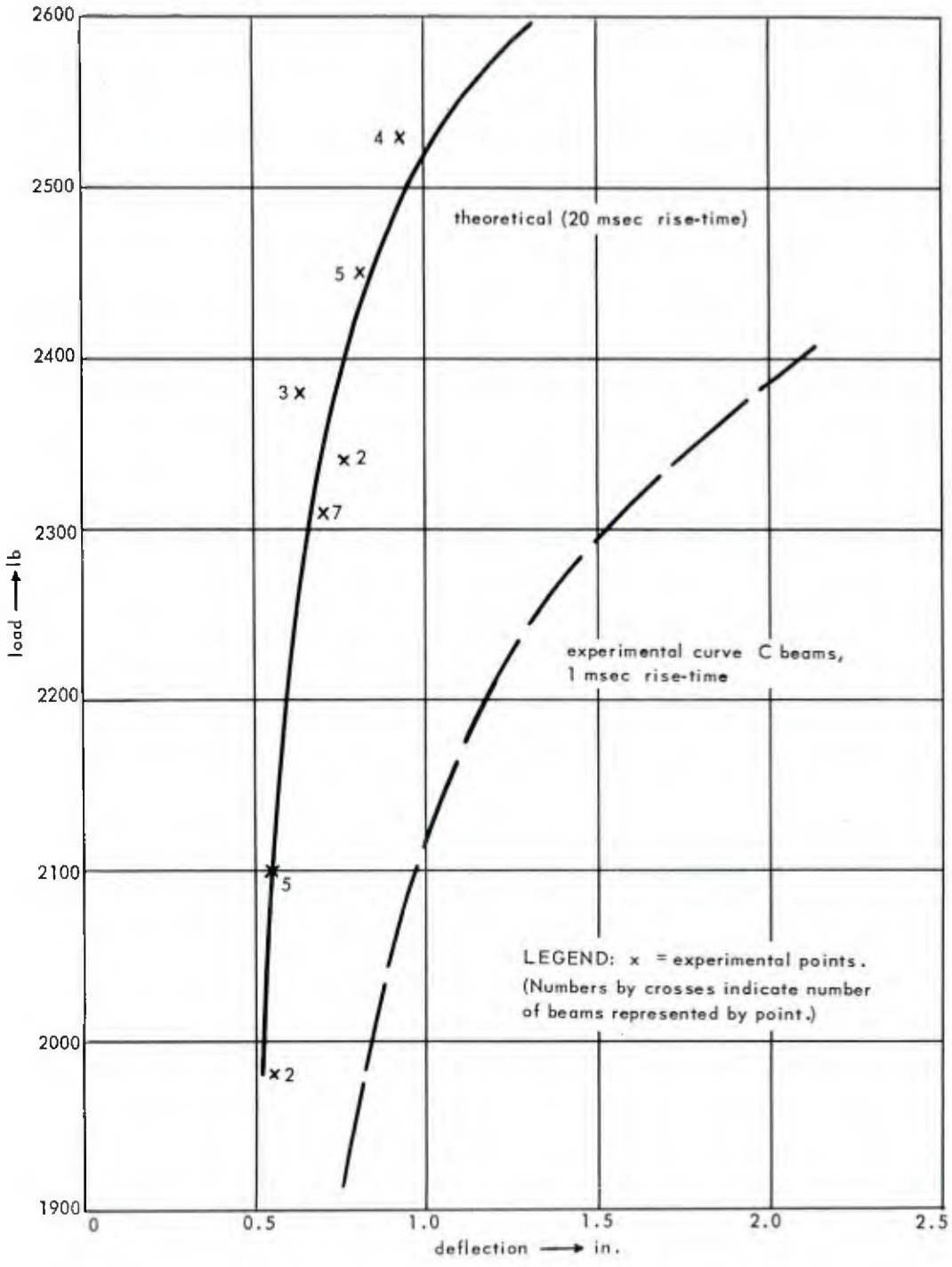

Figure 34. Load-deflection curve - beams with rise-time of load.

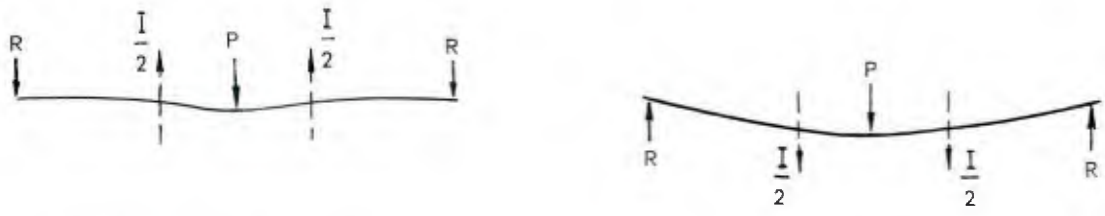

(a) Deflected shape $0 < t < 7$ msec.

(b) Deflected shape $t > 7$ msec.

Figure 35. Deflected shapes of beam.

CONCLUSIONS

It should be kept in mind that all tests reported were for beams of one size and section. Further, the beams essentially were of model proportions. The results, therefore, can be taken only as an indication of the probable behavior of full-size beams.

Elasto-plastic beam action is a complex phenomena involving the interrelation of many parameters; there is still much to learn about it, although some insight into the behavior has been acquired. Conclusions and observations appear to be justified as follows:

1. For design purposes the spring-mass system provides a satisfactory analogy to the symmetrically restrained and loaded beam. Accuracy of the solution is primarily dependent upon the resistance curve employed.

2. Plastic range resistance exhibits a time-dependent character which is of significance only for research purposes.

3. An increase in yield point predicted from Manjoine's curve gives results which agree well with the experimentally determined increase in yield point.

4. Shear is more critical in dynamic loading than in static loading; the peak dynamic reaction is readily predicted and may be as much as two times the static reaction.

5. On loading, the ends of the beams tend to move upward, producing a downward reaction at the supports.

6. The primary influence of damping is reduction of velocity at the time of yield.

7. Elastic damping for loads of zero rise-time can be expected to produce a maximum resistive force of about 12 percent of the static yield load.

8. Dynamic yield of a beam occurs at about 0.8 times the static yield load for loads of zero rise-time.

9. Using the dynamic yield load and the step-load condition $P = 1.35Q_c$ as criteria, the maximum increase in load capacity from plastic action is 70 percent.

10. Compression steel should be used in all beams designed for dynamic load.

11. Actual resistance curves are readily developed from force-equilibrium studies. An equivalent mass of one-half the actual mass gives a theoretical resistance which agrees with the peak resistance determined by experiment.

12. A load of $1.1Q_c$ is a reasonable criteria for design against the loads imposed by side-on pressure from megaton explosions. For this criteria a maximum initial deflection of $3.71y_c$ will result.

13. The method of analysis given in appendix C, exemplified in appendix F, accounts for the basic parameters and provides a rapid comprehensive method for use in the design office.

RECOMMENDATIONS

Design Criteria

The recommendations which follow are based on tests and studies of other investigators as well as the work presented in this report. They are intended as a guide to the designer.

1. Compression steel should be used in all reinforced concrete beams designed for dynamic loads.

2. Vertical stirrups should be used in regions where a plastic hinge is anticipated even though they are not necessary to meet the shear requirement. These stirrups restrict the compression steel from buckling when the concrete fails in compression and, hence, should be closely spaced.

3. Proper anchorage of the ends should be provided to restrain them from jumping the supports.

4. Shear design should be based upon an analysis such as the one given in the text. This type of analysis will generally require a shear load of about 1.5 to 2 times the corresponding static shear. As larger stirrups are required, particular attention must be paid to bond stress and anchorage.

5. The criteria for designing beams to resist the side-on loads imposed by megaton explosions should be a step load with $\frac{P}{Q_c} = 1.1$ and an ultimate deflection of at least 3.7, and preferably 10, times the static yield deflection.

6. For the design for rapidly decaying loads, the design criteria should be based on an allowable elasto-plastic deflection, preferably in the range of $\frac{L}{10}$ to $\frac{L}{20}$.

7. Consideration should be given to the possibility of using rail steel as a means of limiting plastic deflections to values which will not impair the post-shot usefulness of the structure. The use of rail steel for dynamically loaded members is still a subject of some controversy.

8. Consideration should be given to the possibility of reverse loading from the negative phase of a blast.

9. Graphical methods should be considered for the solution of spring-mass problems which cannot be obtained from prepared charts.

Future Work

Recommendations for future work in the field of structural dynamics which the authors consider as among the most likely to yield useful results are as follows:

1. Criteria should be established for determining the optimum section of beams to resist nuclear blast loads.

2. An evaluation should be made of the relative merits of using rail steel versus structural grade steel.

3. Further work should be done on the properties of reinforcing steel under dynamic load conditions such as those which occur in a beam.

4. The effects of asymmetry of load, reaction, and section might be investigated.

5. Emphasis on experimental work in structural dynamics should be shifted to full-size members including beams, frames, arches, shear walls, and connections.

ACKNOWLEDGEMENTS

The authors wish to acknowledge the contribution of Dr. W. T. Thomson of the University of California at Los Angeles, Los Angeles, California, in developing the theory of appendix B and the curves of figures 39 and 40.

NOMENCLATURE

C, C_1, C_2, etc.	=	constants
c	=	damping constant; also distance measured from the neutral axis of beam
E	=	modulus of elasticity of beam
f	=	fixity; ratio of the moment actually developed at the supports to that which would be developed under infinitely rigid supports
I	=	moment of inertia
k_c	=	mid-span stiffness due to concentrated load at mid-span
k_d	=	mid-span stiffness due to distributed load
k_1	=	elastic slope of resistance curve
k_2	=	plastic slope of resistance curve
L	=	span of beam
M	=	bending moment
M_s	=	bending moment at supports
m	=	mass
m_e	=	equivalent mass
P	=	dynamic load
Q	=	resistance of beam
Q_b, Q_c	=	resistance of beam at points on resistance curve
q	=	static uniformly distributed load

q_c, q_g	=	static uniformly distributed load at points on resistance curve indicated by subscript
S	=	unit stress
T	=	kinetic energy
t	=	time
t_l, t_b	=	time to points on load or resistance curve indicated by subscript
t_m	=	time to maximum displacement
U	=	potential energy
v	=	velocity of mid-point of beam
v_l, v_b	=	velocity of mid-point of beam at points on load or resistance curve indicated by subscripts
W	=	work
x	=	distance along beam
y	=	deflection
$\dot{y}$	=	velocity of mid-point of beam
$\ddot{y}$	=	acceleration of mid-point of beam
y_l, y_b	=	deflection of mid-point of beam at points on load or resistance curve indicated by subscripts
y_c	=	deflection of mid-point of beam
y_m	=	initial maximum deflection of mid-point of beam
β	=	load or work factor
β'	=	mass factor

Δ	=	increment of time
δ	=	increment constant
ϵ	=	unit strain
ζ	=	damping factor
$\emptyset$	=	constant
ω	=	natural frequency

REFERENCES

1. Massachusetts Institute of Technology, "Behavior of Reinforced Concrete Structural Elements Under Long Duration Impulsive Loads", J. B. Wilbur, et al, September 1949.

2. University of Illinois, Structural Research Series No. 106, "Inelastic Behavior of Mild Steel Beams Subjected to Transverse Impact", F. L. Howland, August 1953.

3. NCEL Technical Note N-174, An Interval Controller, W. A. Bowen, Jr., 25 November 1953.

4. Massachusetts Institute of Technology Notes for Summer Course, "Structural Design for Dynamic Loads", C. H. Norris and others, August 1956.

5. Manjoine, M. J., "Influence of Rate of Strain and Temperature on Yield Stresses of Mild Steel", JOURNAL APPLIED MECHANICS, Vol. 11, No. 4, December 1944.

6. Davis, E. A., "The Effect of the Speed of Stretching and the Rate of Loading on the Yielding of Mild Steel", JOURNAL APPLIED MECHANICS, Vol. 11, No. 4, December 1944.

7. "The Effects of Nuclear Weapons", Department of Defense and Atomic Energy Commission Publication, June 1957.

8. Frankland, J. M., "Effects of Impact on Elastic Structures", Proceedings, Society for Experimental Stress Analysis, Vol. VI, No. 2, May 1947.

9. Lee, E. H., and Symonds, P. S., "Large Plastic Deformations of Beams Under Transverse Impact", JOURNAL APPLIED MECHANICS, Vol. 19, No. 3, September 1952.

10. Newmark, N. M., "Designing for Atomic Blast Protection", a paper presented at the Structural Engineers Association of California Convention at Reno, Nevada, 12 October 1956, reprinted in the BUDOCKS Technical Digest, March-April 1957.

11. Bureau of Yards and Docks, Design of Protective Structures, A. Amirikian, August 1950.

12. Bleich, H. H., and Salvadori, M. C., "Impulsive Motion of Elasto-Plastic Beams", American Society of Civil Engineers Proceedings, Vol. 79, Separate No. 287, September 1953.

13. Thomson, W. T., "Impulsive Response of Beams in the Elastic and Plastic Regions", JOURNAL APPLIED MECHANICS, September 1954.

14. University of California at Los Angeles, "Dynamic Response of Single Span Beams in the Plastic Region", by W. T. Thomson, Report 57-53, June 1957.

15. Wood, D. S., "Rapid Loading Tests on Three Grades of Reinforcing Steel", Report Under Contract NOy-90922 with the Laboratory, 15 May 1956.

16. Clark, D. S., and Wood, D. S., "The Time Delay for the Initiation of Plastic Deformation at Rapidly Applied Constant Stress", Proceedings, American Society for Testing Materials, Vol. 49, 1949.

17. University of Michigan, "Steel Beams, Connections, Columns and Frames", L. S. Hu, R. C. Byce, Bruce G. Johnston, March 1952, p II-6.

18. Jacobsen, L. S., "On a General Method of Solving Second Order Ordinary Differential Equations by Phase-Plane Displacements," JOURNAL APPLIED MECHANICS, Vol. 19, No. 4, December 1952.

APPENDIX A

DYNAMIC PROPERTIES OF STEEL

It has been recognized that the rate of loading has a decided effect on the strength properties of materials. For steel, an increase in the rate of loading will result in an increase in yield point and ultimate strength. The modulus of elasticity, however, is unaffected by rate of loading. The increase in yield point of steel is of particular importance in the design of blast-resistant structures.

A considerable number of tests of various grades of steel have been performed at rapid rates of strain. Tests performed by Manjoine are among the most reliable made on mild steel at strain rates normally encountered in blast-resistant design.[5] These tests were performed at room temperature on specimens machined from a commercial low-carbon open hearth steel. The finished test specimens were bright-annealed for 1 hr at 920 C in dissociated ammonia. The yield point of this steel is 28,400 psi, when tested at a strain rate of 10 μ-in /in /sec.

The influence of increased rate-of-strain on the yield point of this steel is shown in figure 36, curve A. While this graph does not extend over the range of strain rates reported in Reference 5, it does cover the strain rates of most interest to the designer of blast-resistant construction. It should be realized that this curve is appropriate only when the static yield point is determined at the strain rate mentioned above.

ASTM standard A370-54T permits static tension tests to be performed at a strain rate approximately equal to 1000 μ-in /in /sec. It should be recognized that this is an unrealistic strain rate for accurate determination of static strength properties of steel specimens in the Laboratory. This relatively rapid strain rate was established to apply primarily to regular production procedure in the testing of steel products by the steel manufacturers. Naturally, a rate of strain of this magnitude will result in a yield point considerably higher than that determined at a strain rate of 10 μ-in /in /sec. For the particular steel used in Manjoine's research, the yield point determined by the maximum strain rate permitted by these ASTM standards would be 31,200 psi. Figure 36, curve B shows the influence of strain rate on the increase in yield point using 31,200 psi as the basic yield point.

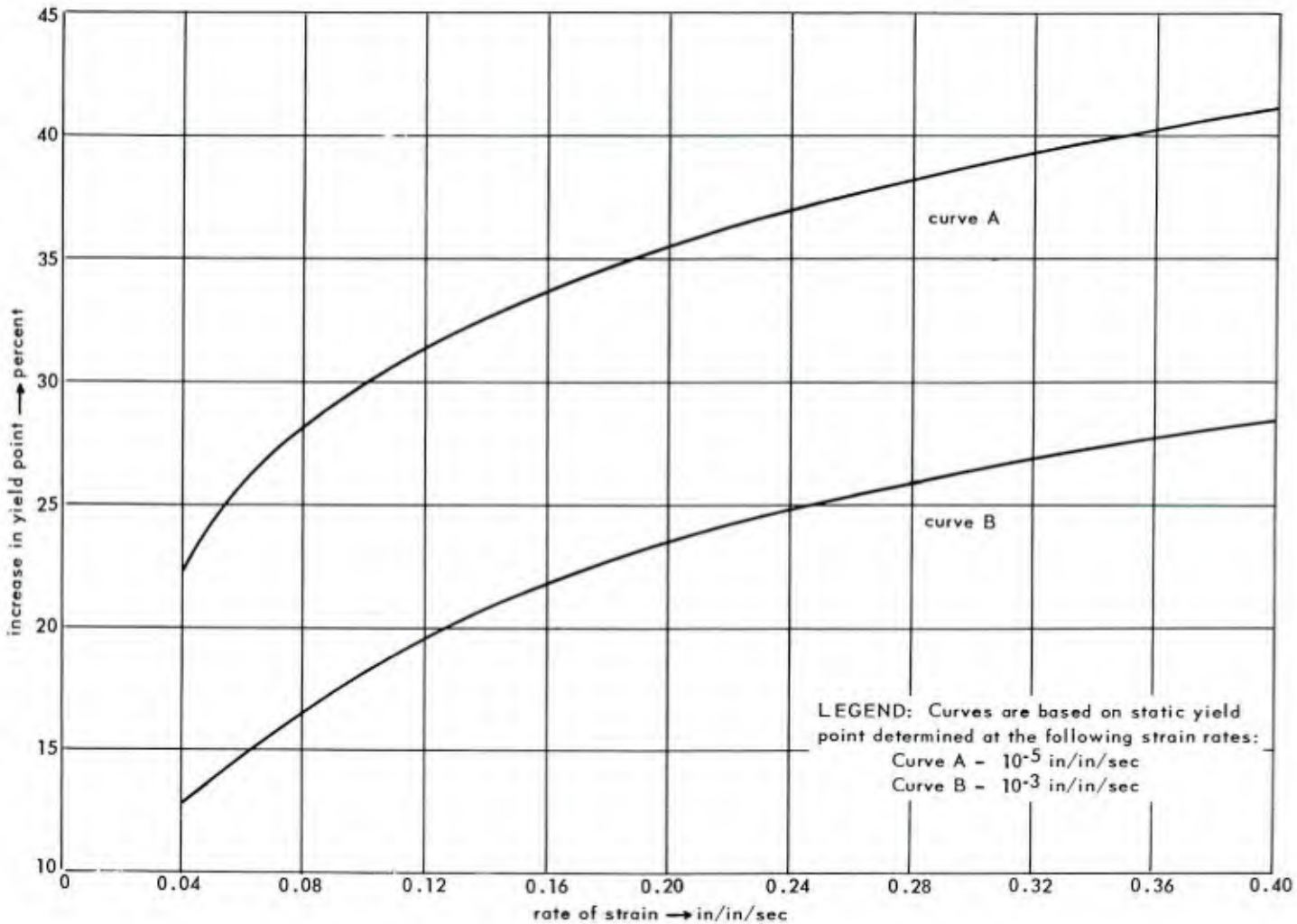

Figure 36. Increase in yield point with strain rate.

So it becomes apparent that, before an increase in yield point of steel is selected, it is important to know the strain rate at which the static yield point is determined. If this yield point is obtained from the steel mill, curve B should be used.

In the literature, the phenomenon of increase in yield point is occasionally associated with the time required to reach the yield point. This method of presenting data on the increased yield point probably originated because the time to yield is readily available from a dynamic analysis.

This approach should be viewed with caution since it does not give an accurate value for strain rate. The yield strain divided by the time to reach yield will give the average strain rate but not the true strain rate at yield. Because of its inertia, the beam will not deflect very much in the first few milliseconds after application of a dynamic load, and the true strain at yield will therefore be greater than the average strain rate. The true strain rate at yield may be determined quite easily by the method of appendix D.

Another disadvantage in the use of the time to reach yield point as the independent variable is that, strictly speaking, such a curve actually applies only to a steel of a given yield point. For a steel of a different yield point the curve would not be accurate. For example, assume that a curve has been prepared having a lower yield level of 40,000 psi. A time to reach of 0.03 sec represents a certain average rate of strain. However, if the curve were used to determine the increase in yield point for a steel with a yield point of 48,000 psi, the same time to reach yield point of 0.03 sec would then represent a strain rate approximately 20 percent greater than for the steel with a yield of 40,000 psi. Thus, the single curve would indicate the same increase in yield point for rates-of-strain differing by 20 percent.

The errors inherent in the determination of increased yield point from curves using time to yield as the independent variable may not be of sufficient magnitude to warrant consideration by the designer of blast-resistant structures. However, these errors are of concern to the research engineer for an accurate analysis.

Under contract with the Laboratory, tension tests were run to determine the influence of strain rate on the yield point of mild steel, and intermediate and hard grades of reinforcing steel.[15] Tests were

performed on 18 machined specimens of each grade of steel at strain rates varying from 1.7×10^{-5} to 0.9 in/in/sec. The test equipment and instrumentation used are described elsewhere in the literature.[16]

These tests on mild steel provide results very close to those obtained by Manjoine, figure 36, and are therefore not repeated. The results of the rapid strain tests on intermediate and hard grades reinforcing steel are shown in figure 37. It should be noted that these curves are valid when the static yield point is determined at a strain rate between the limits of 1.0 to 5.0×10^{-5} in/in/sec.

Consideration should be given also to the probability of deviation from the determined yield point. Tests of structural steel show a probability of deviation from the average yield point of 5.5 percent.[17]

An interesting phenomenon occurs when steel is loaded rapidly to, and held at, a stress between the static lower yield point and the dynamic upper yield point. Then a definite and well defined time elapses during which no straining takes place. It is called the time to initiate plastic strain. This phenomenon is mentioned only to acknowledge the existence of the property; it is of no consequence in the design of beams for dynamic loads. The dynamic step load which produces yielding, $0.8Q_c$, is less than the load established as a design criteria, $1.1Q_c$. Hence, the design load will produce stresses above the maximum stress (dynamic upper yield point) for which time to initiate plastic strain is possible.

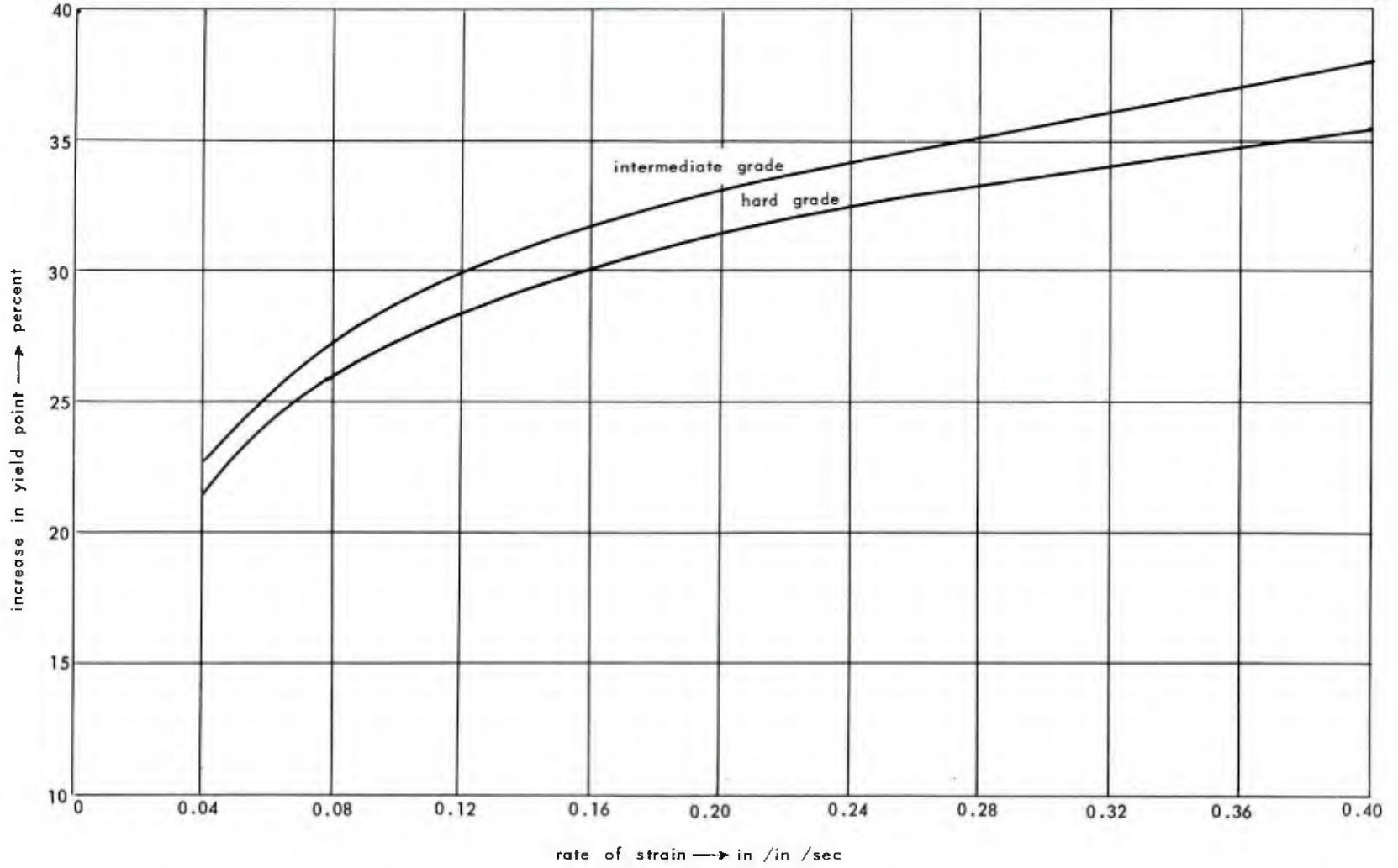

Figure 37. Increase in yield point of reinforcing steel with strain rate.

APPENDIX B

DEVELOPMENT OF EQUIVALENCY FACTORS

Consider the uniform beam with end supports of fixity f (figure 38), loaded by a uniformly distributed force of arbitrary time variation. Fixity f is here defined as the ratio of the moment M_s actually developed

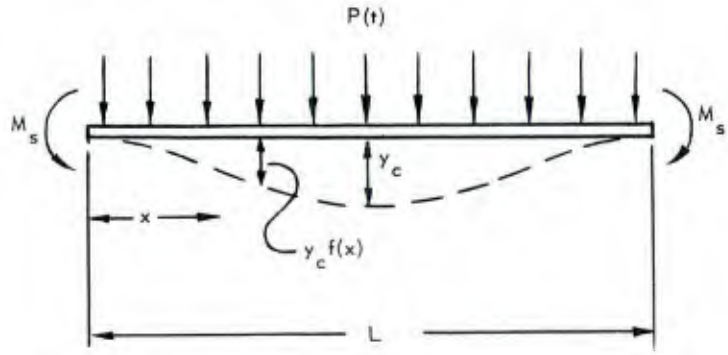

Figure 38. Configuration of uniform beam with end fixity f.

to that which would have developed under infinitely rigid supports. Thus, f = 1.0 represents a fixed end beam while f = 0 indicates a simply supported beam.

Since the procedure for analysis in the plastic region is dependent on certain basic concepts derived for the elastic behavior, the equations of motion in the elastic region will be discussed first. The deflection at any point x in terms of its mid-span value y_c will be expressed by the equation

$$y = y_c f(x) \tag{5}$$

where f(x) must conform to the existing end conditions. The kinetic and potential energies of the beam are then

$$T = \frac{1}{2} m \dot{y}_c^2 \int_0^L f^2(x)\, dx \tag{6}$$

$$U = \frac{1}{2} EI y_c^2 \int_0^L \left[\frac{d^2 f(x)}{dx^2}\right]^2 dx \qquad (7)$$

and the work done by the applied load and the damping force (assumed to be viscous) during an increment of deflection δy_c is

$$\delta W = \frac{P(t)\, \delta y_c}{L} \int_0^L f(x)\, dx - c \dot{y}_c \frac{\delta y_c}{L} \int_0^L f(x)\, dx \qquad (8)$$

Substituting into Lagrange's equation which for this case is

$$\frac{d}{dt}\left(\frac{\delta T}{\delta \dot{y}_c}\right) + \frac{\delta U}{\delta y_c} = \frac{\delta W}{\delta y_c} \qquad (9)$$

we obtain the differential equation

$$\left\{m \int_0^L f^2(x)\, dx\right\} \ddot{y}_c + \left\{EI \int_0^L \left[\frac{d^2 f(x)}{dx^2}\right]^2 dx\right\} y_c = \frac{P(t)}{L} \int_0^L f(x)\, dx - \frac{c\dot{y}_c}{L} \int_0^L f(x)\, dx \qquad (10)$$

The coefficient of y_c in equation 10 deserves further discussion. Letting k_c be the stiffness of the beam at mid-span due to a concentrated load Q at the same point, we have from Castigliano's theorem,

$$k_c = \frac{1}{y_c}\left(\frac{\delta U}{\delta y_c}\right) = EI \int_0^L \left[\frac{d^2 f(x)}{dx^2}\right]^2 dx \qquad (11)$$

It is, however, more convenient for the distributed load problem to express k_c in terms of the mid-span stiffness k_d because of distributed force q. To produce the same mid-span deflection, a larger distributed load qL is required in comparison to the concentrated load Q. By equating the work done by the two types of forces for equal mid-span deflection, we arrive at the result

$$k_c = k_d\left(\frac{1}{L}\right)\int_0^L f(x)\ dx \qquad (12)$$

equation 10 can now be written in the form

$$\beta' m \ddot{y} = \beta \left[P(t) - k_d y_c - c \dot{y}_c\right] \qquad (13)$$

where:

m = total mass of beam

β' = mass factor $= \frac{1}{L}\int_0^L f^2(x)\ dx$

β = load factor $= \frac{1}{L}\int_0^L f(x)\ dx$

It is evident that equation 13 is that of an equivalent spring-mass system where the actual mass of the beam is reduced to $\frac{\beta'}{\beta} m$.

The values of β and β' depend somewhat on the equation chosen for the deflection as indicated in table VI. However, regardless of the type of supports or the equation used, the ratio β'/β remains nearly a constant and a value of 0.769 can be adopted for all conditions without introducing errors beyond those caused by other unknown factors.

Table VI. Equivalency Factors

Type of Beam and Equation Used	β	β'	$\frac{\beta'}{\beta}$
Simply supported			
$\text{Sin}\ \frac{\pi x}{L}$	0.636	0.500	0.787
Concentrated load equation	0.625	0.486	0.775
Distributed load equation	0.640	0.503	0.787
Clamped ends			
$\frac{1}{2}\left(1 - \cos \frac{2\pi x}{L}\right)$	0.50	0.383	0.763

APPENDIX C

FUNDAMENTAL MODE THEORY FOR ZERO RISE-TIME

Motion of the system of figure 21 having the load characteristics of figure 10, diagram (a), is given by two sets of equations. The first set defines the elastic behavior (range 2-3, a-b). For this range Newton's equation of motion is

$$m_e \ddot{y} + c\,\dot{y} + k_1 y = P$$

or

$$\ddot{y} + 2\xi\omega\,\dot{y} + \omega^2 y = \frac{P}{m_e} \tag{14}$$

where:

$$\omega = \sqrt{\frac{k_1}{m_e}} \tag{15}$$

$$\xi = \frac{c}{2\sqrt{k_1 m_e}} \tag{16}$$

$$m_e = \frac{\beta'}{\beta}\, m \tag{17}$$

The solution for displacement and velocity is,

$$y = Ce^{-\xi\omega t} \sin\left(\omega t\sqrt{1-\xi^2} + \phi\right) + \frac{P}{k_1} \tag{18}$$

$$\dot{y} = C\,\omega\sqrt{1-\xi^2}\; e^{-\xi\omega t}\left[\cos\left(\omega t\sqrt{1-\xi^2} + \phi\right)\right]$$

$$- \frac{\xi}{\sqrt{1-\xi^2}} \sin\left(\omega t\sqrt{1-\xi^2} + \phi\right) \tag{19}$$

With the initial conditions $y(0) = 0$ and $\dot{y}(0) = 0$, the undetermined constants become,

$$C = -\frac{P}{k_1}\frac{1}{\sqrt{1-\xi^2}} \tag{20}$$

and

$$\phi = \arctan\frac{\sqrt{1-\xi^2}}{\xi} \tag{21}$$

Using these constants equations 18 and 19 may be expressed in non-dimensional form as follows:

$$\frac{y}{y_b} = \frac{P}{ky_b}\left[1 - \frac{e^{-\xi\omega t}\cos(\omega t\sqrt{1-\xi^2}+\phi)}{\sqrt{1-\xi^2}}\right];\ y<y_b \tag{22}$$

and

$$\frac{v}{v_b} = \frac{P}{ky_b}e^{-\xi\omega t}\left[\sin(\omega t\sqrt{1-\xi^2}+\phi) + \frac{\xi\cos(\omega t\sqrt{1-\xi^2}+\phi)}{\sqrt{1-\xi^2}}\right] \tag{23}$$

Knowing the yield deflection $y = y_b$, the velocity at yield may be readily computed for various values of ξ. This has been accomplished[14] and the results are plotted in figure 39.

For zero damping the time to point "b" is determined explicitly by substituting the condition $t = t_b$ when $y = y_b$ in equation 22 from which

$$t_b = \frac{1}{\omega}\arccos\left(1 - \frac{Q_b}{P}\right) \tag{24}$$

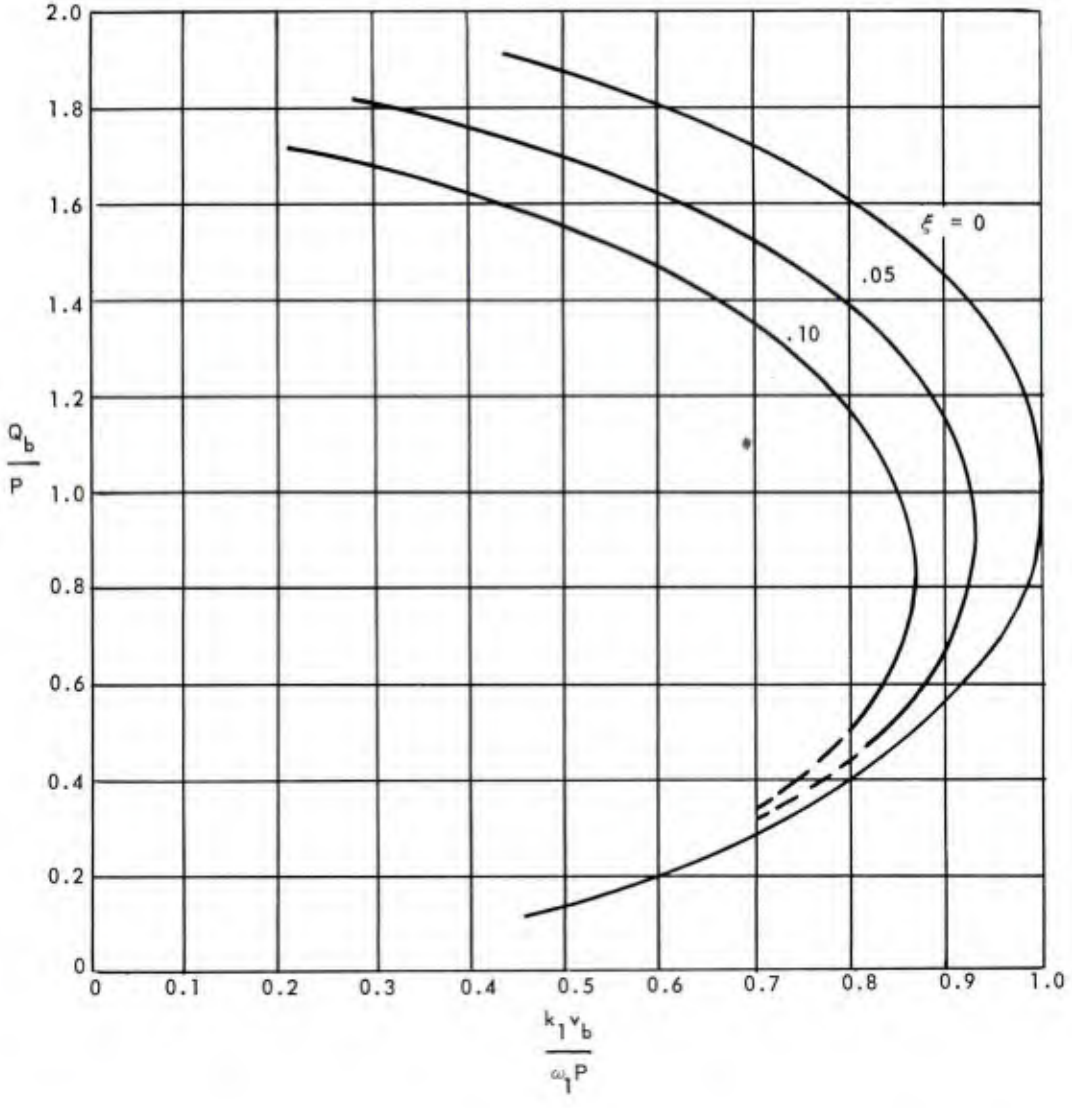

Figure 39. Solution for velocity at yield (step load).

This time equation 23 gives the velocity at "b" as

$$\frac{v_b}{\omega y_b} = \frac{P}{Q_b} \sin\left[\arccos\left(1 - \frac{Q_b}{P}\right)\right] \tag{25}$$

At "b" the beam enters the plastic region (range 2-3, b-d) and a second set of relations must be developed. For this range the equation of motion is

$$\ddot{y} = \frac{P - Q_b}{m_e} = \omega^2 y_b \left(\frac{P}{Q_b} - 1\right) \tag{26}$$

The solution of this equation is

$$y = \omega^2 y_b \left(\frac{P}{Q_b} - 1\right) \frac{t^2}{2} + C_3 t + C_4 \tag{27}$$

From the initial conditions, $y = y_b$ and $v = v_b$, the constants C_3 and C_4 are determined to be

$$C_3 = v_b$$

$$C_4 = y_b$$

Hence,

$$\frac{y}{y_b} = \left(\frac{P}{Q_b} - 1\right) \frac{(\omega t)^2}{2} + \frac{v_b}{\omega y_b} (\omega t) + 1 \tag{28}$$

and

$$\frac{v}{\omega y_b} = \left(\frac{P}{Q_b} - 1 \right) (\omega t) + \frac{v_b}{\omega y_b} \tag{29}$$

The time to zero velocity which is also the time to maximum displacement is obtained by setting equation 29 to zero, which gives

$$\omega t_m = \frac{\frac{v_b}{\omega y_b}}{1 - \frac{P}{Q_b}} \tag{30}$$

Substituting in equation 28,

$$\frac{y_m}{y_b} = 1 + \frac{\left(\frac{v_b}{\omega y_b} \right)^2}{2 \left(1 - \frac{P}{Q_b} \right)} \tag{31}$$

Combining with equation 25,

$$\frac{y_m}{y_b} = 1 + \frac{\left\{ \frac{P}{Q_b} \sin \left[\arccos \left(1 - \frac{Q_b}{P} \right) \right] \right\}^2}{2 \left(1 - \frac{P}{Q_b} \right)} \tag{32}$$

From which the maximum initial displacement, y_m, may be determined. Equation 32 is plotted in figure 40.

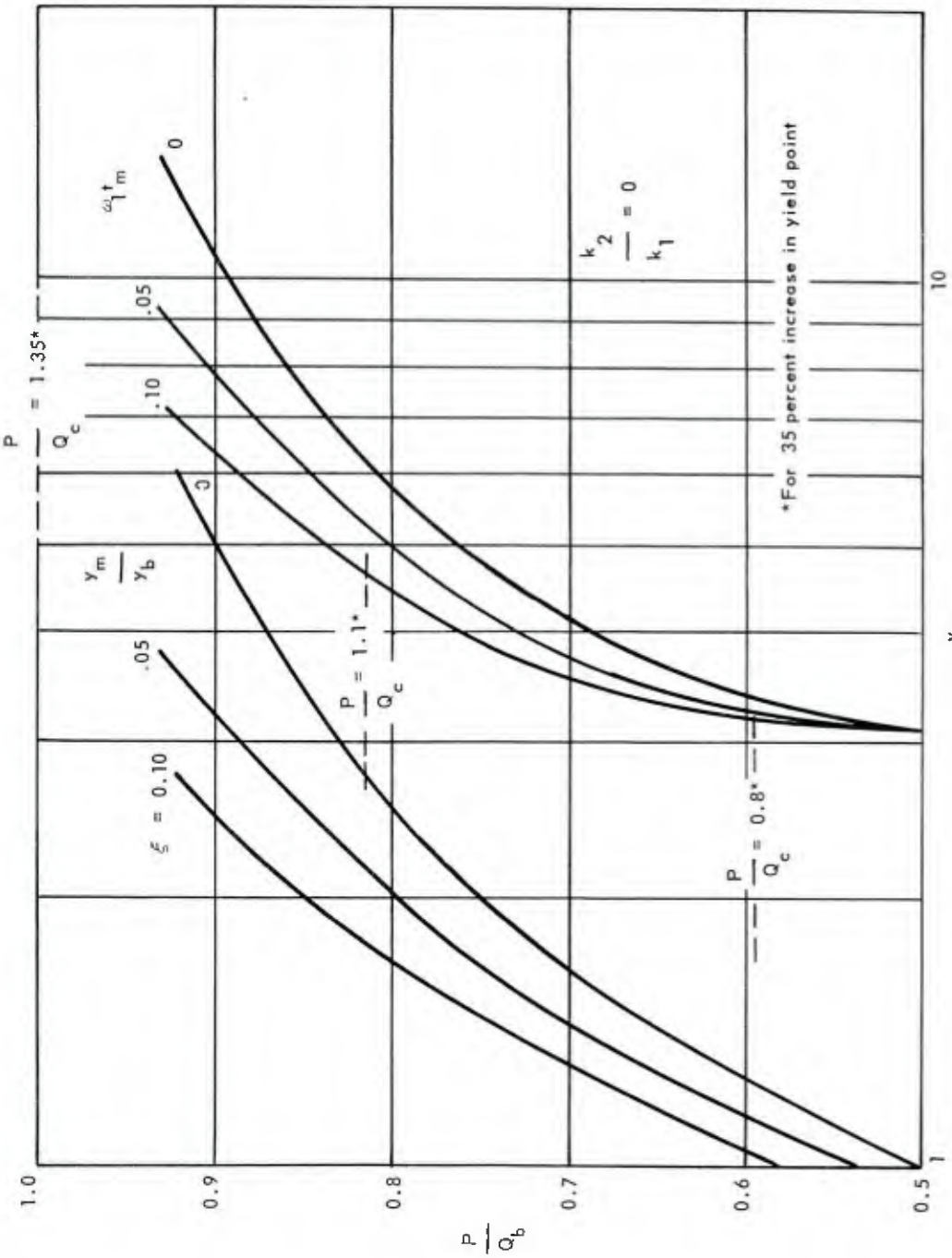

Figure 40. Design curves for step load.

APPENDIX D

METHOD OF ESTIMATING THE PERCENT INCREASE IN YIELD POINT

Simple Beam, Concentrated Load at the Center

For a simple beam loaded at the center the maximum deflection is given by

$$y = \frac{PL^3}{48EI} \tag{33}$$

We may also write

$$\epsilon = \frac{S}{E} = \frac{Mc}{EI} = \frac{PLc}{4EI} \tag{34}$$

Solving equations 33 and 34 for P and equating

$$P = \frac{48yEI}{L^3} = \frac{4\epsilon EI}{Lc} \tag{35}$$

Hence,

$$\epsilon = \frac{12yc}{L^2} \tag{36}$$

Assuming this relation holds for dynamic response, differentiation gives

$$\frac{d\epsilon}{dt} = \frac{12c}{L^2}\left(\frac{dy}{dt}\right) = \frac{12c}{L^2} \quad v \tag{37}$$

let $v = v_b$ = velocity at yield, which may be determined from figure 39.

Using the rate of strain computed from equation 37 and figures 36 or 37, the percent increase in yield point may be determined.

Partially Fixed Beams, Uniformly Distributed Load

For a beam with partially fixed ends subjected to a uniformly distributed load, the moment developed at the supports is given by equation 44 of appendix E.

$$M_s = \frac{fqL^2}{12} \tag{38}$$

And for identical support and mid-span yield moments, when the fixity is 75 percent or greater, the deflection of the center of the beam up to yielding of the supports is given in appendix E (equation 45).

$$y = \frac{qL^4(5 - 4f)}{384EI} \tag{39}$$

Also

$$\epsilon = \frac{S}{E} = \frac{Mc}{EI} = \frac{fqL^2 c}{12EI} \tag{40}$$

Solving equations 39 and 40 for q and equating,

$$q = \frac{12EI\epsilon}{fL^2 c} = \frac{384EIy}{L^4 (5 - 4f)} \tag{41}$$

from which

$$\epsilon = \frac{32 \; f \; c \; y}{L^2 (5 - 4f)} \tag{42}$$

Differentiating $\frac{d\epsilon}{dt} = \frac{32 \; f \; c}{L^2 (5 - 4f)} \left(\frac{dy}{dt} \right)$ (43)

The term $\frac{dy}{dt}$ or v_b, the velocity at yield, and the increase in yield point of the reinforcing steel is determined as mentioned above.

APPENDIX E

DETERMINATION OF STATIC RESISTANCE CURVE FOR BEAMS WITH PARTIALLY FIXED ENDS

It is desired to determine the static resistance curve for beams with partially fixed ends. Figure 41 shows the relationship between moment at the supports and moment at the center for beams of partial fixity.

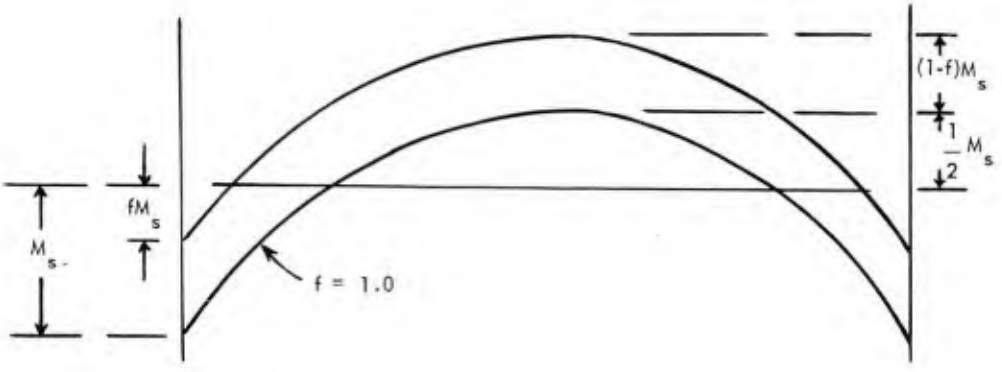

Figure 41. Relation of fixity to moments.

In order to develop equations which can be used to calculate the load-deflection curve of a beam with partially fixed ends, it is necessary to know the values of yield moment at the supports and center of the beam and to assume a value for the degree of fixity.

It is assumed that initial yielding will occur at the supports and the fixity of the ends is accomplished after the beam is in place; therefore the beam is considered to be simply supported for dead load and partially fixed for live loads.

A beam carrying a uniform load of q lb/ft will develop moments at the supports equal to

$$M_s = \frac{fqL^2}{12} \qquad (44)$$

where f is the fixity of the ends.

The deflection of the center of the beam because of this live load is

$$y = \frac{1}{EI}\left[\frac{2}{3}\left(\frac{L}{2}\right)\left(\frac{qL^2}{8}\right)\left(\frac{5}{8}\right)\left(\frac{L}{2}\right) - \left(\frac{L}{2}\right)\left(\frac{fqL^2}{12}\right)\left(\frac{L}{4}\right)\right]$$

$$y = \frac{qL^4(5 - 4f)}{384EI} \tag{45}$$

From these equations, the load q_g that produces yielding at the supports and the deflection y_g of the center of the beam can be determined.

The elastic slope then is

$$k_1 = \frac{qL}{y} \qquad \frac{384EI}{(5 - 4f)\,L^3} \tag{46}$$

In order to determine the loading which will produce yielding at the center of the beam, it is assumed that the moment at the supports does not exceed the yield moment with increase in load and that yielding is confined to a limited region at the supports.

As loading continues, the beam behaves as a simply supported member with constant end moments. The moment diagrams for dead load and live load are shown in figure 42. The moment at the center of the beam is

$$M = \frac{wL^2}{8} + \frac{qL^2}{8} - \frac{fq_gL^2}{12} \tag{47}$$

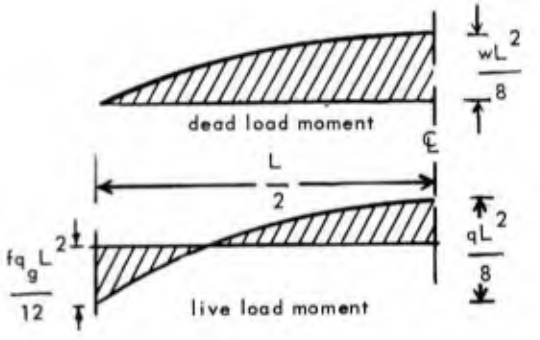

Figure 42. Moment diagram after formation of yield hinges at the supports.

And the deflection of the center of the beam due to live load only is

$$y = \frac{1}{EI}\left[\frac{2}{3}\left(\frac{L}{2}\right)\left(\frac{qL^2}{8}\right) - \left(\frac{L}{2}\right)\left(\frac{fq_gL^2}{12}\right)\left(\frac{L}{4}\right)\right]$$

$$y = \frac{(5q - 4fq_g)L^4}{384EI} \qquad (48)$$

APPENDIX F

EXAMPLE OF BEAM SELECTION AND ANALYSIS

The purpose of this appendix is to give a numerical example demonstrating the use of the information presented in this technical memorandum. It is desired to design a precast roof panel 5 ft wide and 20 ft long to withstand a pressure of 4.5 psi from a megaton explosion.

The procedure is as follows: first, use the design criteria established in the text ($P = 1.1Q_c$) to find the required static resistance; second, by trial select a section which provides the required resistance; third, estimate the increase in yield point; fourth, using the calculated increase in yield point determine the dynamic resistance; and fifth, complete the dynamic analysis by use of the design chart of figure 40.

It is assumed that the panel will have a fixity of 90 percent and that the ends will be fixed after the panel is in place. Therefore, the panel is simply supported for dead load and partially fixed for live loads.

From the criteria recommended the required maximum static resistance is

$$Q_c = \frac{P}{1.1} = \frac{4.5(144)(5)(20)}{1.1} = 58,900 \text{ lb.}$$

By trial, the sections shown in figure 43 are found satisfactory. The yield moments at mid-span and the support are 84,660 ft-lb and 82,840 ft-lb respectively. Total weight of the panel is 5,710 lb or 285.5 lb per foot of length and the stiffness EI is 33.0×10^6 lb-ft.^{2}

The static resistance will have the form given by a-g-h-e, figure 44. However, for simplicity the curve a-c-e is used as a suitable approximation. By equation 44 (appendix E), the load to produce yielding at the supports is

$$q_g = \frac{12M_s}{fL^2} = \frac{12(82,840)}{0.9(20)^2} = 2760 \text{ lb/ft.}$$

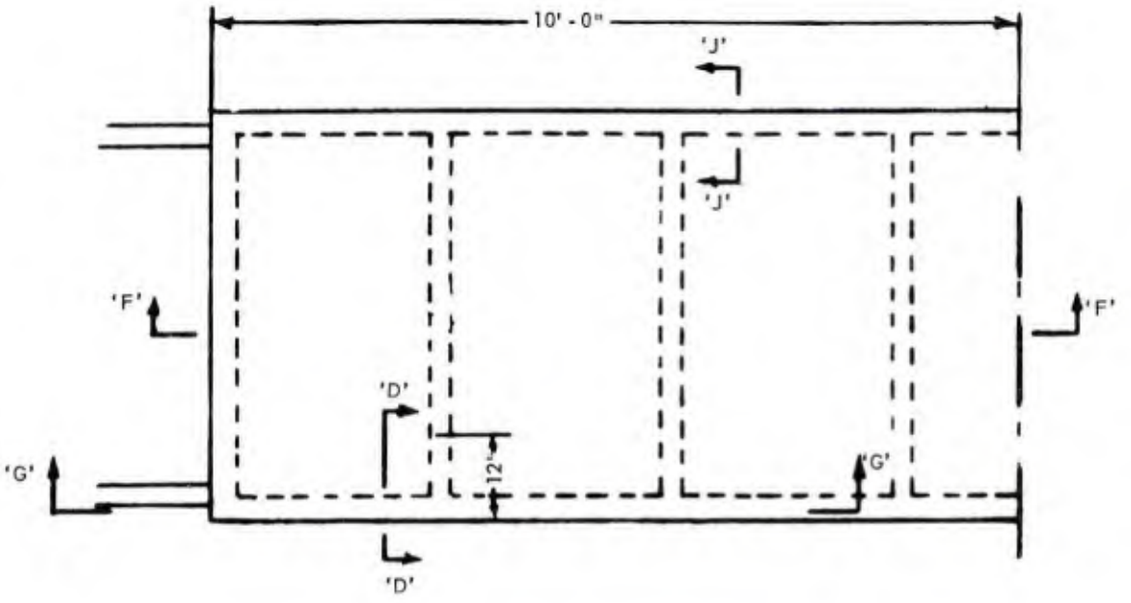

panel B

symmetrical about ℄

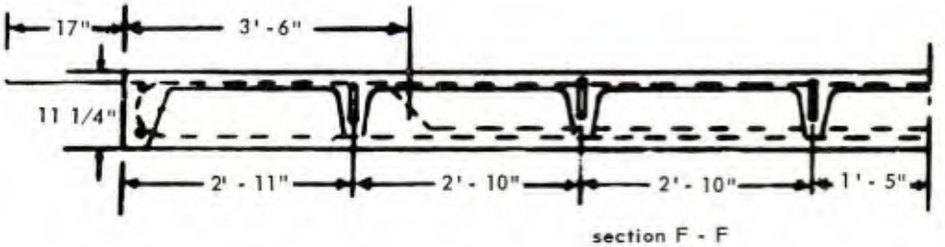

section F - F

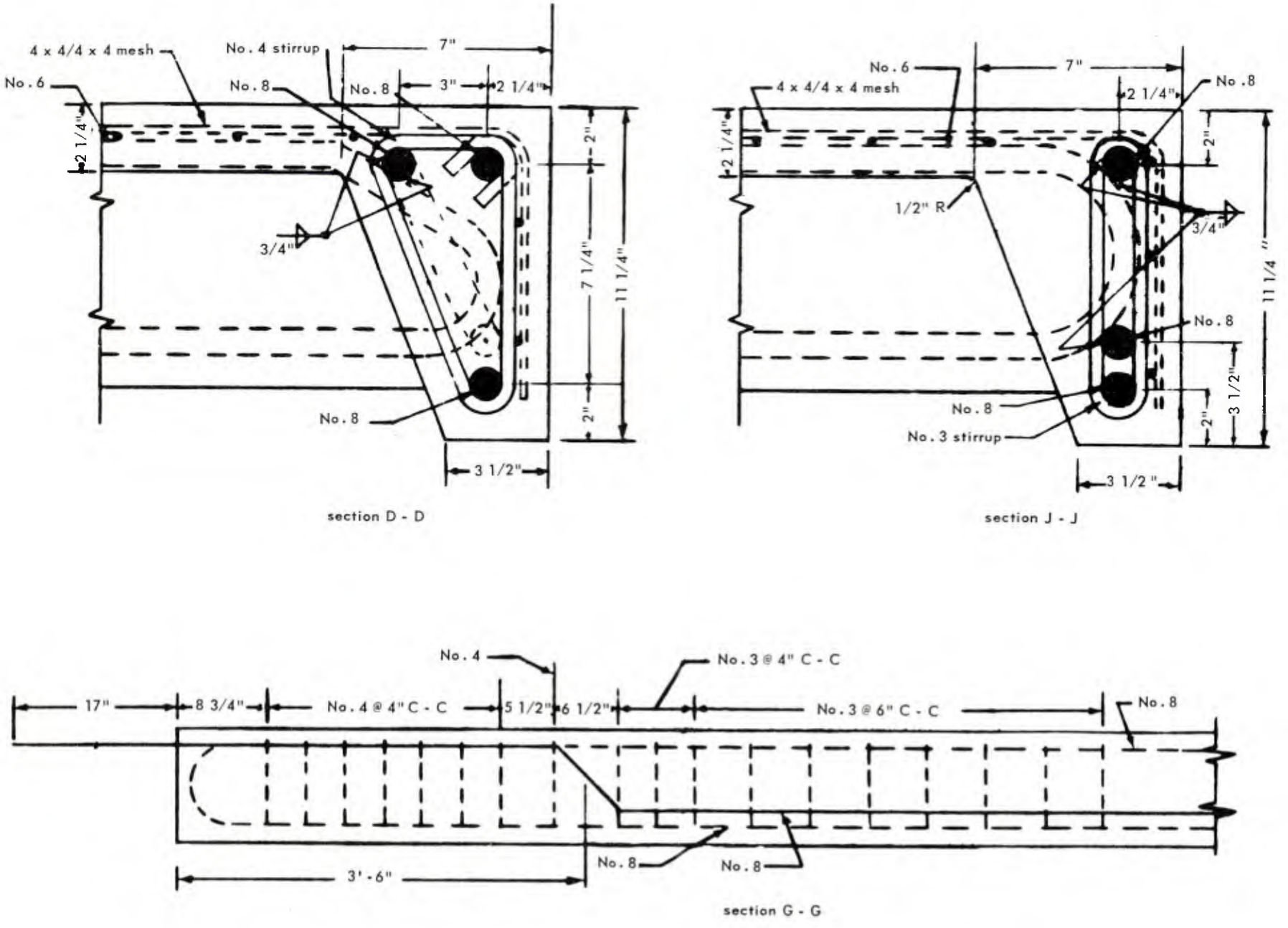

Figure 43. Precast roof panel.

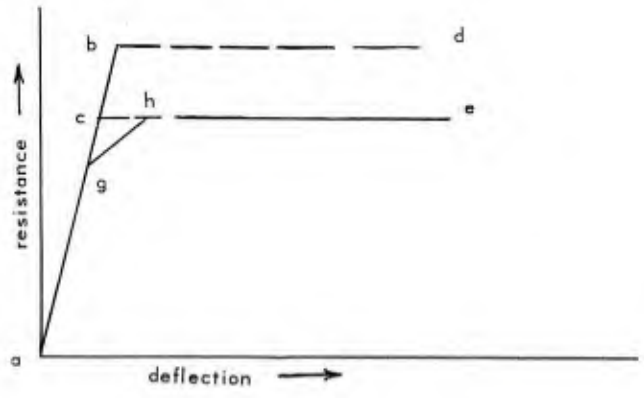

Figure 44. Resistance curve for restrained beams.

The load at c is found from the relation for moment at mid-span. Recalling the condition that the panel is simply supported for dead load and partially fixed for live loads,

$$M = \frac{wL^2}{8} + \frac{q_c L^2}{8} - \frac{fq_g L^2}{12}$$

From which

$$q_c = \frac{8}{L^2}\left[M + \frac{fq_g L^2}{12}\right] - w = \frac{8}{(20)^2}\left[84,660 + 82,840\right] - 285$$

$$q_c = 3350 - 285 = 3065 \text{ lb/ft.}$$

$Q_c = 3065(20) = 61,300$ lb which is slightly greater than the resistance of 58,900 lb established by the design criteria. Next, the slope k_1 is determined from equation 46 (appendix E).

$$k_1 = \frac{384EI}{(5 - 4f)L^3} = \frac{384(33.0 \times 10^6)}{[5 - 4(0.9)](20)^3} = 1,131,000 \text{ lb/ft.}$$

Then the deflection at c is

$$y_c = \frac{Q_c}{k_1} = \frac{61,300}{1,131,000} = 0.0542 \text{ ft} = 0.65 \text{ in.}$$

The next step is to compute the increase in yield point. To do this, assume an increase of 25 percent, find the velocity at yield from figure 39 and substitute in equation 43 (appendix D). The assumed increase in yield gives a dynamic yield load of 1.25(61,300) = 76,630 lb and a dynamic yield deflection of 1.25(0.65) = 0.813 in.

Hence, the ordinate of figure 39 is

$$\frac{Q_b}{P} = \frac{76,630}{64,800} = 1.18 \text{ which, for 6 percent elastic damping, gives}$$

$$\frac{\dot{y}_b k_1}{\omega P} = 0.86 \text{ or, } \dot{y}_b = \frac{0.86\,\omega P}{k_1} = \frac{0.86(91.4)(64,800)}{1,131,000} = 4.50 \text{ ft/sec}$$

$$\text{where } \omega_1 = \sqrt{\frac{\beta}{\beta'}\frac{k_1}{m}} = \sqrt{\frac{1.31(1,131,000)(32,2)}{5710}} = 91.4 \text{ radians/sec}$$

Using this value in equation 43, (appendix D), the strain rate is

$$\frac{d\epsilon}{dt} = \frac{32\,f\,c}{L^2(5 - 4f)}\left(\frac{dy}{dt}\right) = \frac{32(0.9)(0.411)(4.50)}{(20)^2[5 - 4(0.9)]} = 0.095 \text{ in/in/sec}$$

And from Manjoine's curve, figure 37, the increase in yield point is 29.6 percent.

Increasing the yield load Q_c by this percentage, the dynamic yield load is determined as

$$Q_b = 1.296(61,300) = 79,400 \text{ lb.}$$

Maximum displacement and time to maximum displacement are now readily determined from figure 40. With the revised value of the ordinate determined as $\frac{Q_b}{P} = \frac{79,400}{64,800} = 1.23$, we get

$$\frac{y_m}{y_b} = 2.82 \quad ; \quad y_m = 0.813\ (2.82) = 2.29 \text{ in.}$$

and

$$\omega t_m = 6.38 \quad ; \quad t_m = \frac{6.38}{91.4} = 0.070 \text{ sec.}$$

The stiffener ribs and the sub-panels are analyzed in a similar manner. Also the shear requirements may be readily checked by the method demonstrated in the text.

APPENDIX G

FUNDAMENTAL MODE THEORY — LOADS WITH RISE-TIME

When the spring-mass system is subjected to a load with a rise-time, as shown in figure 10, diagram (b), the equation of motion for the elastic range becomes,

$$\ddot{y} + \omega^2 y = \frac{P}{m}\left(\frac{t}{t_2}\right) \tag{49}$$

Using the initial conditions $y = o$ and $\dot{y} = o$,

$$\frac{y}{y_b} = \frac{P}{Q_b t_2}\left(t - \frac{\sin \omega t}{\omega}\right), \quad t \leq t_2 \tag{50}$$

The remainder of the solution depends upon whether the terminal condition (2) or (b) is reached first. For the C beams, the time-to-yield was greater than the time-of-rise; hence, the remaining development will be based on this condition.

Differentiating equation 50, using $t = t_2$ and $y = y_2$

$$\frac{v_2}{\omega y_b} = \frac{P}{Q_b}\,\frac{1}{\omega t_2}\,(1 - \cos \omega t_2) \tag{51}$$

In the range 2-3, a-b, the equation of motion may be written,

$$\ddot{y} + \omega^2 y = \frac{P}{m} - \omega^2 y_2 \tag{52}$$

With the initial conditions $y = 0$ and $\dot{y} = v_2$, the solution becomes,

$$\frac{y}{y_b} = \frac{y_2}{y_b}(\cos \omega t - 1) + \frac{v_2}{\omega y_b} \sin \omega t + \frac{P}{Q_b}(1 - \cos \omega t) \quad ,$$

$$t_2 \leq t \leq t_b \tag{53}$$

When $\dot{y} = v_b$, $t = t_b - t_2$, therefore

$$\frac{v_b}{\omega y_b} = \left(\frac{P}{Q_b} - \frac{y_2}{y_b}\right) \sin \omega(t_b - t_2) + \frac{v_2}{\omega y_b} \cos \omega(t_b - t_2) \tag{54}$$

This may be simplified using $\frac{y_2}{y_b}$ from equation 50 and $\frac{v_2}{\omega y_b}$ from equation 51 to get

$$\frac{v_b}{\omega y_b} = \frac{2P}{Q_b \omega t_2} \sin \omega(t_b - t_2) \sin \frac{\omega t_2}{2} \tag{55}$$

The time to b may be obtained by use of equations 50 and 51 in equation 53 together with the terminal condition that $y = y_b - y_2$, when $t = t_b - t_2$

$$t_b = \frac{t_2}{2} + \frac{1}{\omega} \arccos \left[\frac{\left(1 - \frac{Q_b}{P}\right) \frac{\omega t_2}{2}}{\sin \frac{\omega t_2}{2}} \right] \tag{56}$$

During the final phase before maximum initial displacement is reached (range 2-3, b-d), the equation of motion is

$$\ddot{y} = \frac{P - Q_b}{m} \tag{57}$$

and the solution with initial conditions $y = y_b$, $\dot{y} = v_b$ when $t = 0$ is

$$\frac{y}{y_b} = \left(\frac{P}{Q_b} - 1\right)\frac{(\omega t)^2}{2} + \frac{v_b}{y_b}t + 1 \tag{58}$$

$$\text{and } \frac{\dot{y}}{\omega y_b} = \left(\frac{P}{Q_b} - 1\right)\omega t + \frac{v_b}{\omega y_b} \tag{59}$$

From equation 59 the time to zero velocity is

$$\omega t_m = \frac{\frac{v_b}{\omega y_b}}{1 - \frac{P}{Q_b}} \tag{60}$$

This time in equation 58 gives the initial maximum displacement as

$$\frac{y_m}{y_b} = 1 + \frac{\left(\frac{v_b}{\omega y_b}\right)^2}{2\left(1 - \frac{P}{Q_b}\right)} \tag{61}$$

the same relation as equation 31, (appendix C).

Plots of equations 55 and 61 are shown in figures 45 and 46. From these two curves it is a simple matter to determine the initial maximum deflection of a beam subjected to a step load with a rise-time.

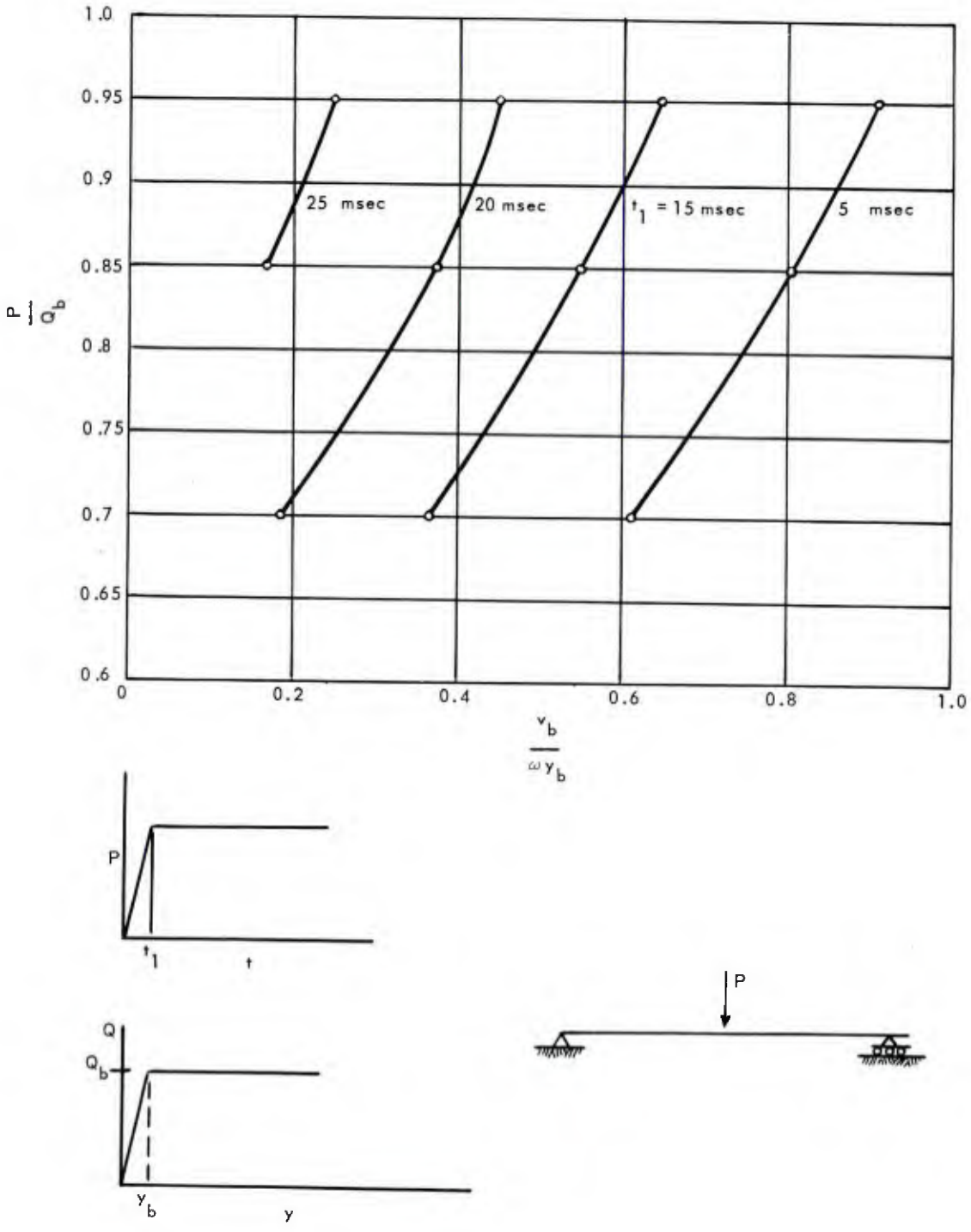

Figure 45. Solution for velocity (load with a rise-time for condition $t_1 < t_b$).

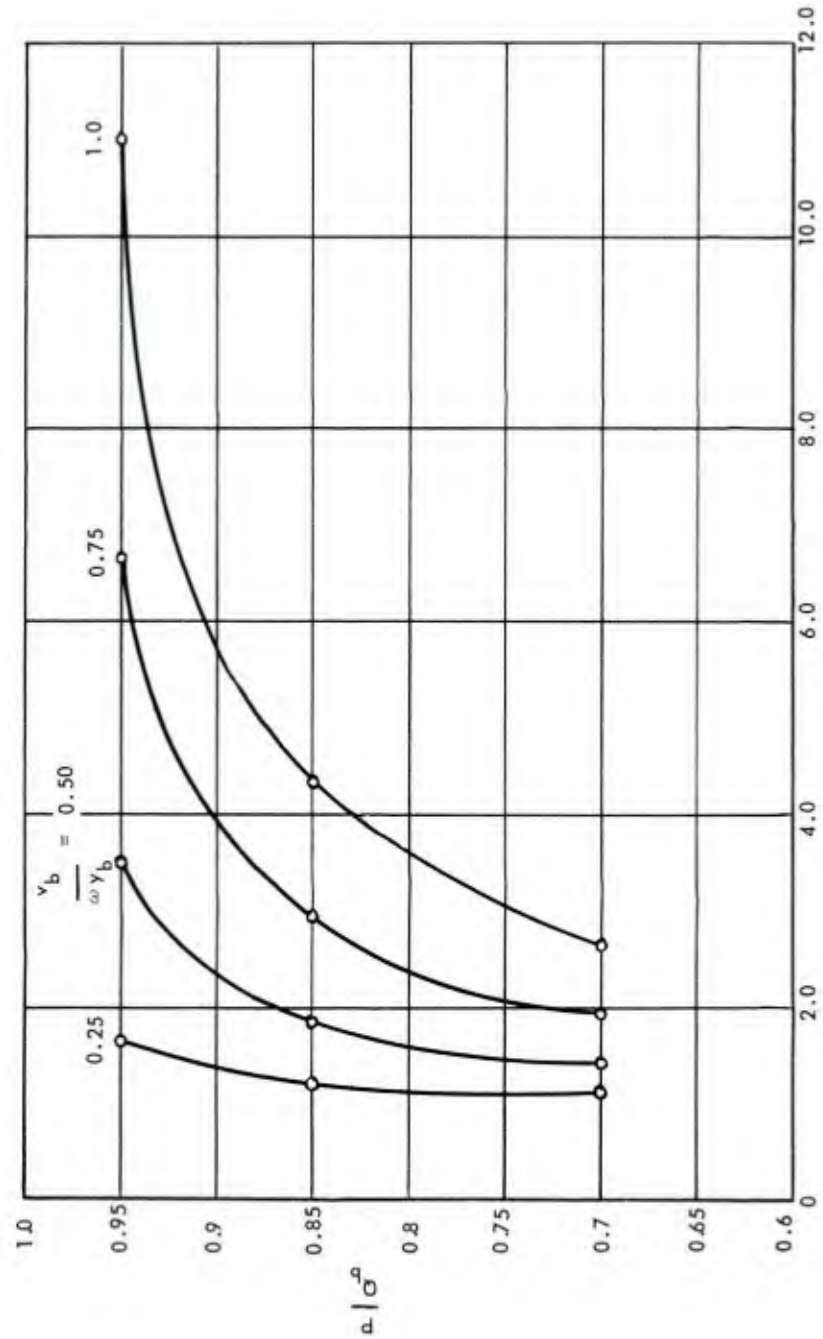

Figure 46. Solution for displacement (load with a rise-time for condition $t_1 < t_b$).

APPENDIX H

GRAPHICAL ANALYSIS OF A DYNAMICALLY LOADED BEAM

The graphical analysis discussed in this appendix is an extension of the method developed by J. Lamoën in 1935 and extended by L. S. Jacobsen in 1952.[18] It is not the intent of this appendix to develop the method here, but rather to demonstrate the use of graphics in determining the response of a beam to a step load with a rise-time.

Briefly the method consists of writing the differential equation for the various ranges or phases of the behavior in the following form:

$$\ddot{y} + \omega^2 (y + \delta) = 0 \qquad (62)$$

The solution of this equation may be plotted on the so-called phase-plane as a series of circular arcs. This requires that the quantity δ be held constant during an increment of arc. Phase-plane coordinates are y as ordinate and $\frac{\dot{y}}{\omega}$ as abscissa. The quantity $(-\delta)$ is also taken on the positive zero displacement ordinate. The angle subtended by the arc is the frequency of the system (ω) times the arbitrary time increment (Δ) during which δ is held constant.

Solution is given below for beam C-14 to demonstrate the ease of graphical analysis as compared to the analytical development. For this beam P = 2470 lb, ω = 194.4 radians/sec, Q_b = 2705 lb, y_b = 0.486 in., and t_2 = 0.016 seconds.

The differential equation of motion in the form of equation 62 is written below for step increments of loads as shown on the curve of figure 47.

Range 1-2, a-b

$$m\ddot{y} + k_1 y = \frac{P}{m} \qquad (63)$$

$$y + \omega^2\left(y - \frac{P}{k_1}\right) = 0 \qquad (64)$$

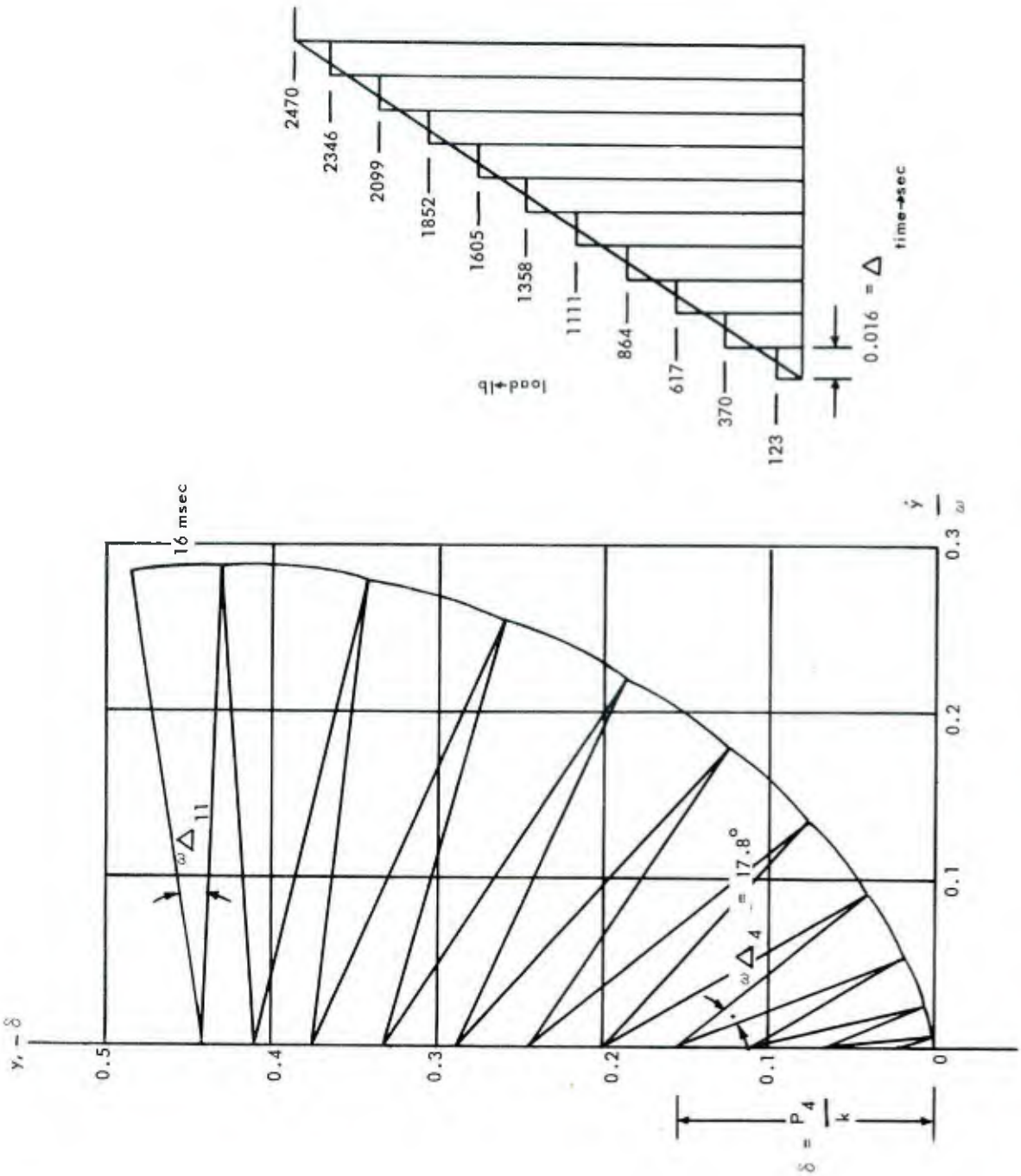

Figure 47. Phase-plane solution for elastic range.

$$\delta = -\frac{P}{k_1} \tag{65}$$

Time increments are 1.6 msec, resulting in an angle of

$$\omega \triangle = 194.4\ (0.0016)\ \frac{180}{\pi} = 17.82^{\circ} \quad .$$

Ten circular segments are laid out successively with their arcs contiguous as shown in figure 47. They represent the passage of 16 msecs at which time point 2 on the load curve has been reached. It is noted that the deflection reached is less than y_b therefore, point b on the resistance curve has not been reached as yet. That is, the beam is elastic and the load is no longer increasing.

It is evident that a new equation of motion must be written for range 2-3, a-b.

Range 2-3, a-b

$$m\,\ddot{y} + k_1 y = P - k_1 y_2 \tag{66}$$

$$\ddot{y} + \omega^2 \left(y - \frac{P}{k_1} + y_2 \right) = 0$$

$$\delta' = -\frac{P}{k_1} + y_2 = -0.4430 + 0.432 = -0.011$$

or for the axis of figure 47.

$$-\delta = y_2 - \delta' = 0.432 + 0.011 = 0.443 \tag{67}$$

This value of $-\delta$ is laid out and an arc is drawn until it intersects the dynamic yield deflection abscissa at 0.486 in.

The remainder of the solution is developed in figure 48. Again the differential equation of motion is written

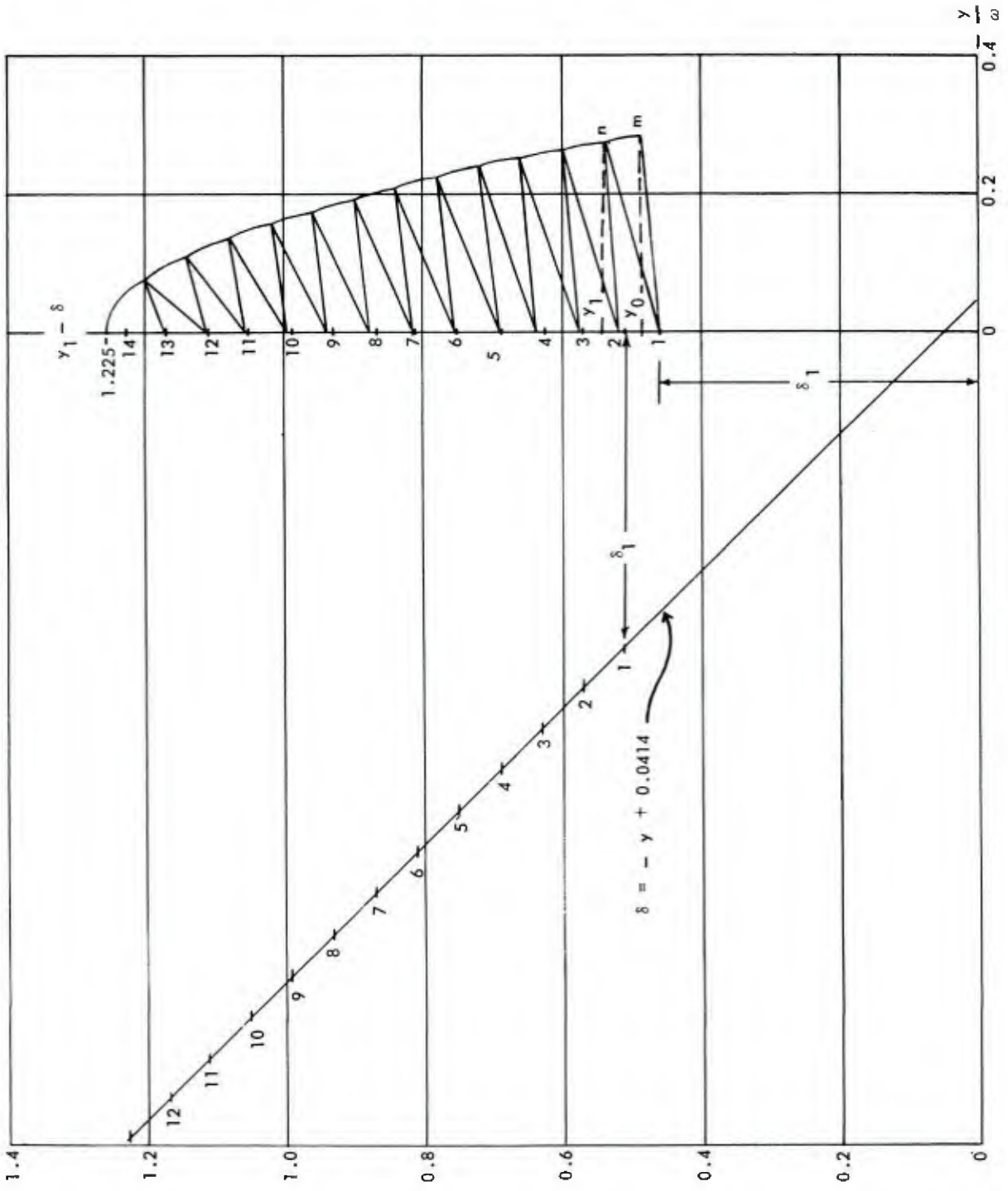

Figure 48. Phase-plane solution for plastic range.

$$\ddot{y} = \frac{1}{m}(P - Q_b) \tag{68}$$

which in the form of equation 62 becomes

$$\ddot{y} + \omega^2\left[y - \left(y + \frac{P - Q_b}{k_1}\right)\right] = 0 \tag{69}$$

$$\delta = -y - \frac{P - Q_b}{k_1} = -y + 0.0414 \tag{70}$$

Here the dependence of δ upon y can be resolved by choosing increments of y and using the average value of δ during this displacement. To do this equation 70 is plotted taking δ as the abscissa.

Then construction of the phase curve is commenced from the initial conditions $y = y_b$, $\frac{\dot{y}}{\omega} = \frac{\dot{y}_b}{\omega}$ taken from figure 47. The first displacement increment is chosen as $y_o\, y_1$, for which the average δ is shown in figure 48 as δ_1. This distance is laid off on the y, $-\delta$ axis, thus locating the center, 1, of the first arc, mn. An identical procedure is used to generate the remainder of the solution. The maximum displacement (1.23 in.) checks the value obtained analytically.

DISTRIBUTION LIST

No. of copies	
15	Chief of Civil Engineers (Code D-400)
1	Chief of Civil Engineers (Code P-300)
1	Navy Secretary, Research and Development Board, Department of Defense
1	Chief of Naval Research (Code 320)
2	Defence Research Member, Canadian Joint Staff (Via ONI-90-321)
1	Dr. Wang, SWRS, Research Director, AFSWC, Kirtland Air Force Base, Albuquerque, New Mexico
1	Chief of Engineers, U. S. Army (Engineer Research and Development Division)
1	Commanding General, Air Materiel Command, Wright-Patterson Air Force Base, Dayton, Ohio (Air Installation Division)
1	Director, National Bureau of Standards (Dr. G. H. Keulegan)
1	Professor C. O. Dohrenwend, Rensselaer Polytechnic Institute, Troy, New York
1	Professor H. J. Hansen, Massachusetts Institute of Technology, Cambridge
1	Dr. N. Newmark, Talbot Laboratory, University of Illinois, Urbana, Illinois
1	Dr. C. P. Seiss, Talbot Laboratory, University of Illinois, Urbana, Illinois
1	Dr. R. C. DeHart, Armed Forces Special Weapons Project, Pentagon
1	Professor W. T. Thomson, University of California at Los Angeles
1	Commanding Officer and Director, David W. Taylor Model Basin, Aerodynamics Laboratory, Washington, D. C. (CDR C. W. Sterling, CEC, USN)
1	Office, Chief of Engineers, Gravely Point, Washington, D. C. (Protective Construction Branch)
3	Officer in Charge, U. S. Naval School, Civil Engineer Corps Officers
1	Library of Congress, (Central Documents Office)
10	Office of Technical Services, Department of Commerce, Washington, D. C.
5	Armed Services Technical Information Agency, Arlington Hall Station, Arlington, Virginia
1	Commander, Air Force Special Weapons Center, Kirtland Air Force Base, New Mexico (SWRS)
1	Commander, Air Force Special Weapons Center, Kirtland Air Force Base, New Mexico (SWOI)

Naval Civil Engineering Research and Evaluation Laboratory. Technical Memorandum M-130.
ELASTO-PLASTIC RESPONSE OF BEAMS TO DYNAMIC LOADS, by J. R. Allgood and W. A. Shaw.
103 p. illus. 3 March 1958. UNCLASSIFIED

A study was made to provide and substantiate a simple method for determining the elasto-plastic response of beams subjected to pulse loads. Design charts are presented. The theory is compared with the results of over sixty beam tests.

1. Beams -- Structural analysis
I. Allgood, J. R.
II. Shaw, W. A.

UNCLASSIFIED

Naval Civil Engineering Research and Evaluation Laboratory. Technical Memorandum M-130.
ELASTO-PLASTIC RESPONSE OF BEAMS TO DYNAMIC LOADS, by J. R. Allgood and W. A. Shaw.
103 p. illus. 3 March 1958. UNCLASSIFIED

A study was made to provide and substantiate a simple method for determining the elasto-plastic response of beams subjected to pulse loads. Design charts are presented. The theory is compared with the results of over sixty beam tests.

1. Beams -- Structural analysis
I. Allgood, J. R.
II. Shaw, W. A.

UNCLASSIFIED

Naval Civil Engineering Research and Evaluation Laboratory. Technical Memorandum M-130.
ELASTO-PLASTIC RESPONSE OF BEAMS TO DYNAMIC LOADS, by J. R. Allgood and W. A. Shaw.
103 p. illus. 3 March 1958. UNCLASSIFIED

A study was made to provide and substantiate a simple method for determining the elasto-plastic response of beams subjected to pulse loads. Design charts are presented. The theory is compared with the results of over sixty beam tests.

1. Beams -- Structural analysis
I. Allgood, J. R.
II. Shaw, W. A.

UNCLASSIFIED

Naval Civil Engineering Research and Evaluation Laboratory. Technical Memorandum M-130.
ELASTO-PLASTIC RESPONSE OF BEAMS TO DYNAMIC LOADS, by J. R. Allgood and W. A. Shaw.
103 p. illus. 3 March 1958. UNCLASSIFIED

A study was made to provide and substantiate a simple method for determining the elasto-plastic response of beams subjected to pulse loads. Design charts are presented. The theory is compared with the results of over sixty beam tests.

1. Beams -- Structural analysis
I. Allgood, J. R.
II. Shaw, W. A.

UNCLASSIFIED